

Numerical solution to a free boundary problem for the Stokes equation using the coupled complex boundary method in shape optimization setting

Julius Fergy Tiongson Rabago and Hirofumi Notsu

Faculty of Mathematics and Physics, Institute of Science and Engineering, Kanazawa University, Kakumamachi, Kanazawa-shi, 920-1192, Ishikawa-ken, Japan.

Contributing authors: jfrabago@gmail.com; notsu@se.kanazawa-u.ac.jp;

Abstract

A new reformulation of a free boundary problem for the Stokes equations, which govern a viscous flow with an overdetermined condition on the free boundary, is proposed. The idea of the method is to transform the governing equations into a boundary value problem with a complex Robin boundary condition that couples the two boundary conditions on the free boundary. The proposed formulation gives rise to a new cost functional that apparently has not been exploited in the context of free surface problems. The shape derivative of the cost function, constructed using the imaginary part of the velocity and pressure solution in the whole domain, is computed in order to identify the free boundary. The shape gradient information is then utilized in a domain variation method based on a preconditioned steepest descent algorithm to solve the shape optimization problem. Numerical results illustrating the applicability of the method are provided in both two and three spatial dimensions. For validation and evaluation of the method, the numerical results are compared with those obtained via the classical tracking Dirichlet data.

Keywords: coupled complex boundary method, free surface flow, shape optimization, shape derivatives, rearrangement method, and adjoint method

1 Introduction

We study a free boundary problem for fluid flows arising in various applications including magnetic shaping processes in which the fluid's shape is influenced by the Lorentz force. The model involves the Stokes flow equations and a pressure balance equation on the free boundary, disregarding surface tension effects [1]. Two model problems can be considered in this context. The first involves fluid confinement in a mould with an unknown internal boundary. The second deals with a portion of the fluid boundary adhering to a solid while the rest is free and interacts with the surrounding air. In this work, we focus on the second case for d -dimensional geometries, where d is 2 or 3. That is, we are particularly interested in the free surface problem, similar to the Bernoulli problem [2, 3], but with the Stokes equations replacing the Laplace equation.

Main Problem. Consider a simply connected bounded domain $\omega \subset \mathbb{R}^d$ with boundary $\Gamma := \partial\omega$. The fluid is considered levitating around ω which is influenced by a gravity-like force \mathbf{f} , and occupies then the domain $\Omega = B \setminus \overline{\omega}$, where B is a larger bounded, simply connected domain with boundary $\Sigma := \partial B$ containing $\overline{\omega}$. The incompressible viscous flow occupying Ω , the velocity field \mathbf{u} , and the pressure p are then supposed to satisfy the overdetermined system of Stokes equations in non-dimensional form:

$$\left\{ \begin{array}{ll} -\alpha\Delta\mathbf{u} + \nabla p = \mathbf{f} & \text{in } \Omega, \\ \nabla \cdot \mathbf{u} = 0 & \text{in } \Omega, \\ \mathbf{u} = \mathbf{g} & \text{on } \Gamma, \\ \mathbf{u} \cdot \mathbf{n} = 0 \quad \text{and} \quad -p\mathbf{n} + \alpha\partial_{\mathbf{n}}\mathbf{u} = \mathbf{0} & \text{on } \Sigma, \end{array} \right. \quad (1)$$

where $\alpha := Re^{-1}$, and $Re > 0$ is the Reynolds number, $\partial_{\mathbf{n}}$ denotes the normal derivative, and \mathbf{n} is the outer unit normal vector to Σ (see [1, 4]).¹ The boundary data \mathbf{g} is a prescribed velocity which triggers the motion of Γ while the boundary condition imposed on the free surface Σ indicate zero ambient pressure and negligible surface tension effects². The slip boundary condition $\mathbf{u} \cdot \mathbf{n} = 0$ on Σ permits tangential velocities on the boundary, but neither inflow or outflow cannot occur. This condition is appropriate for problems that involve free boundaries such as the well-known coating problem [5, 6] and situations where the usual no-slip condition $\mathbf{u} = \mathbf{0}$ is not valid (e.g., flows past chemically reacting walls [7, 8]). The distinctions between slip and no-slip boundary conditions have been heavily discussed in the literature. The no-slip condition has been well established (see, e.g., [9, 10]) for moderate pressures and velocities through direct observations and by comparing numerical simulations with experimental findings across a wide range of intricate flow scenarios. Early experiments revealed that low-temperature slip occurs on solid surfaces, specifically when the Knudsen numbers are sufficiently large, resulting in velocity slip at the wall surface. This phenomenon is also observed in hydraulic fracturing and biological fluids [8], representing examples of nonlinear fluid flows.

Known approaches. Motivated by various applications like ship hydrodynamics [11] and thin film manufacturing [12], numerical solutions for flows with freely moving boundaries are crucial. These problems involve determining both the flow variables and the unknown boundary, referred to as the “free boundary.” Due to the complexity of resolving these unknowns simultaneously, an iterative numerical solution is necessary and can be obtained through different methods [13, 14].

Free surface problems (FSPs) such as (1) consist of overdetermined boundary conditions on the unknown part of the boundary. To handle this issue, we can reframe them as shape optimization problems; see, e.g., [1, 4].³ There are different approaches to doing this. One common strategy is to select one of the boundary conditions on the unknown boundary to establish a well-defined state equation (cf. [17–21]). Then, we can track the remaining boundary data using an appropriate norm; for example, using the L^2 -norm. Another approach involves utilizing the Kohn–Vogelius cost functional. This formulation includes two auxiliary problems each posed with one of the boundary condition on the free boundary (see [22–24] for the Bernoulli problem and [1, 4] for an FSP). More precisely, one considers the minimization problem

$$J_{KV}(\Omega) := \frac{1}{2} \int_{\Omega} |\nabla(\mathbf{u}_N - \mathbf{u}_D)|^2 dx \rightarrow \inf, \quad (2)$$

¹To make the boundary condition on the free part Σ physically relevant, we write (1) in terms of the symmetric deformation tensor $\sigma(\mathbf{u}) = \frac{1}{2}(\nabla\mathbf{u} + \nabla\mathbf{u}^\top)$. Because $\nabla \cdot \mathbf{u} = 0$, we have $2\alpha\nabla \cdot \sigma(\mathbf{u}) = \alpha\Delta\mathbf{u}$ in Ω . Also, we have $-\alpha\partial_{\mathbf{n}}\mathbf{u} + p\mathbf{n} = (-2\mu\sigma(\mathbf{u}) + pid)\mathbf{n}$ on Σ , see [1]. Here, however, we follow [4] for the notations.

²The zero-surface tension assumption is a typical setup in the literature which not only simplifies the discussion, but also allows one to ignore technical difficulties resulting from higher derivative terms.

³The same technique – but in the context of optimal shape design problems – of finding the boundary that minimizes a norm of the residual of one of the free surface conditions, subject to the boundary value problem with the remaining free surface conditions imposed, has also been used for potential free surface flows in [15, 16].

where the state variables $\mathbf{u}_N := \mathbf{u}_N(\Omega)$ and $\mathbf{u}_D = \mathbf{u}_D(\Omega)$ respectively satisfy the following well-posed systems of partial differential equations (PDEs):

$$\begin{cases} -\alpha\Delta\mathbf{u}_D + \nabla p_D = \mathbf{f} & \text{in } \Omega, \\ \nabla \cdot \mathbf{u}_D = \mathbf{0} & \text{in } \Omega, \\ \mathbf{u}_D = \mathbf{g} & \text{on } \Gamma, \\ \mathbf{u}_D \cdot \mathbf{n} = \mathbf{0} \quad \text{and} \quad \alpha\partial_{\mathbf{n}}\mathbf{u}_D \cdot \boldsymbol{\tau} = \mathbf{0} & \text{on } \Sigma; \end{cases} \quad (3)$$

$$\begin{cases} -\alpha\Delta\mathbf{u}_N + \nabla p_N = \mathbf{f} & \text{in } \Omega, \\ \nabla \cdot \mathbf{u}_N = \mathbf{0} & \text{in } \Omega, \\ \mathbf{u}_N = \mathbf{g} & \text{on } \Gamma, \\ -p_N \mathbf{n} + \partial_{\mathbf{n}}\mathbf{u}_N = \mathbf{0} & \text{on } \Sigma. \end{cases} \quad (4)$$

In (3), $\boldsymbol{\tau}$ denotes the tangential vector to Σ . Meanwhile, for tracking-boundary-data cost functional approach, the following minimization problems can be considered:

$$J_D(\Omega) := \frac{1}{2} \int_{\Sigma} (\mathbf{u}_N \cdot \mathbf{n})^2 d\sigma \rightarrow \inf, \quad (5)$$

$$J_N(\Omega) := \frac{1}{2} \int_{\Sigma} |-p_D \mathbf{n} + \partial_{\mathbf{n}}\mathbf{u}_D|^2 d\sigma \rightarrow \inf, \quad (6)$$

where, of course, \mathbf{u}_D and \mathbf{u}_N satisfy problems (3) and (4), respectively.

The equivalence between each of the formulations (2), (5), and (6), and problem (1) can easily be demonstrated, see [4, Rem. 2.2]. Here, it should be noted that the equation $J_{KV}(\Omega) = 0$ is equivalent to the existence of $\lambda_0 \in \mathbb{R}$ such that $(\mathbf{u}_D, p_D) = (\mathbf{u}_N, p_N + \lambda_0)$ [1]. Meanwhile, we note that J_N requires a higher degree of regularity of the state variables to be well-defined. Therefore, using this cost functional in numerical experiments may be impractical without ensuring high regularity of the state variables. In (2), (5), and (6), the infimum has always to be taken over all sufficiently smooth domains. For the feasibility of these approaches, with $\mathbf{g} \equiv \mathbf{0}$, we refer to [4].

Remark 1.1. One may opt to penalize, instead of J_{KV} , by the cost functional

$$J_{L^2}(\Omega) := \frac{1}{2} \int_{\Omega} |\mathbf{u}_N - \mathbf{u}_D|^2 dx.$$

Compared to J_{KV} , however, the shape gradient of J_{L^2} is more complex and computationally expensive to evaluate due to additional systems of PDEs (cf. [25]).

New strategy and novelty. In this study, we offer a novel shape optimization approach to solve (1). We introduce the coupled complex boundary method (CCBM) as a new application in this field. The method's starting point is similar to [26], but we incorporate the concept of complex PDEs. The basic idea is to combine Dirichlet and Neumann data into a Robin boundary condition, where the Dirichlet data represents the real part and the Neumann data represents the imaginary part. This transformation allows us to combine the boundary conditions on the free surface into a single condition that must be satisfied within the domain. Consequently, a new cost functional (see (14)) is introduced, which has not been explored in existing literature. This reformulation seems advantageous as it involves a volume integral and incorporates a more regular adjoint state compared to boundary-data tracking-type cost functions.

CCBM, introduced by Cheng et al. [27, 28], initially addressed an inverse source problem [27] and a Cauchy problem [28]. It was subsequently applied to solve inverse conductivity problems [29] and parameter identification in elliptic problems [30]. Afraites [31] then used CCBM for inverse obstacle problems, and Rabago [32] applied it to the exterior Bernoulli problem. While CCBM has been employed

for solving an inverse Cauchy Stokes problem [33], this work stands out as the first to apply CCBM to tackle free surface problems, specifically in relation to solving (1).

Contributions to the literature. The main contributions and highlights of this study are listed as follows.

- This work introduces a new cost functional for the free surface problem, resulting directly from the CCBM formulation; see (14). Notably, this cost functional has not been examined in the existing literature.
- The study focuses on the rigorous computation of the first-order shape derivative of the cost functional associated with CCBM (see Theorem 3.4), using only the Hölder continuity of the state variables (see Lemma 3.10). This approach differs from the classical approach, which typically relies on either the material or shape derivatives of the states (see, e.g., [1, 4, 32]). In fact, our approach bypasses the need for computing these derivatives.
- The proof of the Hölder continuity of the state variables proceeds in a slightly different manner from the usual strategy found, for instance, in [21, 34, 35]. Applying the technique used in these papers poses challenges in eliminating pressure variables and obtaining a consistent estimate for the velocity difference between transformed and steady cases of the Stokes problem. See the proof of Lemma 3.10 for the details.
- To our knowledge, previous numerical studies on the free boundary problem with the Stokes equations (see [4]) only dealt with two-dimensional (2D) cases. However, our study goes a step further by testing the proposed method in three-dimensional (3D) problems. In fact, the numerical part of the paper reveals that our formulation exhibits a smoothing effect, particularly in 3D cases, when approximating a solution to the overdetermined BVP (1); refer to subsection 4.2.2 for more details.

The remainder of the paper is organized as follows. In Section 2, we will demonstrate how problem (1) is formulated into a shape optimization problem via CCBM. The well-posedness of the CCBM formulation is also discussed in this section. Meanwhile, we devote Section 3 to computing the boundary integral expression of the shape gradient of J . This paper section begins with a brief overview of shape calculus concepts relevant to the study, followed by a concise list of tangential shape calculus identities. The main result, concerning the shape gradient of the cost, is rigorously characterized using the rearrangement method – referencing [21, 35]. Section 4 discretizes the continuous formulation and presents a numerical algorithm based on the Sobolev gradient method for solving the discrete shape optimization problem. This section is divided into two parts: discussing the iterative scheme (subsection 4.1) and presenting numerical experiments in 2D and 3D (subsection 4.2). The paper concludes in Section 5 with a brief summary of the study and a mention of future work.

The paper also contains three appendices wherein we provide some details of the proofs of the well-posedness of the state problem (Appendix A), show the computation of some identities used in the investigation (Appendix B), and demonstrate the derivation of the shape gradient via the chain rule approach (Appendix C).

2 CCBM in shape optimization settings

We present here the proposed coupled complex boundary method formulation of (1) and discuss the well-posedness of the state problem.

2.1 The coupled complex boundary method formulation

CCBM suggests to write the boundary conditions on the free boundary as one condition. This means to consider the complex boundary value problem (BVP)

$$\left\{ \begin{array}{ll} -\alpha\Delta\mathbf{u} + \nabla p = \mathbf{f} & \text{in } \Omega, \\ \nabla \cdot \mathbf{u} = \mathbf{0} & \text{in } \Omega, \\ \mathbf{u} = \mathbf{g} & \text{on } \Gamma, \\ -p\mathbf{n} + \alpha\partial_{\mathbf{n}}\mathbf{u} + iu_n\mathbf{n} = \mathbf{0} & \text{on } \Sigma, \end{array} \right. \quad (7)$$

where $i = \sqrt{-1}$. Letting $(\mathbf{u}, p) := (\mathbf{u}_r + i\mathbf{u}_i, p_r + ip_i)$ denote the solution of (7), it can be shown that the real vector-valued functions \mathbf{u}_r and \mathbf{u}_i , and real-valued functions p_r and p_i , respectively satisfy the real PDE systems:

$$\begin{cases} -\alpha\Delta\mathbf{u}_r + \nabla p_r = \mathbf{f} & \text{in } \Omega, \\ \nabla \cdot \mathbf{u}_r = \mathbf{0} & \text{in } \Omega, \\ \mathbf{u}_r = \mathbf{g} & \text{on } \Gamma, \\ -p_r \mathbf{n} + \alpha \partial_{\mathbf{n}} \mathbf{u}_r = (\mathbf{u}_i \cdot \mathbf{n}) \mathbf{n} & \text{on } \Sigma, \end{cases} \quad (8)$$

$$\begin{cases} -\alpha\Delta\mathbf{u}_i + \nabla p_i = \mathbf{0} & \text{in } \Omega, \\ \nabla \cdot \mathbf{u}_i = \mathbf{0} & \text{in } \Omega, \\ \mathbf{u}_i = \mathbf{0} & \text{on } \Gamma, \\ -p_i \mathbf{n} + \alpha \partial_{\mathbf{n}} \mathbf{u}_i = -(\mathbf{u}_r \cdot \mathbf{n}) \mathbf{n} & \text{on } \Sigma, \end{cases} \quad (9)$$

Hereinafter, if there is no confusion, we represent the real and imaginary parts of a complex-valued function by attaching to it the subscript \cdot_r and \cdot_i , respectively.

Remark 2.1. Observe from (9) that if $\mathbf{u}_i = \mathbf{0}$ and $p_i = 0$ in Ω , then we have $\mathbf{u}_i = \partial_{\mathbf{n}} \mathbf{u}_i = 0$ and $p_i = 0$ on Σ , and thus $\mathbf{u}_r \cdot \mathbf{n} = 0$ on Σ . From (8) and (9), we see that the pair (Ω, \mathbf{u}_r) solves the original free boundary problem (1). Conversely, if (Ω, \mathbf{u}) is the solution to (1), then clearly \mathbf{u}_r and \mathbf{u}_i satisfy (8) and (9).

We can infer from the previous remark that the original free boundary problem (1) can be reformulated as an equivalent shape optimization problem, which is given as follows.

Problem 2.2. Given a fixed interior boundary Γ and a function \mathbf{f} , find an annular domain Ω , with the exterior boundary denoted by $\Sigma := \partial\Omega \setminus \Gamma$, and a function $\mathbf{u} := \mathbf{u}(\Omega)$ such that $\mathbf{u}_i = 0$ in Ω and $\mathbf{u} = \mathbf{u}_r + i\mathbf{u}_i$ solves the PDE system (7).

2.2 Notations and well-posedness of the state problem

We discuss here the well-posedness of the PDE system (7). For simplicity, we carry out the analysis on the basis of homogenous Dirichlet boundary conditions on the fixed boundary Γ , i.e., $\mathbf{g} = \mathbf{0}$. Accordingly, we assume that $\langle \mathbf{u}, \mathbf{n} \rangle_{\Sigma} = 0$. Extension to non-homogeneous Dirichlet boundary conditions can be accomplished by standard techniques. In this case, appropriate assumptions on \mathbf{g} have to be imposed (i.e., $\mathbf{g} \in H_{\text{loc}}^k(\mathbb{R}^d)^d$, for some $k \in \mathbb{N}$, and $\langle \mathbf{u}, \mathbf{n} \rangle_{\Sigma} = -\langle \mathbf{u}, \mathbf{n} \rangle_{\Gamma} \geq 0$; cf. [9, Lem. 2.2, p. 24]).

Notations. We first introduce some notations. We start with the normal derivative $\partial_{\mathbf{n}} := \partial/\partial\mathbf{n} = \mathbf{n} \cdot \nabla = \mathbf{n}^{\top} \nabla = \sum_{i=1}^d n_i (\partial/\partial x_i)$, where $\mathbf{n} = (n_1, \dots, n_d)^{\top} \in \mathbb{R}^d$ is the outward unit normal vector to Ω and $\nabla := (\partial/\partial x_1, \dots, \partial/\partial x_d)^{\top}$. We denote the inner product of two (column) vectors $\mathbf{a}, \mathbf{b} \in \mathbb{R}^d$ in \mathbb{R}^d by $\mathbf{a} \cdot \mathbf{b} := \mathbf{a}^{\top} \mathbf{b} \equiv \langle \mathbf{a}, \mathbf{b} \rangle_{\mathbb{R}^d} = \langle \mathbf{a}, \mathbf{b} \rangle$, respectively, where the latter is used when there is no confusion. We also add that we occasionally write φ_n instead of $\varphi \cdot \mathbf{n}$, where φ is a vector-valued function, for economy of notation and to save space.

For a vector-valued function $\mathbf{u} := (u_1, u_2, \dots, u_d)^{\top} : \Omega \rightarrow \mathbb{R}^d$, the gradient of \mathbf{u} , denoted by $\nabla \mathbf{u}$, is a second-order tensor defined as $\nabla \mathbf{u} = (\nabla \mathbf{u})_{ij} := (\partial u_j / \partial x_i)_{i,j=1,\dots,d}$, where $(\nabla \mathbf{u})_{ij}$ is the entry at the i th row and j th column. Meanwhile, the Jacobian of \mathbf{u} , denoted by $D\mathbf{u}$ (the total derivative of \mathbf{u}), is the transpose of the gradient (i.e., $D\mathbf{u} = (D\mathbf{u})_{ij} = (\partial u_i / \partial x_j)_{i,j=1,\dots,d} = \nabla^{\top} \mathbf{u}$). Appropriately, we write the \mathbf{n} -directional derivative of \mathbf{u} as $\partial_{\mathbf{n}} \mathbf{u} := (D\mathbf{u})\mathbf{n}$. For later use, the second-order normal derivative of a sufficiently smooth function φ is denoted by $\partial_{\mathbf{n}\mathbf{n}}^2 \varphi$.

Let $1 \leq p \leq \infty$ and m be a non-negative integer. The function spaces $W^{m,p}(\Omega)$, $W^{0,p}(\Omega) = L^p(\Omega)$, and $H^m(\Omega) = W^{m,2}(\Omega)$ denote the standard real Sobolev spaces equip with their natural norms also expressed in the usual notations (i.e., $\|\cdot\|_{W^{m,p}(\Omega)}$ and $\|\cdot\|_{H^m(\Omega)}$ are the standard Sobolev norms); see, e.g., [36, Chap. IV].

For vector-valued functions, we define the Sobolev space

$$H^m(\Omega)^d := \{\mathbf{u} = (u_1, u_2, \dots, u_d)^\top : \Omega \rightarrow \mathbb{R}^d \mid u_i \in H^m(\Omega) \text{ for } i = 1, \dots, d\}.$$

Its associated norm is given by $\|\mathbf{u}\|_{H^m(\Omega)^d} = (\sum_{i=1}^d \|u_i\|_{H^m(\Omega)}^2)^{1/2}$. Similar definition is given when Ω is replaced by $\partial\Omega$. Unless stated otherwise, we assume in the paper that $\Omega \subset \mathbb{R}^d$ is a bounded, non-empty, connected set, and at least of class $C^{1,1}$.

Now, in this paper, we let $\mathbf{H}^m(\Omega)^d$ be the complex version of $H^m(\Omega)^d$ with the inner product $((\cdot, \cdot))_{m,\Omega,d}$ and norm $\|\cdot\|_{m,\Omega,d}$ defined respectively as follows:

$$\text{for all } \mathbf{u}, \mathbf{v} \in \mathbf{H}^m(\Omega)^d, \quad ((\mathbf{u}, \mathbf{v}))_{m,\Omega,d} = \sum_{j=1}^d (u_j, \bar{v}_j)_{m,\Omega} \quad \text{and} \quad \|\mathbf{v}\|_{m,\Omega,d} = \sqrt{((\mathbf{v}, \mathbf{v}))_{m,\Omega,d}}.$$

Also, for ease of writing, we will use the following notations in the paper:

$$\begin{aligned} X &:= \mathbf{H}^1(\Omega)^d, \quad V_\Gamma := \mathbf{H}_{\Gamma,0}^1(\Omega)^d, \quad Q := \mathbf{L}^2(\Omega), \quad \overset{\circ}{Q} = \left\{ q \in Q \mid \int_{\Omega} q \, dx = 0 \right\}, \\ \overset{\circ}{V} &:= \mathbf{H}_0^1(\Omega)^d, \quad \overset{\circ}{V}_0 = \left\{ \mathbf{v} \in \overset{\circ}{V} \mid \nabla \cdot \mathbf{v} = 0 \right\}, \quad (\nabla \cdot \mathbf{v}, q) := (\nabla \cdot \mathbf{v}, q)_\Omega = \int_{\Omega} \bar{q} \nabla \cdot \mathbf{v} \, dx, \\ \overset{\circ}{V}_\perp &= \left\{ \mathbf{v} \in \overset{\circ}{V} \mid (\mathbf{v}, \mathbf{w})_X = 0, \forall \mathbf{w} \in \overset{\circ}{V} \right\}, \quad (\mathbf{v}, \mathbf{w})_X := \int_{\Omega} (\nabla \mathbf{v} : \nabla \bar{\mathbf{w}} + \mathbf{v} \cdot \bar{\mathbf{w}}) \, dx. \end{aligned}$$

In above, the operation ‘ $:$ ’ stands for the Frobenius inner product and is defined as

$$\nabla \mathbf{v} : \nabla \bar{\mathbf{w}} = \sum_{i,j=1}^d \frac{\partial v_j}{\partial x_i} \frac{\partial \bar{w}_j}{\partial x_i} = \frac{\partial v_j}{\partial x_i} \frac{\partial \bar{w}_j}{\partial x_i} \in \mathbb{R}.$$

In above equation, Einstein’s notation for summation is applied. We have introduced it here since this notational convention will be heavily utilized in the latter part of subsection 3.3. Meanwhile, because $\overset{\circ}{V}_0$ is a closed subspace of $\overset{\circ}{V}$, we have the decomposition $\overset{\circ}{V} = \overset{\circ}{V}_0 \oplus \overset{\circ}{V}_\perp$. Also, with the above definitions, we sometimes write $\|\mathbf{v}\|_X = \|\mathbf{v}\|_{1,\Omega,d}$ and $\|q\|_Q = \|q\|_{0,\Omega}$, and drop d when there is no confusion.

Lastly, throughout the paper, c will denote a generic positive constant which may have a different value at different places. Also, we occasionally use the symbol “ \lesssim ” which means that if $x \lesssim y$, then we can find some constant $c > 0$ such that $x \leq c y$. Of course, $y \gtrsim x$ is defined as $x \lesssim y$. Other notations are standard and will only be emphasized for clarity.

Now we exhibit the weak-formulation of the complex PDE system (7). On this purpose, we introduce the following forms:

$$\begin{cases} a(\varphi, \psi) = \int_{\Omega} \alpha \nabla \varphi : \nabla \bar{\psi} \, dx + i \int_{\Sigma} (\varphi \cdot \mathbf{n})(\bar{\psi} \cdot \mathbf{n}) \, d\sigma, \quad \forall \varphi, \psi \in V_\Gamma, \\ b(\varphi, \lambda) = - \int_{\Omega} \bar{\lambda} (\nabla \cdot \varphi) \, dx, \quad \forall \varphi \in V_\Gamma, \forall \lambda \in Q, \\ F(\psi) = \int_{\Omega} \mathbf{f} \cdot \bar{\psi} \, dx, \quad \forall \psi \in V_\Gamma. \end{cases} \quad (10)$$

We can then state the weak formulation of (7) as follows: find $(\mathbf{u}, p) \in V_\Gamma \times Q$ such that

$$a(\mathbf{u}, \varphi) + b(\varphi, p) = F(\varphi), \quad \forall \varphi \in V_\Gamma, \quad \text{and} \quad b(\mathbf{u}, \lambda) = 0, \quad \forall \lambda \in Q. \quad (11)$$

Our first proposition is given next.

Proposition 2.3. For a given $\mathbf{f} \in L^2(\Omega)^d$, the weak formulation of (7) given above admits a unique solution $(\mathbf{u}, p) \in V_\Gamma \times Q$ which depends continuously on the data. Moreover, we have

$$\|\mathbf{u}\|_X, \|p\|_Q \lesssim \|\mathbf{f}\|_{0,\Omega}.$$

The proof of the proposition is based on standard arguments as in the real case. Indeed, the validity of the statement follows from the continuity of the sesquilinear form $a(\cdot, \cdot)$ on $V_\Gamma \times V_\Gamma$, its coercivity on $V_\Gamma \subset X$, i.e., to show that there exists a constant $c_a > 0$ such that

$$\Re(a(\varphi, \varphi)) \geq c_a \|\varphi\|_X, \quad \forall \varphi \in V_\Gamma, \quad (12)$$

the continuity of F on V_Γ , and on an inf-sup condition. For the final condition, the bilinear form b must satisfy the requirement that there exists constant β_0 such that

$$\inf_{\substack{\lambda \in Q \\ \lambda \neq 0}} \sup_{\substack{\varphi \in V_\Gamma \\ \varphi \neq 0}} \frac{b(\varphi, \lambda)}{\|\varphi\|_X \|\lambda\|_Q} \geq \beta_0 > 0. \quad (13)$$

Some details of the argumentation is provided in Appendix A for reference.

2.3 The proposed shape optimization formulation

To solve Problem 2.2, we introduce the cost functional

$$J(\Omega) = \frac{1}{2} \|\mathbf{u}_i\|_{L^2(\Omega)^d}^2 + \frac{1}{2} \|p_i\|_{L^2(\Omega)}^2 = \frac{1}{2} \int_\Omega (|\mathbf{u}_i|^2 + |p_i|^2) dx, \quad (14)$$

where (\mathbf{u}_i, p_i) is subject to the state problem (7). Notice that compared to J_{KV} , the cost functional J only requires the solution of a single complex PDE problem to be solved. The optimization problem we consider here is the problem of minimizing $J(\Omega)$ over a set of admissible domains \mathcal{O}_{ad} , where \mathcal{O}_{ad} is essentially the set of $\mathcal{C}^{k,1}$, $k \geq 1$, $k \in \mathbb{N}$, (non-empty) doubly connected domains with (fixed) interior boundary Γ and (free) exterior boundary Σ . In other words, we consider the shape optimization problem that reads as follows: find Ω such that

$$J(\Omega) = \min_{\tilde{\Omega} \in \mathcal{O}_{ad}} J(\tilde{\Omega}). \quad (15)$$

We note that it is actually enough to consider Γ to be only Lipschitz regular to derive the shape derivative of J , but for simplicity we also assume it to be $\mathcal{C}^{k,1}$ regular. We emphasize that, in this paper, we will not tackle the interesting question of existence of optimal solution to (15). Instead, we will tacitly assume the existence of the solution to (1) and adopt the minimization approach (15) to resolve the problem numerically.

To numerically solve (15), we will apply a shape-gradient-based descent method based on the finite element method (FEM). The shape derivative of the cost will be exhibited in the next section using *shape calculus* [37–41].

3 Computation of the shape derivative

The main purpose of this section is to prove our main result given by Theorem 3.4.

3.1 Some concepts from shape calculus

Prior to computing the shape gradient of the cost functional J , we provide in this section a concise overview of key concepts and results from shape calculus.

Consider a (convex) bounded hold-all domain U of class $C^{k,1}$, $k \geq 1$, strictly containing $\bar{\Omega}$ (the closure of Ω). Given a t -independent deformation field $\boldsymbol{\theta} := (\theta_1, \theta_2, \dots, \theta_d)^\top$ belonging to the admissible space⁴

$$\Theta^k := \{\boldsymbol{\theta} \in C^{k,1}(\bar{U})^d \mid \boldsymbol{\theta} = \mathbf{0} \text{ on } \Gamma \cup \partial U\}, \quad (16)$$

where $k \in \mathbb{N}$ (later on specified as what is needed), we define T_t as the *perturbation of the identity id*⁵ given by the map

$$T_t = T_t(\boldsymbol{\theta}) = id + t\boldsymbol{\theta}, \quad T_0 = id, \quad (T_t : \bar{U} \mapsto \mathbb{R}^d). \quad (17)$$

We express the perturbation of the reference domain Ω as $\Omega_t := T_t(\Omega)$. Then, accordingly, we write $\Sigma_t := T_t(\Sigma)$, and we have $\Gamma_t := T_t(\Gamma) \equiv \Gamma$ since $\boldsymbol{\theta} = \mathbf{0}$ on Γ . In addition, of course, $\Omega_0 = \Omega$ and $\Sigma_0 = \Sigma$.

Now, for a fixed $\varepsilon > 0$ (which is assumed sufficiently small for technical reasons), we define the set of all admissible domains \mathcal{O}_{ad} as follows

$$\mathcal{O}_{ad} = \left\{ T_t(\boldsymbol{\theta})(\bar{\Omega}) \subset U \mid \Omega \in C^{k,1}, k \in \mathbb{N}, t \in \mathcal{I} := [0, \varepsilon], \boldsymbol{\theta} \in \Theta^k \right\}. \quad (18)$$

The functional $J : \mathcal{O}_{ad} \rightarrow \mathbb{R}$ has a directional *first-order Eulerian derivative* at Ω in the direction of the field $\boldsymbol{\theta}$ if the limit

$$\lim_{t \searrow 0} \frac{J(\Omega_t) - J(\Omega)}{t} =: dJ(\Omega)[\boldsymbol{\theta}] \quad (19)$$

exists [37, Eq. (3.6), p. 172]. The functional J is said to be *shape differentiable* at Ω if the limit exists for all $\boldsymbol{\theta} \in \Theta^k$ and the map $\boldsymbol{\theta} \mapsto dJ(\Omega)[\boldsymbol{\theta}]$ is linear and continuous on Θ^k . In this case, we refer to the map as the *shape gradient* of J .

We introduce a few more notations for ease of writing. We denote by DT_t the Jacobian matrix of T_t and write the inverse and inverse transpose of this matrix by $(DT_t)^{-1}$ and $(DT_t)^{-\top} := ((DT_t)^\top)^{-1}$, respectively. Also, we define the following:

$$I_t := \det DT_t, \quad A_t := I_t(DT_t^{-1})(DT_t)^{-\top}, \quad B_t := I_t|M_t \mathbf{n}|, \quad M_t := (DT_t)^{-\top}. \quad (20)$$

At $t = 0$, it is evident that $I_0 = 1$, $DT_0^{-1} = (DT_0)^{-\top} = id$, $A_0 = id$, and $B_0 = 1$.

We also introduce the following notations for frequent use in subsection 3.3:

$$\mathfrak{d}_t := I_t - 1, \quad \mathfrak{m}_t := M_t^\top - id, \quad \mathfrak{a}_t := A_t - id, \quad \text{and} \quad \mathfrak{b}_t := B_t|M_t \mathbf{n}|^{-2} - 1. \quad (21)$$

Now, let – for the rest of this subsection – $\mathcal{I} = [-\varepsilon, \varepsilon]$. For sufficiently small $\varepsilon > 0$, I_t is positive, and the following regularity properties of T_t can be shown (see, e.g., [21, 35, 37]):

$$\begin{aligned} [t \mapsto T_t] &\in C^1(\mathcal{I}, C^{1,1}(\bar{U})^d), & [t \mapsto DT_t] &\in C^1(\mathcal{I}, C^{0,1}(\bar{U})^{d \times d}), \\ [t \mapsto T_t^{-1}] &\in C(\mathcal{I}, C^1(\bar{U})^d), & [t \mapsto (DT_t)^{-\top}] &\in C^1(\mathcal{I}, C(\bar{U})^{d \times d}), \\ [t \mapsto I_t] &\in C^1(\mathcal{I}, C^{0,1}(\bar{U})), & \frac{d}{dt}(DT_t)^{\pm 1}|_{t=0} &= \lim_{t \rightarrow 0} \frac{(DT_t)^{\pm 1} - id}{t} = \pm D\boldsymbol{\theta}, \\ [t \mapsto I_t] &\in C^1(\mathcal{I}, C(\bar{\Omega})), & \frac{d}{dt}I_t|_{t=0} &= \lim_{t \rightarrow 0} \frac{I_t - 1}{t} = \lim_{t \rightarrow 0} \frac{\mathfrak{d}_t}{t} = \operatorname{div} \boldsymbol{\theta}, \\ [t \mapsto A_t] &\in C(\mathcal{I}, C(\bar{U})^{d \times d}), & \frac{d}{dt}A_t|_{t=0} &= \lim_{t \rightarrow 0} \frac{A_t - id}{t} = \lim_{t \rightarrow 0} \frac{\mathfrak{a}_t}{t} = A, \\ [t \mapsto A_t] &\in C^1(\mathcal{I}, C(\bar{\Omega})^{d \times d}), & A &:= (\operatorname{div} \boldsymbol{\theta})id - D\boldsymbol{\theta} - (D\boldsymbol{\theta})^\top, \\ [t \mapsto B_t] &\in C^1(\mathcal{I}, C(\Sigma)), & \frac{d}{dt}B_t|_{t=0} &= \lim_{t \rightarrow 0} \frac{B_t - 1}{t} = \operatorname{div}_\Sigma \boldsymbol{\theta}, \end{aligned} \quad (22)$$

⁴Here, and throughout the paper, $C^{k,1}(\cdot)^d := C^{k,1}(\cdot; \mathbb{R}^d)$. Similarly, $C^{k,1}(\cdot)^{d \times d} := C^{k,1}(\cdot; \mathbb{R}^{d \times d})$.

⁵Here, *id* is also used to denote the identity matrix in d -dimension. If there is no confusion, this abuse of notation is used throughout the paper.

where $\operatorname{div}_\Sigma \boldsymbol{\theta} = \operatorname{div} \boldsymbol{\theta}|_\Sigma - (D\boldsymbol{\theta}\mathbf{n}) \cdot \mathbf{n}$ denotes the tangential divergence of the vector $\boldsymbol{\theta}$ on Σ . Based on the above properties of T_t , we note that there is a constant $C > 0$ such that $|DT_t^{-1}(x)|_\infty < C < \infty$, for all $x \in \overline{U}$; see, e.g., [19, eq. (2.9)].

Additionally to the above properties, we assume that for $t \in \mathcal{I}$, we have

$$0 < \Lambda_1 \leq I_t \leq \Lambda_2 \quad \text{and} \quad 0 < \Lambda_3 |\xi|^2 \leq A_t \xi \cdot \xi \leq \Lambda_4 |\xi|^2, \quad (23)$$

for all $\xi \in \mathbb{R}^d$, for some constants $\Lambda_1, \Lambda_2, \Lambda_3$, and Λ_4 ($\Lambda_1 < \Lambda_2, \Lambda_3 < \Lambda_4$).

Furthermore, as we intend to refer a function $\varphi_t : \Omega_t \rightarrow \mathbb{C}^d$ to the reference domain Ω using T_t , we make use of the notation $\varphi^t := \varphi_t \circ T_t : \Omega \rightarrow \mathbb{C}^d$.

To close the section, we state some auxiliary results that will be helpful with our investigation. Let $\boldsymbol{\theta} \in \Theta^k$, $k \geq 1$, $\overline{\Omega}_t \subset\subset U$ for all sufficiently small $t \geq 0$. Then, for a vector-valued function $\boldsymbol{\varphi} = (\varphi_1, \varphi_2, \dots, \varphi_d)^\top \in H^2(U)^d$, we have

$$\lim_{t \rightarrow 0} \|\boldsymbol{\varphi} \circ T_t - \boldsymbol{\varphi}\|_{H^1(U)^d} = \lim_{t \rightarrow 0} \left(\sum_{i=1}^d \|\varphi_i \circ T_t - \varphi_i\|_{H^1(U)} \right)^{1/2} = 0. \quad (24)$$

Moreover, the maps $t \mapsto \boldsymbol{\varphi} \circ T_t$ from $\mathcal{I} \rightarrow H^1(\Omega)^d$ and $t \mapsto I_t \boldsymbol{\varphi} \circ T_t$ from \mathcal{I} to $L^2(\Omega)^d$ are differentiable at $t = 0$, and we have

$$\lim_{t \rightarrow 0} \frac{1}{t} (\boldsymbol{\varphi} \circ T_t - \boldsymbol{\varphi}) = D\boldsymbol{\varphi}\boldsymbol{\theta} \quad \text{and} \quad \lim_{t \rightarrow 0} \frac{1}{t} (I_t \boldsymbol{\varphi} \circ T_t - \boldsymbol{\varphi}) = \nabla \cdot (\boldsymbol{\varphi} \otimes \boldsymbol{\theta}), \quad (25)$$

where $\nabla \cdot (\boldsymbol{\varphi} \otimes \boldsymbol{\theta}) = (\operatorname{div}(\varphi_1 \boldsymbol{\theta}), \operatorname{div}(\varphi_2 \boldsymbol{\theta}), \dots, \operatorname{div}(\varphi_d \boldsymbol{\theta}))^\top$, and \otimes denotes the outer product; i.e., $\boldsymbol{\varphi} \otimes \boldsymbol{\theta} = \boldsymbol{\varphi} \boldsymbol{\theta}^\top = (\varphi_j \theta_k)_{jk}$ where $j, k = 1, \dots, d$.

The proofs of the above results are omitted since they are standard and follow similar arguments used for the case of scalar functions, see, e.g., [21, 37].

3.2 Some identities from trangential shape calculus

In the next section, we will observe that the shape gradient of J incorporates elements from tangential shape calculus (see, e.g., [37, Chap. 9, Sec. 5] or [38, Sec. 5.4.3, pp. 216–221]). To aid our investigation, we gather here some expressions that will be referenced in our subsequent discussions.

Definition 3.1 ([37, eq. (5.17) – (5.19), p. 497]). *Let Ω be a domain in \mathbb{R}^d with $\mathcal{C}^{1,1}$ smooth boundary $\Gamma := \partial\Omega$. Then, for any given functions $\psi \in \mathcal{C}^1(\Gamma)$ and $\boldsymbol{\varphi} \in \mathcal{C}^1(\Gamma; \mathbb{R}^d)$, with \mathcal{C}^1 extensions $\tilde{\psi}$ and $\tilde{\boldsymbol{\varphi}}$ into a neighborhood of Γ , the following expressions are well-defined:*

- $\nabla_\Gamma \psi := \nabla \tilde{\psi}|_\Gamma - \partial_\mathbf{n} \tilde{\psi} \mathbf{n} \in \mathcal{C}^0(\Gamma)^d$;
- $D_\Gamma \boldsymbol{\varphi} = D\tilde{\boldsymbol{\varphi}}|_\Gamma - D\tilde{\boldsymbol{\varphi}} \mathbf{n} \otimes \mathbf{n} \in \mathcal{C}^0(\Gamma)^{d \times d}$;
- $\nabla_\Gamma \cdot \boldsymbol{\varphi} := \operatorname{div}_\Gamma \boldsymbol{\varphi} = \operatorname{div} \tilde{\boldsymbol{\varphi}}|_\Gamma - D\tilde{\boldsymbol{\varphi}} \mathbf{n} \cdot \mathbf{n} \in \mathcal{C}^0(\Gamma)$.

With the above definitions, the formulas in the next lemma can easily be verified.

Lemma 3.2 ([37, eq. (5.26) – (5.27), p. 498]). *Consider a $\mathcal{C}^{1,1}$ domain Ω with boundary $\Gamma := \partial\Omega$ and let κ be the mean curvature of Γ . Then, for $\psi \in H^1(\Gamma)$ and $\boldsymbol{\varphi} \in \mathcal{C}^1(\Gamma; \mathbb{R}^d)$ the following identities hold:*

- *Tangential divergence formula:* $\operatorname{div}_\Gamma(\psi \boldsymbol{\varphi}) = \nabla_\Gamma \psi \cdot \boldsymbol{\varphi} + \psi \operatorname{div}_\Gamma \boldsymbol{\varphi}$;
- *Tangential Stokes' formula:* $\int_\Gamma \operatorname{div}_\Gamma \boldsymbol{\varphi} d\sigma = \int_\Gamma \kappa \boldsymbol{\varphi} \cdot \mathbf{n} d\sigma$;

- *Tangential Green's formula:* $\int_{\Gamma} (\nabla_{\Gamma}\psi \cdot \varphi + \psi \operatorname{div}_{\Gamma} \varphi) d\sigma = \int_{\Gamma} \kappa\psi \varphi \cdot \mathbf{n} d\sigma.$

Another version of the tangential Green's formula (whose proof can be found, for instance, in [39]) is given in the next lemma (see, e.g., [41], eq. (2.144), p. 92]).

Lemma 3.3. *Let U be a bounded domain of class $C^{1,1}$ and $\Omega \subset U$ with boundary $\Gamma := \partial\Omega$. Consider the functions $\varphi \in C^{1,1}(\overline{U}; \mathbb{R}^d)$ and $\psi \in W^{2,1}(U)$. Then,*

$$\int_{\Sigma} (\nabla\psi \cdot \varphi + \psi \operatorname{div}_{\Sigma} \varphi) d\sigma = \int_{\Sigma} (\partial_{\mathbf{n}}\psi + \psi \operatorname{div}_{\Sigma} \mathbf{n}) \varphi \cdot \mathbf{n} d\sigma.$$

Let $\mathcal{M}_{d \times d}$ be the space of matrices of size $d \times d$. In what follows, we write the tangential differential operators over Γ with the subscript \cdot_{Γ} . For $\varphi \in \mathbf{W}^{1,1}(\partial\Omega)$ and $\mathbf{M} \in W^{1,1}(\partial\Omega; \mathcal{M}_{d \times d})$, the following operators are defined on $\Gamma := \partial\Omega$:

- $\nabla_{\Gamma}\varphi := \nabla\varphi - (\nabla\varphi\mathbf{n}) \otimes \mathbf{n}$;⁶
- $\operatorname{div}_{\Gamma} \mathbf{M} := \operatorname{div} \mathbf{M} - (\nabla \mathbf{M} \mathbf{n}) \mathbf{n}$ (see, e.g., [37], eq. (5.11), p. 496);
- $\Delta_{\Gamma}\varphi := \operatorname{div}_{\Gamma}(\nabla_{\Gamma}\varphi)$ (see, e.g., [37], eq. (5.12), p. 496]).

In the next section, we will exhibit the computation of the shape gradient of J . Throughout the paper, we shall refer to the proposed shape optimization approach (15) simply as CCBM.

3.3 Computation of the shape gradient

In this subsection we compute the shape derivative of J rigorously via rearrangement method in the spirit of [21, 35] given that $\mathbf{f} \in H^1(U)^d$, Ω is of class $C^{1,1}$, and $\boldsymbol{\theta} \in \Theta^1$. Before we proceed, we will discuss below the advantages of the method we use to calculate the shape derivative of the cost functional J and comment on other studies that deal with the computation of shape derivatives for the Stokes equations.

- The rearrangement method, introduced and developed in [21, 35], allows the computation of the shape derivatives of cost functionals without involving the shape derivative of the state variables where high regularity of the domain is required. In fact, one only require the state variables to be Lipschitz continuous with respect to geometry perturbations. Consequently, a mild $C^{1,1}$ regularity assumption on the domain is sufficient. In [1], the authors required Ω to be of class $C^{2,1}$ in order to establish the shape derivative of the cost function J_{KV} .
- In [4], Kasumba calculated the shape gradients of J_D , J_N , and J_{KV} using the *strong form* of the shape derivative of the states \mathbf{u}'_D , \mathbf{u}'_N , p'_D , and p'_N . This necessitates higher regularity assumptions on the state variables, implying that Ω needs to be $C^{2,1}$ smooth. However, in our approach, we only require the Hölder continuity of the states \mathbf{u}^t, p^t . Accordingly, a $C^{1,1}$ smoothness assumption on Ω is enough.
- The shape derivative for the Stokes equations with a Dirichlet boundary condition (on the free boundary) are well-known for a long time since the pioneering work of Simon [42] (see also the work of Caubet et al. [43] for a recent related work, but for an inverse problem). The computations of the shape gradients carried out in [42, 43] require the strong form of the shape derivative of the states. The existence of the strong solutions to the shape derivative equations requires a $C^{2,1}$ regularity assumption on the boundary of the domain, and the sufficient smoothness of the data.
- We emphasize that even in the class of $C^{2,1}$ domains, the shape derivative of the states may *not* always exist. This occurs when the data lacks the required regularity for the shape derivative of the state solution to be in the H^1 space. Consequently, the chain rule cannot be used to derive the

⁶Given a vector $\varphi := (\varphi_1, \dots, \varphi_d)^T$, we note the relation $(D_{\Gamma}\varphi)^T = (\nabla_{\Gamma}\varphi_1, \dots, \nabla_{\Gamma}\varphi_d) = \nabla_{\Gamma}\varphi$, where $\nabla_{\Gamma}\varphi_i$, $i = 1, \dots, d$, is a column vector.

shape derivative of the cost due to this lack of shape differentiability. However, the rearrangement technique remains applicable in this case, which is one of the main features of this approach. For a more in-depth discussion, we refer readers to [35, Sec. 3.5].

- We also mention that in [35], the authors derived the shape derivative of the stationary Navier-Stokes equation, but again with pure Dirichlet boundary condition.

In summary, the main advantage of the method we will employ to prove the main result lies in its independence from the existence of the weak solution of the shape derivative of the states. Such a key feature is especially advantageous when dealing with less regular data and domains. As a result, the proposed demonstration of shape sensitivity analysis in this study serves as a reference for computing shape derivatives of cost functionals in free surface problems with less smooth data. This topic will be considered in our future study.

Given the compatibility condition

$$\int_{\Sigma} \mathbf{v} \cdot \mathbf{n} d\sigma = - \int_{\Omega} p_i dx.$$

for the *adjoint variable* \mathbf{v} (which we assume without further notice), our main result is given in the following theorem.

Theorem 3.4. *Let $\mathbf{f} \in H^1(U)^d$, Ω be of class $C^{1,1}$, and $\boldsymbol{\theta} \in \Theta^1$. Then, J is shape differentiable and its shape derivative is given by $dJ(\Omega)[\boldsymbol{\theta}] = \int_{\Sigma} g_{\Sigma} \mathbf{n} \cdot \boldsymbol{\theta} d\sigma$ where⁷*

$$\begin{aligned} g_{\Sigma} \theta_n &= \Im \{ \mathbf{B}[\theta_n] \cdot \bar{\mathbf{v}} \} + \frac{1}{2} (|\mathbf{u}_i|^2 + |p_i|^2) \theta_n, \\ \mathbf{B}[\theta_n] &= \mathbf{f} \theta_n - \nabla_{\Sigma}(p \theta_n) + \operatorname{div}_{\Sigma} [\alpha(\nabla_{\Sigma} \mathbf{u}) \theta_n] + i \operatorname{div}_{\Sigma}(\theta_n \mathbf{u}) \mathbf{n} \\ &\quad + i u_n \nabla_{\Sigma} \theta_n + \kappa [p \mathbf{n} - i u_n \mathbf{n}] \theta_n, \end{aligned} \tag{26}$$

and κ denotes the mean curvature of the free boundary Σ , $\mathbf{u} = \mathbf{u}_r + i \mathbf{u}_i$ and $p = p_r + i p_i$ is the unique pair of solution to (7), and the pair of adjoints (\mathbf{v}, q) , where $\mathbf{v} = \mathbf{v}_r + i \mathbf{v}_i$ and $q = q_r + i q_i$, uniquely solves the adjoint system

$$\begin{cases} -\alpha \Delta \mathbf{v} + \nabla q = \mathbf{u}_i & \text{in } \Omega, \\ -\nabla \cdot \mathbf{v} = p_i & \text{in } \Omega, \\ \mathbf{v} = \mathbf{0} & \text{on } \Gamma, \\ -q \mathbf{n} + \alpha \partial_{\mathbf{n}} \mathbf{v} - i(\mathbf{v} \cdot \mathbf{n}) \mathbf{n} = \mathbf{0} & \text{on } \Sigma. \end{cases} \tag{27}$$

The proof of the proposition relies on several lemmas that we first prove below. To start, we present the weak formulation of (27). Let us then introduce the following forms:

$$\begin{cases} \tilde{a}(\boldsymbol{\varphi}, \boldsymbol{\psi}) = \int_{\Omega} \alpha \nabla \boldsymbol{\varphi} : \nabla \bar{\boldsymbol{\psi}} dx - i \int_{\Sigma} (\boldsymbol{\varphi} \cdot \mathbf{n})(\bar{\boldsymbol{\psi}} \cdot \mathbf{n}) d\sigma, & \forall \boldsymbol{\varphi}, \boldsymbol{\psi} \in V_{\Gamma}, \\ \tilde{F}(\boldsymbol{\psi}) = \int_{\Omega} \mathbf{u}_i \cdot \bar{\boldsymbol{\psi}} dx, & \forall \boldsymbol{\psi} \in V_{\Gamma}. \end{cases} \tag{28}$$

Hence, the weak formulation of (27) can be stated as follows:

$$\text{find } (\mathbf{v}, q) \in V_{\Gamma} \times Q \text{ such that } \begin{cases} \tilde{a}(\mathbf{v}, \boldsymbol{\psi}) + b(\boldsymbol{\psi}, q) = \tilde{F}(\boldsymbol{\psi}), & \forall \boldsymbol{\psi} \in V_{\Gamma}, \\ b(\mathbf{v}, \mu) = (\mu, p_i), & \forall \mu \in Q. \end{cases} \tag{29}$$

Remark 3.5. *Given the compatibility condition $\langle \mathbf{v}, \mathbf{n} \rangle_{\Sigma} = -(p_i, 1)_{\Omega}$, the well-posedness of the above problem (cf. [10, Chap. 4, exercise 6.2]) can be verified using similar arguments issued in subsection*

⁷Here ∇_{Σ} is the tangential gradient operator on Σ . The intrinsic definition of the operator is given, for instance, in [37, Chap. 5., Sec. 5.1, p. 492].

2.2 for the state problem (7) (provided, of course, (11) admits a unique solution $(\mathbf{u}, p) \in V_\Gamma \times Q$). Particularly, one can show that an inf-sup condition (cf. (13)) holds for the above variational problem.

Remark 3.6. For $\mathbf{f} \in H^k(\Omega)^d$ and Ω of class $C^{k+1,1}$, k a non-negative integer, it can be shown that the weak solution $(\mathbf{u}, p) \in X \times Q$ to the variational problem (11) is also $\mathbf{H}^{k+2}(\Omega)^d \times \mathbf{H}^{k+1}(\Omega)$. In particular, $\mathbf{u}_i \in H^{k+2}(\Omega)^d$ and $p_i \in H^{k+1}(\Omega)$. Consequently, we find that the weak solution (\mathbf{v}, q) of problem (29) is not only in $V_\Gamma \times Q$, but is also an element of $\mathbf{H}^{k+2}(\Omega)^d \times \mathbf{H}^{k+1}(\Omega)$.

At this juncture, we introduce the following sesquilinear forms $a^t, \tilde{a}^t \in V_\Gamma \times V_\Gamma \rightarrow \mathbb{R}$ and linear forms, $b^t : V_\Gamma \times Q \rightarrow \mathbb{R}$ and $F^t, \tilde{F}^t : V_\Gamma \rightarrow \mathbb{R}$ (which are essentially the transformed versions of the forms listed in (10) and (28)) defined as follows:

$$\begin{cases} a^t(\varphi, \psi) = \int_{\Omega} \alpha A_t \nabla \varphi : \nabla \bar{\psi} dx + i \int_{\Sigma} \frac{B_t}{|M_t \mathbf{n}|^2} (M_t^\top \varphi \cdot \mathbf{n}) (M_t^\top \bar{\psi} \cdot \mathbf{n}) d\sigma, \\ b^t(\varphi, \lambda) = - \int_{\Omega} I_t \bar{\lambda} (M_t^\top : \nabla \varphi) dx, \\ F^t(\varphi) = \int_{\Omega} I_t \mathbf{f}^t \cdot \bar{\varphi} dx, \quad \text{where } \mathbf{f}^t = \mathbf{f}_t \circ T_t \in H^1(U)^d, \\ \tilde{a}^t(\varphi, \psi) = \int_{\Omega} \alpha A_t \nabla \varphi : \nabla \bar{\psi} dx - i \int_{\Sigma} \frac{B_t}{|M_t \mathbf{n}|^2} (M_t^\top \varphi \cdot \mathbf{n}) (M_t^\top \bar{\psi} \cdot \mathbf{n}) d\sigma, \\ \tilde{F}^t(\varphi) = \int_{\Omega} I_t \mathbf{u}_i \cdot \bar{\varphi} dx, \quad \text{where } \mathbf{u}_i \in V_\Gamma. \end{cases} \quad (30)$$

In the definition of \tilde{F}^t given above, of course, \mathbf{u}_i is the imaginary part of the velocity solution $\mathbf{u} \in V_\Gamma$ to the state system (7).

Now, the first of the several lemmas that we need is given as follows.

Lemma 3.7. For $t \in \mathcal{I}$, the sesquilinear forms a^t and \tilde{a}^t defined on $X \times X$ are bounded and coercive on $X \times X$. In addition, the linear forms $F^t(\varphi)$ and $\tilde{F}^t(\varphi)$ are also bounded. Moreover, the bilinear form b^t satisfies the condition that there is a constant $\beta_1 > 0$ such that

$$\inf_{\substack{\lambda \in Q \\ \lambda \neq 0}} \sup_{\substack{\varphi \in V_\Gamma \\ \varphi \neq 0}} \frac{b^t(\varphi, \lambda)}{\|\varphi\|_X \|\lambda\|_Q} \geq \beta_1. \quad (31)$$

Proof. The proof is similar to the arguments used in the discussion issued in subsection 2.2. This time, however, one has to take into account the properties of A_t and B_t in (22) and the bounds given in (23) to prove the given results. \square

The next lemma is concerned about the well-posedness of the transported perturbed version of (11). Concerning the result, we emphasize that the compatibility condition $\int_{\Gamma_t} \mathbf{u}_t \cdot \mathbf{n}_t d\sigma_t = 0$ we assumed hereinafter is equivalent to

$$\int_{\Sigma} B_t \mathbf{u}^t \cdot \frac{M_t \mathbf{n}}{|M_t \mathbf{n}|} d\sigma = 0,$$

which follows from the transformation $(\mathbf{u} \cdot \mathbf{n})_t = (\mathbf{u}_t \cdot \mathbf{n}_t) \circ T_t = \mathbf{u}^t \cdot \mathbf{n}^t = \mathbf{u}^t \cdot \frac{M_t \mathbf{n}}{|M_t \mathbf{n}|}$ [37, Thm. 4.4, p. 488].

Lemma 3.8. The pair $(\mathbf{u}^t, p^t) := (\mathbf{u}_r^t + i\mathbf{u}_i^t, p_r^t + ip_i^t)$ uniquely solves in $V_\Gamma \times Q$ the variational equations

$$a^t(\mathbf{u}^t, \varphi) + b^t(\varphi, p^t) = F^t(\varphi), \quad \forall \varphi \in V_\Gamma, \quad \text{and} \quad b^t(\mathbf{u}^t, \lambda) = 0, \quad \forall \lambda \in Q. \quad (32)$$

Proof. The functions $\mathbf{u}_t \in \mathbf{H}^1(\Omega_t)^d$ and $p_t \in \mathbf{L}^2(\Omega_t)$ solve the variational equation

$$\left\{ \begin{array}{l} \int_{\Omega_t} \alpha \nabla \mathbf{u}_t : \nabla \bar{\varphi} dx_t + i \int_{\Sigma_t} (\mathbf{u}_t \cdot \mathbf{n}_t) (\bar{\varphi} \cdot \mathbf{n}_t) d\sigma_t - \int_{\Omega_t} p_t (\nabla \cdot \bar{\varphi}) dx_t \\ \quad = \int_{\Omega_t} \mathbf{f}_t \cdot \bar{\varphi} dx_t, \quad \forall \varphi \in \mathbf{H}_{\Gamma,0}^1(\Omega_t)^d, \\ - \int_{\Omega_t} \bar{\lambda} (\nabla \cdot \mathbf{u}_t) dx_t = 0, \quad \forall \lambda \in \mathbf{L}^2(\Omega_t). \end{array} \right.$$

By change of variables (see [37, pp. 482–484]), together with the identities

$$\begin{aligned} \mathbf{u}^t &= \mathbf{u}_t \circ T_t, \quad \text{where } \mathbf{u}_t = \mathbf{u}_{rt} + i \mathbf{u}_{it}, \\ (\nabla \varphi_t) \circ T_t &= M_t \nabla \varphi^t, \quad (\nabla \cdot \varphi_t) \circ T_t = M_t^\top : \nabla \varphi^t, \quad \text{where } \varphi_t \in \mathbf{H}^1(\Omega_t)^d, \quad \varphi^t \in \mathbf{H}^1(\Omega)^d, \end{aligned}$$

and the transformation $(\mathbf{u} \cdot \mathbf{n})_t = \mathbf{u}^t \cdot \frac{M_t \mathbf{n}}{|M_t \mathbf{n}|}$ [37, Thm. 4.4, p. 488], we get

$$\left\{ \begin{array}{l} \int_{\Omega} \alpha A_t \nabla \mathbf{u}^t : \nabla \bar{\varphi} dx + i \int_{\Sigma} \frac{B_t}{|M_t \mathbf{n}|^2} (\mathbf{u}^t \cdot M_t \mathbf{n}) (\bar{\varphi} \cdot M_t \mathbf{n}) d\sigma - \int_{\Omega} I_t p^t (M_t^\top : \nabla \bar{\varphi}) dx \\ \quad = \int_{\Omega} I_t \mathbf{f}^t \cdot \bar{\varphi} dx, \quad \forall \varphi \in V_{\Gamma}, \\ - \int_{\Omega} I_t \bar{\lambda} (M_t^\top : \nabla \mathbf{u}^t) dx = 0, \quad \forall \lambda \in Q. \end{array} \right.$$

In light of the notations listed in (30), we recover (32).

The rest of the proof is similar to the arguments used in subsection 2.2 combined with the properties of A_t and B_t given in (22) and in (23), and together with Lemma 3.7. Concerning uniqueness of solution, the proof is also standard, so we omit it. \square

Lemma 3.9. *For $t \in \mathcal{I}$, the solutions (\mathbf{u}^t, p^t) of (32) are uniformly bounded in $X \times Q$. That is, for $t \in \mathcal{I}$, there is a constant $c > 0$ independent of t such that*

$$\|\mathbf{u}^t\|_X, \|p^t\|_Q \leq c \|\mathbf{f}\|_{1,U}.$$

Proof. For the (uniform) boundedness of \mathbf{u}^t in X for $t \in \mathcal{I}$, the result is established by taking $\varphi = \mathbf{u}^t \in V_{\Gamma}$ in (32), and then applying the properties of A_t and B_t given in (22) and (23), and the coercivity of a^t on $X \times X$ (Lemma 3.7). Indeed, taking $(\varphi, \lambda) = (\mathbf{u}^t, p^t) \in V_{\Gamma} \times Q$ in (32), we get $a^t(\mathbf{u}^t, \mathbf{u}^t) + b^t(\mathbf{u}^t, p^t) = F^t(\mathbf{u}^t)$, or equivalently, $a^t(\mathbf{u}^t, \mathbf{u}^t) = F^t(\mathbf{u}^t)$. This yields the following inequality

$$c \|\mathbf{u}^t\|_X^2 \leq \Re\{a^t(\mathbf{u}^t, \mathbf{u}^t)\} \leq |a^t(\mathbf{u}^t, \mathbf{u}^t)| \leq \left| \int_{\Omega} I_t \mathbf{f}^t \cdot \bar{\mathbf{u}}^t dx \right| \leq \|I_t \mathbf{f}^t\|_{0,\Omega} \|\bar{\mathbf{u}}^t\|_{0,\Omega},$$

where the constant $c > 0$ appearing on the leftmost side of the inequality is the coercivity constant of a^t whose existence is ensured by Lemma 3.7. To further get an estimate for the rightmost side of the above inequality, we note that

$$\|I_t \mathbf{f}^t\|_{0,\Omega}^2 = \int_{\Omega_t} I_t \circ T_t^{-1} \mathbf{f}^2 dx_t \leq \Lambda_2 \|\mathbf{f}\|_{0,U}^2, \tag{33}$$

where in the inequality we used the bound for I_t given in (23). Hence, we have

$$\|\mathbf{u}^t\|_X^2 \leq c^{-1} \sqrt{\Lambda_2} \|\mathbf{f}\|_{0,U} \|\bar{\mathbf{u}}^t\|_{0,\Omega} \leq c^{-1} \sqrt{\Lambda_2} \|\mathbf{f}\|_{0,U} \|\mathbf{u}^t\|_X.$$

This gives us a priori estimate

$$\|\mathbf{u}^t\|_X \leq c\|\mathbf{f}\|_{0,U}, \quad (34)$$

for some constant $c \in \mathbb{R}^+$, which shows that \mathbf{u}^t is bounded in X for $t \in \mathcal{I}$.

For the boundedness of p^t in Q for $t \in \mathcal{I}$, we use (31), which is equivalent to

$$\sup_{\substack{\varphi \in V_\Gamma \\ \varphi \neq 0}} \frac{b^t(\varphi, \lambda)}{\|\varphi\|_X} \geq \beta_1 \|\lambda\|_Q, \quad \forall \lambda \in Q.$$

We let $\lambda = p^t \in Q$. Then, from (3.8), the bounds in (23), and equation (33), we have the following calculation

$$\begin{aligned} \beta_1 \|p^t\|_Q &\leq \sup_{\substack{\varphi \in V_\Gamma \\ \varphi \neq 0}} \frac{b^t(\varphi, p^t)}{\|\varphi\|_X} = \sup_{\substack{\varphi \in V_\Gamma \\ \varphi \neq 0}} \|\varphi\|_X^{-1} \left\{ F^t(\varphi) - a^t(\mathbf{u}^t, \varphi) \right\} \\ &\leq \sup_{\substack{\varphi \in V_\Gamma \\ \varphi \neq 0}} \|\varphi\|_X^{-1} \left\{ \int_\Omega I_t \mathbf{f}^t \cdot \bar{\varphi} dx - \int_\Omega \alpha A_t \nabla \mathbf{u}^t : \nabla \bar{\varphi} dx \right. \\ &\quad \left. - \int_\Sigma \frac{I_t}{|M_t \mathbf{n}|} (\mathbf{u}^t \cdot M_t \mathbf{n}) (\bar{\varphi} \cdot M_t \mathbf{n}) d\sigma \right\} \\ &\leq c \sup_{\substack{\varphi \in V_\Gamma \\ \varphi \neq 0}} \|\varphi\|_X^{-1} \left\{ \|\mathbf{f}\|_{0,U} \|\bar{\varphi}\|_{0,\Omega} + \|\nabla \mathbf{u}^t\|_{0,\Omega} \|\nabla \bar{\varphi}\|_{0,\Omega} + \|\mathbf{u}^t\|_{0,\Sigma} \|\bar{\varphi}\|_{0,\Sigma} \right\} \\ &\leq c (\|\mathbf{f}\|_{0,U} + \|\mathbf{u}^t\|_X). \end{aligned}$$

Therefore, using the estimate for $\|\mathbf{u}^t\|_X$ given in (34), we arrive at

$$\|p^t\|_Q \leq c\|\mathbf{f}\|_{0,U},$$

for some $c \in \mathbb{R}^+$. The desired results then follow from the fact that $\mathbf{f} \in H^1(U)^d$. \square

To complete our preparations, we next prove the following lemma concerning the Hölder continuity of the state variables \mathbf{u}^t and p^t with respect to t .

Lemma 3.10. *Let $(\mathbf{u}, p) \in V_\Gamma \times Q$ be the solution of (11). Then,*

$$\lim_{t \rightarrow 0^+} \frac{1}{\sqrt{t}} \left(\|\mathbf{u}^t - \mathbf{u}\|_X + \|p^t - p\|_Q \right) = 0,$$

where $(\mathbf{u}^t, p^t) \in V_\Gamma \times Q$ solves (32), for $t \in \mathcal{I}$.

Proof. Let us first note that the assumption that $\boldsymbol{\theta} \in \Theta^1$ implies that⁸

$$\|\boldsymbol{\theta}\|_{C^{1,1}(\bar{U})^d} = |\boldsymbol{\theta}|_\infty + |D\boldsymbol{\theta}|_\infty + \sup_{x \neq y} \frac{|D\boldsymbol{\theta}(x) - D\boldsymbol{\theta}(y)|_\infty}{|x - y|} < \infty$$

which implies further that $|\boldsymbol{\theta}|_\infty$ and $|D\boldsymbol{\theta}|_\infty$ are both finite.

Hereafter, we proceed in two steps:

⁸Here and throughout the paper, we use $|\cdot|_\infty$ to denote the $L^\infty(\bar{U})$ norm for simplicity.

Step 1. We first show that $\lim_{t \rightarrow 0} \mathbf{u}^t = \mathbf{u}$ in X and $\lim_{t \rightarrow 0} p^t = p$ in Q .

Step 2. Then, we validate our claim that $\lim_{t \rightarrow 0^+} \frac{1}{\sqrt{t}} \left(\|\mathbf{u}^t - \mathbf{u}\|_X + \|p^t - p\|_Q \right) = 0$.

Step 1. We consider the difference between the variational equations (32) and (11) and define $\mathbf{y}^t := \mathbf{u}^t - \mathbf{u}$ and $r^t := p^t - p$. By making $\varepsilon > 0$ smaller if necessary, it can be shown that the following expansions hold for sufficiently small $t \in \mathcal{I}$,

$$\begin{cases} I_t = 1 + t \operatorname{div} \boldsymbol{\theta} + t^2 \tilde{\rho}(t, \boldsymbol{\theta}), \quad \text{where } \tilde{\rho} \in \mathcal{C}(\mathbb{R}, \mathcal{C}^{0,1}(U)), \\ M_t^\top = (DT_t)^{-1} = (id + tD\boldsymbol{\theta})^{-1} = \sum_{j=0}^{\infty} (-1)^j t^j (D\boldsymbol{\theta})^j, \quad \text{where } 0 \leq |t| \leq \varepsilon < |\lambda_{max}|^{-1}, \end{cases}$$

where λ_{max} is the maximum singular value of $D\boldsymbol{\theta}$. Below we use the above expansions and specifically write M_t^\top as follows

$$M_t^\top = (DT_t)^{-1} = (id + tD\boldsymbol{\theta})^{-1} = id - tD\boldsymbol{\theta} + O(t^2)id. \quad (35)$$

Henceforth, we denote⁹

$$\rho(t) := t^2 \tilde{\rho}(t, \boldsymbol{\theta}), \quad R(t) := O(t^2)id, \quad \rho_1(t) := t\tilde{\rho}(t, \boldsymbol{\theta}), \quad \text{and} \quad R_1(t) := O(t)id. \quad (36)$$

Now, let us consider the variational equation

$$b^t(\mathbf{u}^t, \lambda) - b(\mathbf{u}, \lambda) = - \int_{\Omega} I_t \bar{\lambda} (M_t^\top : \nabla \mathbf{u}^t) dx - \left(- \int_{\Omega} \bar{\lambda} \nabla \cdot \mathbf{u} dx \right) = 0, \quad \forall \lambda \in Q.$$

Applying (35) to the above equation, we get

$$\begin{aligned} b^t(\mathbf{u}^t, \lambda) - b(\mathbf{u}, \lambda) &= - \int_{\Omega} \bar{\lambda} \nabla \cdot (\mathbf{u}^t - \mathbf{u}) dx - \int_{\Omega} (t \nabla \cdot \boldsymbol{\theta} + \rho(t)) \bar{\lambda} (M_t^\top : \nabla \mathbf{u}^t) dx \\ &\quad - \int_{\Omega} \bar{\lambda} [(-tD\boldsymbol{\theta} + R(t)) : \nabla \mathbf{u}^t] dx \\ &= 0, \quad \forall \lambda \in Q. \end{aligned} \quad (37)$$

Taking $\lambda = r^t = p^t - p \in Q$, we get

$$\begin{aligned} \int_{\Omega} r^t \nabla \cdot \bar{\mathbf{y}}^t dx &= - \int_{\Omega} (t \nabla \cdot \boldsymbol{\theta} + \rho(t)) r^t (M_t^\top : \nabla \bar{\mathbf{u}}^t) dx \\ &\quad + \int_{\Omega} r^t [(-tD\boldsymbol{\theta} + R(t)) : \nabla \bar{\mathbf{u}}^t] dx. \end{aligned} \quad (38)$$

On the other hand, we also have the equation $a^t(\mathbf{u}^t, \boldsymbol{\varphi}) + b^t(\boldsymbol{\varphi}, p^t) - a(\mathbf{u}, \boldsymbol{\varphi}) - b(\boldsymbol{\varphi}, p) = F^t(\boldsymbol{\varphi}) - F(\boldsymbol{\varphi})$, for all $\boldsymbol{\varphi} \in V_\Gamma$, which is equivalent to

$$a(\mathbf{u}^t - \mathbf{u}, \boldsymbol{\varphi}) + b(\boldsymbol{\varphi}, p^t - p) = \Phi^t(\boldsymbol{\varphi}), \quad \forall \boldsymbol{\varphi} \in V_\Gamma, \quad (39)$$

⁹On certain occasions, the remainder $\rho(t)$ and $R(t)$ may have distinct structures in their exact expressions. Nevertheless, these expressions are always of order $O(t^2)$. The same is true for $\rho_1(t)$ and $R_1(t)$. We abuse the use of these notations since the exact expressions are not actually of interest in our argumentations.

where, for $\varphi \in V_\Gamma$, $\Phi^t(\varphi)$ is given by

$$\begin{aligned}\Phi^t(\varphi) = & -\int_{\Omega} \alpha \mathfrak{a}_t \nabla \mathbf{u}^t : \nabla \bar{\varphi} dx - i \int_{\Sigma} \mathfrak{b}_t (M_t^\top \mathbf{u}^t \cdot \mathbf{n}) (M_t^\top \bar{\varphi} \cdot \mathbf{n}) d\sigma \\ & - i \int_{\Sigma} (\mathfrak{m}_t \mathbf{u}^t \cdot \mathbf{n}) (M_t^\top \bar{\varphi} \cdot \mathbf{n}) d\sigma - i \int_{\Sigma} (M_t^\top \mathbf{u}^t \cdot \mathbf{n}) (\mathfrak{m}_t \bar{\varphi} \cdot \mathbf{n}) d\sigma \\ & + \int_{\Omega} \mathfrak{d}_t p^t (M_t^\top : \nabla \bar{\varphi}) dx + \int_{\Omega} p^t (\mathfrak{m}_t : \nabla \bar{\varphi}) dx + \int_{\Omega} (I_t \mathbf{f}^t - \mathbf{f}) \cdot \bar{\varphi} dx,\end{aligned}\quad (40)$$

and $a : V_\Gamma \times V_\Gamma \rightarrow \mathbb{R}$ and $b : V_\Gamma \times Q \rightarrow \mathbb{R}$ are respectively the sesquilinear and linear forms given in (10), while \mathfrak{d}_t , \mathfrak{m}_t , \mathfrak{a}_t , and \mathfrak{b}_t are the notations specified in (21).

By choosing $\varphi = \mathbf{y}^t \in V_\Gamma$ in (39) and utilizing identity (38), it follows that

$$\begin{aligned}c_a \|\mathbf{y}^t\|_X^2 & \leq \Re\{a(\mathbf{y}^t, \mathbf{y}^t)\} \\ & \leq \left| \Phi^t(\mathbf{y}^t) + \int_{\Omega} r^t \nabla \cdot \bar{\mathbf{y}}^t dx \right| \\ & = \left| -\int_{\Omega} \alpha \mathfrak{a}_t \nabla \mathbf{u}^t : \nabla \bar{\mathbf{y}}^t dx - i \int_{\Sigma} \mathfrak{b}_t (M_t^\top \mathbf{u}^t \cdot \mathbf{n}) (M_t^\top \bar{\mathbf{y}}^t \cdot \mathbf{n}) d\sigma \right. \\ & \quad - i \int_{\Sigma} (\mathfrak{m}_t \mathbf{u}^t \cdot \mathbf{n}) (M_t^\top \bar{\mathbf{y}}^t \cdot \mathbf{n}) d\sigma - i \int_{\Sigma} (M_t^\top \mathbf{u}^t \cdot \mathbf{n}) (\mathfrak{m}_t \bar{\mathbf{y}}^t \cdot \mathbf{n}) d\sigma \\ & \quad + \int_{\Omega} \mathfrak{d}_t p^t (M_t^\top : \nabla \bar{\mathbf{y}}^t) dx + \int_{\Omega} p^t (\mathfrak{m}_t : \nabla \bar{\mathbf{y}}^t) dx + \int_{\Omega} (I_t \mathbf{f}^t - \mathbf{f}) \cdot \bar{\mathbf{y}}^t dx \\ & \quad \left. - t \int_{\Omega} (\nabla \cdot \boldsymbol{\theta} + \rho_1(t)) r^t (M_t^\top : \nabla \bar{\mathbf{u}}^t) dx - t \int_{\Omega} r^t [(-D\boldsymbol{\theta} + R_1(t)) : \nabla \bar{\mathbf{u}}^t] dx \right| \\ & \leq |\alpha| |\mathfrak{a}_t|_\infty \|\nabla \mathbf{u}^t\|_{0,\Omega} \|\nabla \bar{\mathbf{y}}^t\|_{0,\Omega} \\ & \quad + (|\mathfrak{b}_t|_\infty |M_t^\top|_\infty^2 + 2 |\mathfrak{m}_t|_\infty |M_t^\top|_\infty) \|\mathbf{u}^t\|_{0,\Sigma} \|\bar{\mathbf{y}}^t\|_{0,\Sigma} \\ & \quad + (|\mathfrak{d}_t|_\infty |M_t^\top|_\infty + |\mathfrak{m}_t|_\infty) \|p^t\|_{0,\Omega} \|\nabla \bar{\mathbf{y}}^t\|_{0,\Omega} + \|I_t \mathbf{f}^t - \mathbf{f}\|_{0,\Omega} \|\bar{\mathbf{y}}^t\|_{0,\Omega} \\ & \quad + t (|\nabla \cdot \boldsymbol{\theta}|_\infty + |\rho_1(t)|_\infty) |M_t^\top|_\infty \|r^t\|_{0,\Omega} \|\nabla \bar{\mathbf{u}}^t\|_{0,\Omega} \\ & \quad + t (|D\boldsymbol{\theta}|_\infty + |R_1(t)|_\infty) \|r^t\|_{0,\Omega} \|\nabla \bar{\mathbf{u}}^t\|_{0,\Omega}.\end{aligned}$$

Therefore, we have the estimate

$$c_a \|\mathbf{y}^t\|_X^2 \leq m_t \|\mathbf{y}^t\|_X + t \Xi_t \|r^t\|_Q, \quad (41)$$

where

$$\begin{cases} m_t := (|\alpha| |\mathfrak{a}_t|_\infty + |\mathfrak{b}_t|_\infty |M_t^\top|_\infty^2 + 2 |\mathfrak{m}_t|_\infty |M_t^\top|_\infty) \|\mathbf{u}^t\|_X \\ \quad + (|\mathfrak{d}_t|_\infty |M_t^\top|_\infty + |\mathfrak{m}_t|_\infty) \|p^t\|_Q + \|I_t \mathbf{f}^t - \mathbf{f}\|_{0,\Omega}, \\ \Xi_t := [(|\nabla \cdot \boldsymbol{\theta}|_\infty + |\rho_1(t)|_\infty) |M_t^\top|_\infty + |D\boldsymbol{\theta}|_\infty + |R_1(t)|_\infty] \|\mathbf{u}^t\|_X. \end{cases} \quad (42)$$

Refer to (20), (21), and (36) to recall the meaning of the notations used.

Now, let us take $\lambda = r^t = p^t - p \in Q$ in the inf-sup condition (A.65) and consider equation (39). We have

$$\begin{aligned} \beta_0 \|r^t\|_Q &\leq \sup_{\substack{\varphi \in V_\Gamma \\ \varphi \neq 0}} \|\varphi\|_X^{-1} \left\{ |\alpha| |\mathbf{a}_t|_\infty \|\nabla \mathbf{u}^t\|_{0,\Omega} \|\nabla \bar{\varphi}\|_{0,\Omega} \right. \\ &\quad + (|\mathbf{b}_t|_\infty |M_t^\top|_\infty + 2 |\mathbf{m}_t|_\infty |M_t^\top|_\infty) \|\mathbf{u}^t\|_{0,\Sigma} \|\bar{\varphi}\|_{0,\Sigma} \\ &\quad + (|\mathbf{d}_t|_\infty |M_t^\top|_\infty + |\mathbf{m}_t|_\infty) \|p^t\|_{0,\Omega} \|\nabla \bar{\varphi}\|_{0,\Omega} \\ &\quad + \|I_t \mathbf{f}^t - \mathbf{f}\|_{0,\Omega} \|\bar{\varphi}\|_{0,\Omega} \\ &\quad \left. + |\alpha| \|\nabla \mathbf{y}^t\|_{0,\Omega} \|\nabla \bar{\varphi}\|_{0,\Omega} + \|\mathbf{y}^t\|_{0,\Sigma} \|\bar{\varphi}\|_{0,\Sigma} \right\} \\ &\leq m_t + \max\{|\alpha|, 1\} \|\mathbf{y}^t\|_X. \end{aligned} \tag{43}$$

Therefore, we have the inequality

$$\|r^t\|_Q \leq \beta_0^{-1} (m_t + \max\{|\alpha|, 1\} \|\mathbf{y}^t\|_X). \tag{44}$$

Going back (41) and utilizing the above estimate, we get

$$\begin{aligned} c_a \|\mathbf{y}^t\|_X^2 &\leq m_t \|\mathbf{y}^t\|_X + t \Xi_t [\beta_0^{-1} (m_t + \max\{|\alpha|, 1\} \|\mathbf{y}^t\|_X)] \\ &= t \Xi_t \beta_0^{-1} m_t + (m_t + t \Xi_t \beta_0^{-1} \max\{|\alpha|, 1\}) \|\mathbf{y}^t\|_X. \end{aligned} \tag{45}$$

We apply the Peter-Paul inequality to $(m_t + t \Xi_t \beta_0^{-1} \max\{|\alpha|, 1\}) \|\mathbf{y}^t\|_X$ to obtain the estimate

$$(m_t + t \Xi_t \beta_0^{-1} \max\{|\alpha|, 1\}) \|\mathbf{y}^t\|_X \leq \frac{(m_t + t \Xi_t \beta_0^{-1} \max\{|\alpha|, 1\})^2}{2\varepsilon_1} + \frac{\varepsilon_1}{2} \|\mathbf{y}^t\|_X^2,$$

for some constant $\varepsilon_1 > 0$. We choose (and fixed) ε_1 such that $\bar{c} := c(c_a, \varepsilon_1) := 2c_a - \varepsilon_1 > 0$ so that, from our first estimate (45), we have

$$\|\mathbf{y}^t\|_X \leq \bar{c}^{-\frac{1}{2}} \left(t \Xi_t \beta_0^{-1} m_t + \frac{(m_t + t \Xi_t \beta_0^{-1} \max\{|\alpha|, 1\})^2}{2\varepsilon_1} \right)^{1/2}. \tag{46}$$

We note that, at $t = 0$, $I_t |M_t \mathbf{n}|^{-1} = (1)(|id\mathbf{n}|^{-1}) = 1$. Thus, in view of (42) together with Lemma 3.9, (24) and (25), we see that $m_t \rightarrow 0$ as $t \rightarrow 0$. Moreover, it is not hard to see that Ξ_t is (uniformly) bounded for all $t \in \mathcal{I}$ because of Lemma 3.9. Therefore, we conclude – by Lebesgue's dominated convergence theorem – that

$$\lim_{t \rightarrow 0} \|\mathbf{y}^t\|_X = 0 \iff \lim_{t \rightarrow 0} \mathbf{u}^t = \mathbf{u} \text{ in } X. \tag{47}$$

Similarly, based from the above discussion and from (43), we know that the terms on the right side of the said inequality vanish as $t \rightarrow 0$. Thus, we also have the limit

$$\lim_{t \rightarrow 0} \|r^t\|_Q = 0 \iff \lim_{t \rightarrow 0} p^t = p \text{ in } Q. \tag{48}$$

Step 2. Before we proceed to the last part of the proof, we note that, for sufficiently small $t > 0$, $\frac{1}{t} \mathbf{y}^t \in V_\Gamma$ and $\frac{1}{t} r^t \in Q$. In addition, we recall that the derivatives of I_t and M_t with respect to t exists in $L^\infty(\Omega)$ and $L^\infty(\Omega)^{d \times d}$, respectively.

Now, to finish the proof, we go back to the computations in the previous step (referring particularly to (46)), to obtain, after dividing by $t > 0$,

$$\frac{1}{t} \|\mathbf{y}^t\|_X^2 \leq \bar{c}^{-1} \left(\Xi_t \beta_0^{-1} m_t + \frac{1}{2\varepsilon_1} \left(\frac{1}{\sqrt{t}} m_t + \sqrt{t} \Xi_t \beta_0^{-1} \max\{|\alpha|, 1\} \right)^2 \right).$$

Observe that we have

$$\begin{aligned} \frac{1}{\sqrt{t}} m_t &= \sqrt{t} \left(|\alpha| \left| \frac{\mathbf{a}_t}{t} \right|_\infty + \left| \frac{\mathbf{b}_t}{t} \right|_\infty |M_t^\top|_\infty^2 + 2 \left| \frac{\mathbf{m}_t}{t} \right|_\infty |M_t^\top|_\infty \right) \|\mathbf{u}^t\|_X \\ &\quad + \sqrt{t} \left(\left| \frac{\mathbf{d}_t}{t} \right|_\infty |M_t^\top|_\infty + \left| \frac{\mathbf{m}_t}{t} \right|_\infty \right) \|p^t\|_Q + \sqrt{t} \left\| \frac{I_t \mathbf{f}^t - \mathbf{f}}{t} \right\|_{0,\Omega}. \end{aligned}$$

Thus, from (22), (25), Lemma 3.9, (47), and (48), we deduce the following limit

$$\lim_{t \rightarrow 0} \frac{1}{t} \|\mathbf{u}^t - \mathbf{u}\|_X^2 = 0 \iff \lim_{t \rightarrow 0^+} \frac{1}{\sqrt{t}} \|\mathbf{u}^t - \mathbf{u}\|_X = 0. \quad (49)$$

Similarly, from estimate (44), we know that (after dividing by $\sqrt{t} > 0$)

$$\frac{1}{\sqrt{t}} \|r^t\|_Q \leq \beta_0^{-1} \left[\frac{1}{\sqrt{t}} m_t + \max\{|\alpha|, 1\} \left(\frac{1}{\sqrt{t}} \|\mathbf{y}^t\|_X \right) \right].$$

Again, from (22), (25), and Lemma 3.9, but now combined with (49), we infer that

$$\lim_{t \rightarrow 0} \frac{1}{t} \|p^t - p\|_Q^2 = 0 \iff \lim_{t \rightarrow 0^+} \frac{1}{\sqrt{t}} \|p^t - p\|_Q = 0. \quad (50)$$

In above argumentations of taking the limit (equations (49) and (50)), it is understood that we are taking a sequence $\{t_n\}$ such that $\lim_{n \rightarrow \infty} t_n = 0$ and we have exploited the fact that the following sequences $\{\mathbf{d}_{t_n}/t_n\}$, $\{\mathbf{m}_{t_n}/t_n\}$, $\{\mathbf{a}_{t_n}/t_n\}$, and $\{\mathbf{b}_{t_n}/t_n\}$ are (uniformly) bounded in L^∞ (because of (22) and (23)). In addition, Lemma 3.9 was employed above in the manner that, for the sequence $\{t_n\}$ (passing to a subsequence if necessary), the solutions $(\mathbf{u}^{t_n}, p^{t_n})$ of (32) are uniformly bounded in $X \times Q$. These results allow us to interchange the limit and the supremum in obtaining, particularly, equation (50). Finally, combining (49) and (50) concludes the lemma. \square

We can now prove Theorem 3.4 without relying on the shape derivative of \mathbf{u} and p . Before diving into the proof, we will establish four lemmas that contain important identities. These lemmas will aid us in deriving and simplifying the boundary expression for the shape gradient in accordance with the Hadamard-Zolésio structure theorem [37, Thm. 3.6, p. 479].

Lemma 3.11. *The following equation is satisfied by the state solution $\mathbf{u} \in X$ of (11):*

$$\lim_{t \rightarrow 0} b(\mathbf{u}^t - \mathbf{u}, \lambda) = - \lim_{t \rightarrow 0} \int_{\Omega} \bar{\lambda} \nabla \cdot \left(\frac{\mathbf{u}^t - \mathbf{u}}{t} \right) dx = - \int_{\Omega} \bar{\lambda} (D\boldsymbol{\theta} : \nabla \mathbf{u}) dx, \quad \forall \lambda \in Q.$$

Proof. Let $(\mathbf{u}^t, p^t) \in V_{\Gamma} \times Q$ be as in Lemma 3.8. We recall equation (37) and divide both sides by $t > 0$, to obtain the following equation

$$\begin{aligned} - \int_{\Omega} \bar{\lambda} \nabla \cdot \left(\frac{\mathbf{u}^t - \mathbf{u}}{t} \right) dx &= \int_{\Omega} \left(\nabla \cdot \boldsymbol{\theta} + \frac{\rho(t)}{t} \right) \bar{\lambda} (M_t^\top : \nabla \mathbf{u}^t) dx \\ &\quad + \int_{\Omega} \bar{\lambda} \left[\left(-D\boldsymbol{\theta} + \frac{R(t)}{t} \right) : \nabla \mathbf{u}^t \right] dx, \quad \forall \lambda \in Q. \end{aligned} \quad (51)$$

Using the properties of $\rho(t)$ and $R(t)$, we get – by letting t goes to zero in (51) and in view of the last paragraph in the proof of the previous lemma – the following limit

$$-\lim_{t \rightarrow 0} \int_{\Omega} \bar{\lambda} \nabla \cdot \left(\frac{\mathbf{u}^t - \mathbf{u}}{t} \right) dx = \int_{\Omega} (\nabla \cdot \boldsymbol{\theta}) \bar{\lambda} (\nabla \cdot \mathbf{u}) dx - \int_{\Omega} \bar{\lambda} (D\boldsymbol{\theta} : \nabla \mathbf{u}) dx, \quad \forall \lambda \in Q.$$

Because $\operatorname{div} \mathbf{u} = 0$ in Ω , we finally arrive at the desired equation. \square

Lemma 3.12. *Let $\boldsymbol{\theta} \in \Theta^1$ and $\boldsymbol{\varphi}$ be sufficiently smooth vector such that $\operatorname{div} \boldsymbol{\varphi} = 0$ in $\Omega \in \mathcal{C}^{1,1}$. Then, we have the following identity*

$$\langle D\boldsymbol{\theta}\boldsymbol{\varphi} - D\boldsymbol{\varphi}\boldsymbol{\theta}, \mathbf{n} \rangle = \langle \boldsymbol{\varphi}, \nabla_{\Sigma}\theta_n \rangle + \langle (D\boldsymbol{\theta}\mathbf{n} \otimes \mathbf{n})\boldsymbol{\varphi}, \mathbf{n} \rangle - \langle \boldsymbol{\theta}, \nabla_{\Sigma}(\varphi_n) \rangle + \theta_n \operatorname{div}_{\Sigma} \boldsymbol{\varphi} \quad (52)$$

$$= \operatorname{div}_{\Sigma}(\theta_n \boldsymbol{\varphi}) + \langle (D\boldsymbol{\theta}\mathbf{n} \otimes \mathbf{n})\boldsymbol{\varphi}, \mathbf{n} \rangle - \langle \boldsymbol{\theta}, \nabla_{\Sigma}(\boldsymbol{\varphi} \cdot \mathbf{n}) \rangle. \quad (53)$$

We omit the proof of the lemma since it proceeds in a similar fashion as in the proof of Lemma 5.4 in [44] using the identities $D\boldsymbol{\varphi} = D_{\Sigma}\boldsymbol{\varphi} + D\boldsymbol{\varphi}\mathbf{n} \otimes \mathbf{n}$, $\operatorname{div}_{\Sigma} \boldsymbol{\varphi} = \operatorname{div} \boldsymbol{\varphi} - \partial_{\mathbf{n}} \boldsymbol{\varphi} \cdot \mathbf{n}$, and $\nabla_{\Sigma}(\boldsymbol{\varphi} \cdot \mathbf{n}) = D_{\Sigma}\boldsymbol{\varphi}^{\top} \mathbf{n} + D_{\Sigma}\mathbf{n}^{\top} \boldsymbol{\varphi} = D_{\Sigma}\boldsymbol{\varphi}^{\top} \mathbf{n} + D_{\Sigma}\mathbf{n}\boldsymbol{\varphi}$.

Lemma 3.13. *Let $\boldsymbol{\theta} = (\theta_1, \dots, \theta_d)^{\top} \in \Theta^1$ and $\boldsymbol{\varphi} = (\varphi_1, \dots, \varphi_d)^{\top}$. Then,*

$$\mathbf{n} \cdot (D\boldsymbol{\theta}\mathbf{n} \otimes \mathbf{n})\boldsymbol{\varphi} = (D\boldsymbol{\theta}\mathbf{n} \cdot \mathbf{n})(\boldsymbol{\varphi} \cdot \mathbf{n}). \quad (54)$$

Moreover, if $\boldsymbol{\varphi}$ is sufficiently smooth, then it also holds that

$$\operatorname{div}(\nabla \boldsymbol{\varphi}^{\top} \boldsymbol{\theta}) = (\boldsymbol{\theta} \cdot \nabla)(\nabla \cdot \boldsymbol{\varphi}) + D\boldsymbol{\theta} : \nabla \boldsymbol{\varphi} = (\boldsymbol{\theta} \cdot \nabla)(\nabla \cdot \boldsymbol{\varphi}) + \nabla \boldsymbol{\varphi}^{\top} : D\boldsymbol{\theta}^{\top}. \quad (55)$$

Proof. Because $D\boldsymbol{\theta}\mathbf{n} \otimes \mathbf{n} = n_j [(\theta_{ki} n_i) \mathbf{e}_k] \mathbf{e}_j^{\top}$ and $(D\boldsymbol{\theta}\mathbf{n} \otimes \mathbf{n})\boldsymbol{\varphi} = \varphi_j n_j [(\theta_{ki} n_i) \mathbf{e}_k] \mathbf{e}_j^{\top}$, then $\mathbf{n} \cdot (D\boldsymbol{\theta}\mathbf{n} \otimes \mathbf{n})\boldsymbol{\varphi} = [n_k(\varphi_j n_j)] (\theta_{ki} n_i) = [n_k (\theta_{ki} n_i)] (\varphi_j n_j) = (D\boldsymbol{\theta}\mathbf{n} \cdot \mathbf{n})(\boldsymbol{\varphi} \cdot \mathbf{n})$, proving (54). Moreover, if $\boldsymbol{\varphi}$ is sufficiently smooth, then the desired identity (55) is easily verified as follows:

$$\operatorname{div}(\nabla \boldsymbol{\varphi}^{\top} \boldsymbol{\theta}) = \frac{\partial^2 \varphi_j}{\partial x_i \partial x_j} \theta_i + \frac{\partial \varphi_j}{\partial x_i} \frac{\partial \theta_i}{\partial x_j} = (\boldsymbol{\theta} \cdot \nabla)(\nabla \cdot \boldsymbol{\varphi}) + D\boldsymbol{\theta} : \nabla \boldsymbol{\varphi}.$$

\square

We now provide the proof of Theorem 3.4.

Proof of Theorem 3.4. The proof essentially proceeds in two parts. Firstly, we evaluate the limit $\lim_{t \rightarrow 0} \frac{1}{t} (J(\Omega_t) - J(\Omega))$. Then, using the regularity of the domain as well as the state and adjoint variables (to be introduced below), we characterized the boundary integral expression for the computed limit. We begin by applying the domain transformation formula $\int_{\Omega_t} \varphi_t dx_t = \int_{\Omega} \varphi_t \circ T_t I_t dx = \int_{\Omega} \varphi^t I_t dx$, for a function $\varphi_t \in L^1(\Omega_t)$ [37, eq. (4.2), p. 482] and the identity $\eta^2 - \zeta^2 = (\eta - \zeta)^2 + 2\zeta(\eta - \zeta)$ to obtain the following calculations:

$$\begin{aligned} & J(\Omega_t) - J(\Omega) \\ &= \int_{\Omega} \frac{\mathfrak{d}_t}{2} (|\mathbf{u}_i^t|^2 - |\mathbf{u}_i|^2) dx + \int_{\Omega} \frac{\mathfrak{d}_t}{2} |\mathbf{u}_i|^2 dx + \frac{1}{2} \int_{\Omega} (|\mathbf{u}_i^t - \mathbf{u}_i|^2) dx + \int_{\Omega} (\mathbf{u}_i^t - \mathbf{u}_i) \cdot \mathbf{u}_i dx \\ &+ \int_{\Omega} \frac{\mathfrak{d}_t}{2} (|p_i^t|^2 - |p_i|^2) dx + \int_{\Omega} \frac{\mathfrak{d}_t}{2} |p_i|^2 dx + \frac{1}{2} \int_{\Omega} (|p_i^t - p_i|^2) dx + \int_{\Omega} (p_i^t - p_i) p_i dx \end{aligned}$$

$$=: \sum_{i=1}^8 J_i(t).$$

From (22) and using Lemma 3.10, we infer that $\dot{J}_1(0) = \dot{J}_3(0) = \dot{J}_5(0) = \dot{J}_7(0) = 0$. Moreover, the properties of T_t in (22) reveals that

$$\dot{J}_2(0) + \dot{J}_6(0) = \frac{1}{2} \int_{\Omega} \operatorname{div} \boldsymbol{\theta} (|\mathbf{u}_i|^2 + |p_i|^2) dx.$$

Applying the expansion $\operatorname{div}(\psi \boldsymbol{\varphi}) = \psi \operatorname{div} \boldsymbol{\varphi} + \boldsymbol{\varphi} \cdot \nabla \psi$ and Green's theorem, we get

$$\dot{J}_2(0) + \dot{J}_6(0) = - \int_{\Omega} (\mathbf{u}_i \cdot \nabla \mathbf{u}_i^\top \boldsymbol{\theta} + p_i \boldsymbol{\theta} \cdot \nabla p_i) dx + \frac{1}{2} \int_{\Sigma} (|\mathbf{u}_i|^2 + |p_i|^2) \theta_n d\sigma. \quad (56)$$

The computations of the expressions $\dot{J}_4(0)$ and $\dot{J}_8(0)$ need much more work. This requires using the adjoint system (29). Indeed, since $\mathbf{y}^t = \mathbf{u}^t - \mathbf{u} \in V_\Gamma$ and $r^t = p^t - p \in Q$, we can write

$$\begin{aligned} J_4(t) + J_8(t) &= \Im \left\{ \int_{\Omega} \alpha \nabla \bar{\mathbf{v}} \cdot \nabla \mathbf{y}^t dx + i \int_{\Sigma} \bar{v}_n y_n^t d\sigma - \int_{\Omega} \bar{q} \operatorname{div} \mathbf{y}^t dx - \int_{\Omega} r^t \operatorname{div} \mathbf{v} dx \right\} \\ &\equiv \Im \{ a(\mathbf{u}^t - \mathbf{u}, \mathbf{v}) + b(\mathbf{v}, p_t - p) + b(\mathbf{u}^t - \mathbf{u}, q) \}. \end{aligned}$$

Therefore, in light of (39) with $\boldsymbol{\varphi} = \mathbf{v} \in V_\Gamma$, the sum $J_4(t) + J_8(t)$ equates to the expression $\Im \{ \Phi^t(\mathbf{v}) + b(\mathbf{u}^t - \mathbf{u}, q) \}$, where $\Phi^t(\mathbf{v})$ is given by (40) with $\boldsymbol{\varphi} = \mathbf{v}$. Using (22), (25), and Lemma 3.11, we obtain the following limit

$$\begin{aligned} \dot{J}_4(0) + \dot{J}_8(0) &= \lim_{t \rightarrow 0} \frac{1}{t} [\Im \{ \Phi^t(\mathbf{v}) + b(\mathbf{u}^t - \mathbf{u}, q) \}] \\ &= \Im \left\{ - \int_{\Omega} \alpha A \nabla \mathbf{u} : \nabla \bar{\mathbf{v}} dx - i \int_{\Sigma} (\operatorname{div} \boldsymbol{\theta} + D\boldsymbol{\theta} \mathbf{n} \cdot \mathbf{n}) u_n \bar{v}_n d\sigma \right. \\ &\quad - i \int_{\Sigma} [(-D\boldsymbol{\theta}) \mathbf{u} \cdot \mathbf{n}] \bar{v}_n d\sigma - i \int_{\Sigma} u_n [(-D\boldsymbol{\theta}) \bar{\mathbf{v}} \cdot \mathbf{n}] d\sigma \\ &\quad + \int_{\Omega} (\nabla \cdot \boldsymbol{\theta}) p (\nabla \cdot \bar{\mathbf{v}}) dx + \int_{\Omega} p [(-D\boldsymbol{\theta}) : \nabla \bar{\mathbf{v}}] dx \\ &\quad \left. + \int_{\Omega} [\nabla \cdot (\mathbf{f} \otimes \boldsymbol{\theta})] \cdot \bar{\mathbf{v}} dx - \int_{\Omega} \bar{q} (D\boldsymbol{\theta} : \nabla \mathbf{u}) dx \right\} \\ &=: \Im \left\{ \sum_{i=1}^8 K_i \right\} \end{aligned} \quad (57)$$

Before we go further with our computation, we gather in the next few lines some identities that will be useful in our calculations. We put into use the weak formulation of the state and the adjoint state problem given in (11) and (29), respectively. In these variational equations – since $\boldsymbol{\theta} \in \Theta$ and $\mathbf{u}, \mathbf{v} \in \mathbf{H}^2(\Omega)^d$ – we can respectively take $\boldsymbol{\varphi} = \nabla \mathbf{v}^\top \boldsymbol{\theta} \in V_\Gamma$ and $\boldsymbol{\psi} = \nabla \mathbf{u}^\top \boldsymbol{\theta} \in V_\Gamma$, apply integration by parts (IBP) twice, and then use the boundary conditions on Σ to obtain the following equations:

$$\begin{aligned} &- \int_{\Omega} \alpha \Delta \mathbf{u} \cdot \nabla \bar{\mathbf{v}}^\top \boldsymbol{\theta} dx + \int_{\Sigma} \alpha \partial_{\mathbf{n}} \mathbf{u} \cdot \nabla \bar{\mathbf{v}}^\top \boldsymbol{\theta} d\sigma + \int_{\Omega} \nabla p \cdot \nabla \bar{\mathbf{v}}^\top \boldsymbol{\theta} dx - \int_{\Sigma} p \mathbf{n} \cdot \nabla \bar{\mathbf{v}}^\top \boldsymbol{\theta} d\sigma \\ &= - \int_{\Omega} \alpha \Delta \mathbf{u} \cdot \nabla \bar{\mathbf{v}}^\top \boldsymbol{\theta} dx + \int_{\Sigma} \alpha \partial_{\mathbf{n}} \mathbf{u} \cdot \nabla \bar{\mathbf{v}}^\top \boldsymbol{\theta} d\sigma - \int_{\Omega} p \operatorname{div}(\nabla \bar{\mathbf{v}}^\top \boldsymbol{\theta}) dx \\ &= \int_{\Omega} \mathbf{f} \cdot \nabla \bar{\mathbf{v}}^\top \boldsymbol{\theta} dx - i \int_{\Sigma} u_n \mathbf{n} \cdot \nabla \bar{\mathbf{v}}^\top \boldsymbol{\theta} d\sigma \end{aligned} \quad (58)$$

and

$$\begin{aligned}
& - \int_{\Omega} \alpha \Delta \bar{\mathbf{v}} \cdot \nabla \mathbf{u}^T \boldsymbol{\theta} dx + \int_{\Sigma} \alpha \partial_{\mathbf{n}} \bar{\mathbf{v}} \cdot \nabla \mathbf{u}^T \boldsymbol{\theta} d\sigma + \int_{\Omega} \nabla \bar{q} \cdot \nabla \mathbf{u}^T \boldsymbol{\theta} dx - \int_{\Sigma} \bar{q} \mathbf{n} \cdot \nabla \mathbf{u}^T \boldsymbol{\theta} d\sigma \\
& = - \int_{\Omega} \alpha \Delta \bar{\mathbf{v}} \cdot \nabla \mathbf{u}^T \boldsymbol{\theta} dx + \int_{\Sigma} \alpha \partial_{\mathbf{n}} \bar{\mathbf{v}} \cdot \nabla \mathbf{u}^T \boldsymbol{\theta} d\sigma - \int_{\Omega} \bar{q} \operatorname{div}(\nabla \mathbf{u}^T \boldsymbol{\theta}) dx \\
& = \int_{\Omega} \mathbf{u}_i \cdot \nabla \mathbf{u}^T \boldsymbol{\theta} dx - i \int_{\Sigma} \bar{v}_n \mathbf{n} \cdot \nabla \mathbf{u}^T \boldsymbol{\theta} d\sigma.
\end{aligned} \tag{59}$$

Now, let us simplify or expand some of the integrals K_i above.

- Rewriting K_7 . For the last integral, we make use of the expansion $[\nabla \cdot (\mathbf{f} \otimes \boldsymbol{\theta})] \cdot \bar{\mathbf{v}} = (\boldsymbol{\theta} \cdot \nabla f_j + f_j \operatorname{div} \boldsymbol{\theta}) \bar{v}_j = \nabla \mathbf{f}^T \boldsymbol{\theta} \cdot \bar{\mathbf{v}} + (\mathbf{f} \cdot \bar{\mathbf{v}}) \operatorname{div} \boldsymbol{\theta}$. Therefore, we have

$$\int_{\Omega} [(\mathbf{f} \cdot \bar{\mathbf{v}}) \operatorname{div} \boldsymbol{\theta} + \mathbf{f} \cdot \nabla \bar{\mathbf{v}}^T \boldsymbol{\theta} + \nabla \mathbf{f}^T \boldsymbol{\theta} \cdot \bar{\mathbf{v}}] dx = \int_{\Omega} \operatorname{div}[(\mathbf{f} \cdot \bar{\mathbf{v}}) \boldsymbol{\theta}] dx.$$

Thus, by the previous computation together with the divergence theorem, we obtain

$$K_7 = \int_{\Omega} [\nabla \cdot (\mathbf{f} \otimes \boldsymbol{\theta})] \cdot \bar{\mathbf{v}} dx = \int_{\Sigma} (\mathbf{f} \cdot \bar{\mathbf{v}}) \theta_n d\sigma - \int_{\Omega} \mathbf{f} \cdot \nabla \bar{\mathbf{v}}^T \boldsymbol{\theta} dx =: K_{71} + K_{72}. \tag{60}$$

- Rewriting K_5 . Using the definition of the tangential divergence of a vector function (cf. (C.76)) and the identity $-\int_{\Omega} (\boldsymbol{\theta} \cdot \nabla p)(\nabla \cdot \bar{\mathbf{v}}) dx = \int_{\Omega} (\boldsymbol{\theta} \cdot \nabla p)p_i dx$ which was obtained by taking $\mu = \boldsymbol{\theta} \cdot \nabla p \in Q$ in the second equation of (29), we have

$$\begin{aligned}
\int_{\Omega} (\nabla \cdot \boldsymbol{\theta})p(\nabla \cdot \bar{\mathbf{v}}) dx &= \int_{\Sigma} p(\nabla \cdot \bar{\mathbf{v}})\theta_n d\sigma - \int_{\Omega} (\boldsymbol{\theta} \cdot \nabla)[p(\nabla \cdot \bar{\mathbf{v}})] dx \\
&= \int_{\Sigma} [p \operatorname{div}_{\Sigma} \bar{\mathbf{v}} + \partial_{\mathbf{n}} \bar{\mathbf{v}} \cdot (p \mathbf{n})]\theta_n d\sigma - \int_{\Omega} (\boldsymbol{\theta} \cdot \nabla)[p(\nabla \cdot \bar{\mathbf{v}})] dx \\
&\quad - \int_{\Omega} (\nabla \cdot \bar{\mathbf{v}})\boldsymbol{\theta} \cdot \nabla p dx - \int_{\Omega} p(\boldsymbol{\theta} \cdot \nabla)(\nabla \cdot \bar{\mathbf{v}}) dx \\
&= \int_{\Sigma} [kp\mathbf{n}\theta_n - \nabla_{\Sigma}(p\theta_n)] \cdot \bar{\mathbf{v}} d\sigma + \int_{\Sigma} \partial_{\mathbf{n}} \bar{\mathbf{v}} \cdot p\mathbf{n}\theta_n d\sigma \\
&\quad + \int_{\Omega} (\boldsymbol{\theta} \cdot \nabla p)p_i dx - \int_{\Omega} p(\boldsymbol{\theta} \cdot \nabla)(\nabla \cdot \bar{\mathbf{v}}) dx \\
&= K_{51} + K_{52} + K_{53} + K_{54}.
\end{aligned}$$

- Rewriting K_2 . Using the identity $\operatorname{div}_{\Sigma} \boldsymbol{\theta} = \operatorname{div} \boldsymbol{\theta} - D\boldsymbol{\theta} \mathbf{n} \cdot \mathbf{n}$ on Σ and the tangential formula, we can expand K_2 as follows:

$$\begin{aligned}
K_2 &= -i \int_{\Sigma} \theta_n \kappa u_n \mathbf{n} \cdot \bar{\mathbf{v}} d\sigma + \int_{\Sigma} \nabla_{\Sigma}[u_n \bar{v}_n] \cdot \boldsymbol{\theta} d\sigma - 2i \int_{\Sigma} D\boldsymbol{\theta} \mathbf{n} \cdot \mathbf{n} u_n \bar{v}_n d\sigma \\
&=: K_{21} + K_{22} + K_{23}.
\end{aligned}$$

- Rewriting K_1 . For the first integral, we make use of the following formula:

$$\begin{aligned}
& - \int_{\Omega} A \nabla \varphi \cdot \nabla \bar{\psi} dx \\
& = - \int_{\Omega} (\Delta \varphi) \boldsymbol{\theta} \cdot \nabla \bar{\psi} dx - \int_{\Omega} (\Delta \bar{\psi}) \boldsymbol{\theta} \cdot \nabla \varphi dx + \int_{\Sigma} \partial_{\mathbf{n}} \varphi (\boldsymbol{\theta} \cdot \nabla \bar{\psi}) d\sigma \\
& \quad + \int_{\Sigma} \partial_{\mathbf{n}} \bar{\psi} (\boldsymbol{\theta} \cdot \nabla \varphi) d\sigma - \int_{\Sigma} (\nabla \bar{\psi} \cdot \nabla \varphi) \theta_n d\sigma,
\end{aligned} \tag{61}$$

which holds for all functions $\varphi, \psi \in V_\Gamma \cap \mathbf{H}^2(\Omega)$ and $\boldsymbol{\theta} \in \Theta^1$ (see for example the proof of Lemma 32 in [34]). Hence, with reference to equation (58) and (59), we get the following computations

$$\begin{aligned}
& - \int_{\Omega} \alpha A \nabla \mathbf{u} : \nabla \bar{\mathbf{v}} dx \\
& = \int_{\Omega} \mathbf{f} \cdot \nabla \bar{\mathbf{v}}^\top \boldsymbol{\theta} dx - i \int_{\Sigma} u_n \mathbf{n} \cdot \nabla \bar{\mathbf{v}}^\top \boldsymbol{\theta} d\sigma + \int_{\Omega} \mathbf{u}_i \cdot \nabla \mathbf{u}^\top \boldsymbol{\theta} dx - i \int_{\Sigma} \bar{v}_n \mathbf{n} \cdot \nabla \mathbf{u}^\top \boldsymbol{\theta} d\sigma \\
& \quad - \int_{\Sigma} \alpha (\nabla_{\Sigma} \mathbf{u} : \nabla_{\Sigma} \bar{\mathbf{v}}) \theta_n d\sigma - \int_{\Sigma} \alpha \partial_{\mathbf{n}} \mathbf{u} \cdot \partial_{\mathbf{n}} \bar{\mathbf{v}} \theta_n d\sigma \\
& \quad + \int_{\Omega} p \operatorname{div}(\nabla \bar{\mathbf{v}}^\top \boldsymbol{\theta}) dx + \int_{\Omega} \bar{q} \operatorname{div}(\nabla \mathbf{u}^\top \boldsymbol{\theta}) dx \\
& =: K_{11} + K_{12} + K_{13} + K_{14} + K_{15} + K_{16} + K_{17} + K_{18}.
\end{aligned}$$

Notice here that K_{11} will cancel out with K_{72} . Moreover, in light of identity (55), the sum $K_6 + K_{54} + K_{17}$ actually equates to zero. Similarly, using equation (55) and the fact that $\operatorname{div} \mathbf{u} = 0$ in Ω , we get

$$K_{18} = \int_{\Omega} \bar{q} \operatorname{div}(\nabla \mathbf{u}^\top \boldsymbol{\theta}) dx = \int_{\Omega} \bar{q} [(\boldsymbol{\theta} \cdot \nabla)(\nabla \cdot \mathbf{u}) + D\boldsymbol{\theta} : \nabla \mathbf{u}] dx = \int_{\Omega} \bar{q} D\boldsymbol{\theta} : \nabla \mathbf{u} dx.$$

This integral also vanishes when combined with K_8 because of Lemma 3.11.

In the above, we have an expression where we can use Lemma 3.12. Considering the sum $K_3 + K_{14}$, we can apply identity (53) to obtain the following equation

$$\begin{aligned}
K_3 + K_{14} & = i \int_{\Sigma} \bar{v}_n \operatorname{div}_{\Sigma}(\theta_n \mathbf{u}) d\sigma + i \int_{\Sigma} \bar{v}_n \mathbf{n} \cdot (D\boldsymbol{\theta} \mathbf{n} \otimes \mathbf{n}) \mathbf{u} d\sigma - i \int_{\Sigma} \bar{v}_n \boldsymbol{\theta} \cdot \nabla_{\Sigma} u_n d\sigma \\
& =: J_1 + J_2 + J_3.
\end{aligned}$$

Meanwhile, for the sum $K_4 + K_{12}$, we have

$$\begin{aligned}
K_4 + K_{12} & = i \int_{\Sigma} u_n \mathbf{n} \cdot D\boldsymbol{\theta} \bar{\mathbf{v}} d\sigma - i \int_{\Sigma} u_n \mathbf{n} \cdot \nabla \bar{\mathbf{v}}^\top \boldsymbol{\theta} d\sigma \\
& = i \int_{\Sigma} u_n \nabla_{\Sigma} \theta_n \cdot \bar{\mathbf{v}} d\sigma + i \int_{\Sigma} u_n \mathbf{n} \cdot (D\boldsymbol{\theta} \mathbf{n} \otimes \mathbf{n}) \bar{\mathbf{v}} d\sigma \\
& \quad - i \int_{\Sigma} u_n \boldsymbol{\theta} \cdot \nabla_{\Sigma} \bar{v}_n d\sigma - i \int_{\Sigma} u_n \mathbf{n} \cdot \partial_{\mathbf{n}} \bar{\mathbf{v}} \theta_n d\sigma \\
& =: H_1 + H_2 + H_3 + H_4.
\end{aligned}$$

Adding this to $K_{16} + K_{52}$ and noting that $-p\mathbf{n} + \alpha \partial_{\mathbf{n}} \mathbf{u} + iu_n \mathbf{n} = 0$ on Σ , we further get

$$K_4 + K_{12} + K_{16} + K_{52} = H_1 + H_2 + H_3.$$

At this point, we underline the observation that the sum $K_{22} + J_3 + H_3$ vanishes. Moreover, applying identity (54), we also observe that the sum $J_2 + H_2 + K_{23}$ also disappears because

$$i \int_{\Sigma} \bar{v}_n \mathbf{n} \cdot (D\boldsymbol{\theta} \mathbf{n} \otimes \mathbf{n}) \mathbf{u} d\sigma + i \int_{\Sigma} u_n \mathbf{n} \cdot (D\boldsymbol{\theta} \mathbf{n} \otimes \mathbf{n}) \bar{\mathbf{v}} d\sigma - 2i \int_{\Sigma} D\boldsymbol{\theta} \mathbf{n} \cdot \mathbf{n} u_n \bar{v}_n d\sigma = 0.$$

Finally, summarizing our computations – and after applying the tangential Green's formula and using the fact that $\nabla_{\Sigma} \mathbf{u} \mathbf{n} = \mathbf{0}$ [37, eq. (5.20), p. 497] – we get the following equivalent expression for the sum

$\dot{J}_2(0) + \dot{J}_6(0) + \dot{J}_4(0) + \dot{J}_8(0)$ (see (56) and (57)):

$$\begin{aligned}
& \dot{J}_2(0) + \dot{J}_6(0) + \dot{J}_4(0) + \dot{J}_8(0) \\
&= - \int_{\Omega} [\mathbf{u}_i \cdot \nabla \mathbf{u}_i^\top \boldsymbol{\theta} + p_i(\boldsymbol{\theta} \cdot \nabla p_i)] dx + \frac{1}{2} \int_{\Sigma} (|\mathbf{u}_i|^2 + |p_i|^2) \theta_n d\sigma \\
&\quad + \Im \left\{ \int_{\Omega} \mathbf{u}_i \cdot \nabla \mathbf{u}^\top \boldsymbol{\theta} dx + \int_{\Omega} p_i(\boldsymbol{\theta} \cdot \nabla p) dx \right. \\
&\quad \left. + \int_{\Sigma} [\mathbf{f}\theta_n - \nabla_{\Sigma}(p\theta_n) + \operatorname{div}_{\Sigma}[\alpha(\nabla_{\Sigma}\mathbf{u})\theta_n] + i \operatorname{div}_{\Sigma}(\theta_n \mathbf{u})\mathbf{n} + i u_n \nabla_{\Sigma}\theta_n] \cdot \bar{\mathbf{v}} d\sigma \right\} \\
&= \int_{\Sigma} \left[\Im \{ \mathbf{B}[\theta_n] \cdot \bar{\mathbf{v}} \} + \frac{1}{2} (|\mathbf{u}_i|^2 + |p_i|^2) \theta_n \right] d\sigma,
\end{aligned}$$

which is the desired expression of the shape derivative. \square

Remark 3.14. The computed expression (26) for the shape gradient of J obtained via rearrangement method clearly agrees with the structure of the same derivative derived through the classical chain rule approach issued in Appendix C. In fact, after some manipulations, the expression can equivalently be expressed as (see (C.77))

$$\mathbf{B}[\theta_n] = [\alpha \nabla \mathbf{u} + (u_n - p)i\mathbf{d}] \nabla_{\Sigma}\theta_n + [\partial_{\mathbf{n}} p \mathbf{n} - \partial_{\mathbf{n}\mathbf{n}}^2 \mathbf{u} - i(\partial_{\mathbf{n}} u_n)\mathbf{n}] \theta_n - i(\mathbf{u} \cdot \nabla_{\Sigma}\theta_n) \mathbf{n}.$$

The following results can be drawn easily from (26), (27), and Remark 2.1.

Corollary 3.15 (Necessary optimality condition). Let the domain Ω^* be such that the state $(\mathbf{u}, p) = (\mathbf{u}(\Omega^*), p(\Omega^*))$, where $\mathbf{u} = \mathbf{u}_r + i\mathbf{u}_i$ and $p = p_r + ip_i$, satisfies the free surface problem (1), i.e., we have $-p\mathbf{n} + \alpha\partial_{\mathbf{n}}\mathbf{u} = \mathbf{0}$ and $\mathbf{u} \cdot \mathbf{n} = 0$ on Σ^* , or equivalently,

$$\mathbf{u}_i = \mathbf{0} \quad \text{and} \quad p_i = 0 \quad \text{on } \Omega^*, \tag{62}$$

with (\mathbf{u}, p) satisfying (7). Then, the domain Ω^* is stationary for the shape problem (15) (the minimization problem $J(\Omega) = \frac{1}{2} \int_{\Omega} (|\mathbf{u}_i|^2 + |p_i|^2) dx \rightarrow \inf$, where (\mathbf{u}_i, p_i) is subject to the state problem (7)). That is, it fulfills the necessary optimality condition

$$dJ(\Omega^*)[\boldsymbol{\theta}] = 0, \quad \text{for all } \boldsymbol{\theta} \in \Theta^1. \tag{63}$$

Proof. By the assumption that $\mathbf{u}_i = \mathbf{0}$ and $p_i = 0$ on Ω^* , one obtains – in view of (27) – that $\mathbf{v}_i = \mathbf{0}$ and $q_i = 0$ on Ω^* . Thus, it follows that $g_{\Sigma} = 0$ on Σ^* which therefore gives us the conclusion $dJ(\Omega^*)[\boldsymbol{\theta}] = 0$, for any $\boldsymbol{\theta} \in \Theta^1$. \square

Regarding the previous conclusion, it should be noted that while solutions satisfying the necessary condition (63) may exist, they might not satisfy equation (62) (see Fig. 2 and Fig. 3 for numerical examples). However, when the boundary data perfectly matches, a stationary domain Ω^* becomes a global minimum as $J(\Omega^*) = 0$.

4 Numerical approximation

We employ a Sobolev gradient-based approach to numerically resolve our proposed shape optimization method (1). Building upon the author's previous work [45], we implement this approach using the finite element method. Consequently, this section is divided into two subsections: the first part presents algorithm details, while the second part offers concrete test examples for the problem.

4.1 Numerical algorithm

For completeness, we give below the important details of our algorithm.

Choice of descent direction. To solve the problem, we employ the finite element method, utilizing the Riesz representation of the shape gradient (26). This is necessary because the gradient given by g_Σ is only supported on the free boundary Σ . If we directly use $g_\Sigma \mathbf{n}$ as the descent vector $\boldsymbol{\theta}$, undesired oscillations may occur on the free boundary. So, we apply an extension-regularization technique by taking the descent direction $\boldsymbol{\theta}$ as the solution in $\mathbf{H}_{\Gamma,0}^1(\Omega)$ to the variational problem

$$a(\boldsymbol{\theta}, \boldsymbol{\varphi}) = - \int_{\Sigma} g_\Sigma \mathbf{n} \cdot \boldsymbol{\varphi} d\sigma, \quad \text{for all } \boldsymbol{\varphi} \in \mathbf{H}_{\Gamma,0}^1(\Omega), \quad (64)$$

where a is the $\mathbf{H}^1(\Omega)$ ($= H^1(\Omega; \mathbb{R}^d)$)-inner product in d -dimension. By this method, the *Sobolev gradient* $\boldsymbol{\theta}$ [46] becomes a smoothed preconditioned extension of $-g_\Sigma \mathbf{n}$ over the domain Ω . For further details, we refer the readers to [47].

The main steps to compute the k th domain Ω^k is given as follows:

1. *Initialization* Choose an initial guess for Σ^0 (this gives us Ω^0).

2. *Iteration* For $k = 0, 1, 2, \dots$, do the following:

- 2.1 solve equations (11) and (29) on the current domain $\Omega = \Omega^k$;
- 2.2 choose $t^k > 0$, and compute $\boldsymbol{\theta}^k$ by solving (64) on $\Omega = \Omega^k$;
- 2.3 update the domain by setting $\Omega^{k+1} := \{x + t^k \boldsymbol{\theta}^k(x) \in \mathbb{R}^d \mid x \in \Omega^k\}$.

3. *Stop Test* Repeat *Iteration* until convergence.

For the *Stop Test*, we terminate the algorithm after it has reached a maximum number of iterations or when the absolute value of the difference between two consecutive cost values is small enough. Meanwhile, in Step 2.2, the step size t^k is computed via a backtracking line search procedure using the formula $t^k = \mu J(\Omega^k) / |\boldsymbol{\theta}^k|_{\mathbf{H}^1(\Omega^k)}^2$ at each iteration, where $\mu \in \mathbb{R}^+$ is fixed. This method is adapted from [45, p. 281]. However, differently from [45], our approach allows the step size parameter μ to extend beyond the interval $(0, 1)$. By doing so, we can maximize the initial length of the descent vector and depend on the backtracking procedure to determine a suitable step size.

Remark 4.1 (Evaluating the mean curvature). The mean curvature κ of Σ is evaluated as $\nabla \cdot \mathbf{N}$, where $\mathbf{N} \in \mathbf{H}^1(\Omega)$ is an extension of the (outward) unit normal \mathbf{n} satisfying the equation $c_N \int_{\Omega} \nabla \mathbf{N} : \nabla \boldsymbol{\varphi} dx + \int_{\Sigma} \mathbf{N} \cdot \boldsymbol{\varphi} d\sigma = \int_{\Sigma} \mathbf{n} \cdot \boldsymbol{\varphi} d\sigma$, for all $\boldsymbol{\varphi} \in \mathbf{H}^1(\Omega)$, for some $c_N \in \mathbb{R}^{+}$ ¹⁰. We emphasize that \mathbf{N} must be a unitary extension of \mathbf{n} for the formula $\kappa = \operatorname{div}_{\Sigma} \mathbf{n} = \operatorname{div} \mathbf{N} - (\nabla \mathbf{N} \mathbf{n}) \mathbf{n} = \operatorname{div} \mathbf{N}$ (on Σ) to hold [41, Lem. 2.14, p. 92]. So, the proposed extension of \mathbf{n} may not be accurate. However, the approximation suffices to obtain a descent direction for optimization. Additionally, this strategy readily applies to three-dimensional cases. While a more precise numerical calculation of κ is possible, we are satisfied with the results achieved using this approximation technique. In our numerical experiments, we set $c_N = 10^{-8}$.

Remark 4.2. We can improve the convergence of our scheme by using the shape Hessian information in the numerical procedure. However, second-order methods require more computation and time, especially for complicated Hessians [48, 49]. Since the first-order method already provides an excellent approximation of the optimal solution, we will not use a second-order method to solve the optimization problem.

¹⁰This follows the same idea in computing the Riesz representation of the shape gradient.

4.2 Numerical examples

We now demonstrate the feasibility of the shape optimization approach (15) for solving concrete numerical examples of problem (1). While previous studies focused mainly on 2D free surface problems (see [4]), we extend our analysis to include three-dimensional cases. Additionally, we compare the proposed method with the minimization approach (5) to showcase its advantages numerically.

Remark 4.3 (Details of the computational setup and environment). *The simulations in this study were implemented using the programming software FREEFEM++ [50]. Variational problems, except for those corresponding to equations (7) and (27), were solved using a P_1 finite element discretization. Additionally, mesh deformations were performed without adaptive mesh refinement, which differs from previous works [45]. This approach allows us to evaluate the stability of CCBM compared to the classical approach of tracking Dirichlet data in a least-squares sense. The computations were carried out on a MacBook Pro with an Apple M1 chip with 16GB RAM main memory.*

Remark 4.4. We implement the Sobolev-gradient method by solving the discretized version of equation (64). That is, we find $\boldsymbol{\theta}_h^k \in P_1(\Omega_h^k)^d$ such that

$$-\Delta \boldsymbol{\theta}_h^k + \boldsymbol{\theta}_h^k = \mathbf{0} \quad \text{in } \Omega_h^k, \quad \boldsymbol{\theta}_h^k = \mathbf{0} \quad \text{on } \Gamma^h, \quad \nabla \boldsymbol{\theta}_h^k \cdot \mathbf{n}_h^k = -g_\Sigma^k \mathbf{n}_h^k \quad \text{on } \Sigma_h^k,$$

where we suppose a polygonal domain $\overline{\Omega_h^k}$ and its triangulation $\mathcal{T}_h(\overline{\Omega_h^k}) = \{K_l^k\}_{l=1}^{N_e}$ (K_l^k is a closed triangle for $d = 2$, or a closed tetrahedron for $d = 3$) are given, and $P_1(\Omega_h^k)^d$ denotes the \mathbb{R}^d -valued piecewise linear function space on $\mathcal{T}_h(\overline{\Omega_h^k})$. Accordingly, we define Ω_h^{k+1} and $\mathcal{T}_h(\overline{\Omega_h^{k+1}}) = \{K_l^{k+1}\}_{l=1}^{N_e}$ (N_e denotes the number of elements) respectively as $\overline{\Omega_h^{k+1}} := \left\{ x + t^k \boldsymbol{\theta}_h^k(x) \mid x \in \overline{\Omega_h^k} \right\}$ and $K_l^{k+1} := \left\{ x + t^k \boldsymbol{\theta}_h^k(x) \mid x \in K_l^k \right\}$, for all $k = 0, 1, \dots$

4.2.1 Examples in two dimensions

We now provide some numerical examples in 2D. We begin by replicating the numerical experiment described in [4, Subsec. 5.3, p. 833]. A gravity-like force $\mathbf{f} = (-10x, -10y)^\top$ is applied to maintain the fluid on the circular domain with a radius of 0.4. The fluid's initial velocity triggers its flow within the domain until it eventually reaches a steady state, resulting in a free surface position that aligns concentrically with the circular domain. A homogeneous Dirichlet boundary condition ($\mathbf{g} = \mathbf{0}$) is enforced on the fixed boundary Γ , and we take $\alpha = 0.01$. We set the initial geometry of the fluid's free-boundary Σ^0 as follows

$$\Sigma^0 = E(a, b) := \left\{ (x, y) \in \mathbb{R}^2 \mid \frac{x^2}{a^2} + \frac{y^2}{b^2} = 1 \right\},$$

with $(a, b) = (1.0, 1.1)$. We use the built-in bi-dimensional anisotropic mesh generator of FREEFEM++ [50] to discretize the computational domain into triangular elements. The exterior and interior boundaries are discretized with 70 and 30 nodal points, respectively. The Galerkin finite-element method is employed to discretize the Stokes equations (7) and the adjoint system (27). We utilize Taylor-Hood elements (P_2-P_1 finite elements) to approximate the velocity and pressure. This results in a set of linear algebraic equations represented as $\mathbf{K}\bar{\mathbf{u}} = \mathbf{F}$ where \mathbf{K} is the global system matrix, $\bar{\mathbf{u}}$ is the global vector of unknowns (velocities and pressures), and \mathbf{F} is a vector encompassing the effects of body forces and boundary conditions. The linear system is solved using the default LU-solver of FREEFEM++.

The results of the experiment are presented in Fig. 1, which displays a cross comparison of computed shapes, and histories of costs and H^1 gradient norms. CCBM achieves the same solution as formulation (5) (hereinafter referred to as TD). Both methods exhibit comparable convergence behavior in terms of cost values and H^1 gradient norms. Currently, there does not appear to be a significant advantage in using CCBM. However, the advantage will be apparent in 3D cases.

We also plotted the initial and final imaginary parts of the Stokes' and the adjoint's velocity and pressure profiles in Figures 2 and Fig. 3, respectively. The imaginary parts significantly decreased to very small magnitudes in the optimal shape solution. The computed magnitudes of the Stokes and adjoint pressure at the approximate optimal shape were on the order of 10^{-5} and 10^{-7} , respectively. This numerical confirmation aligns with Remark 2.1 and the optimality condition stated in Corollary 3.15.

Another set of examples but with different source function and higher aspect ratio for the initial guess. Let Γ_1 and Γ_2 be defined as follows:

$$\begin{aligned}\Gamma_1 &:= \left\{ \begin{pmatrix} 0.4 \cos t \\ 0.4 \sin t \end{pmatrix} \in \mathbb{R}^2 \mid t \in [0, 2\pi] \right\}; \\ \Gamma_2 &:= \left\{ \begin{pmatrix} (0.37 + 0.03 \cos 5t) \cos t \\ (0.37 + 0.03 \cos 5t) \sin t \end{pmatrix} \in \mathbb{R}^2 \mid t \in [0, 2\pi] \right\}.\end{aligned}$$

Then, we consider the following setups for our next set of examples:

$$\mathbf{f} = (-10x^3, -10y^3)^\top, \quad \Gamma = \Gamma_1, \quad (\text{P1})$$

$$\mathbf{f} = (-10x^3, -10y^3)^\top, \quad \Gamma = \Gamma_2, \quad (\text{P2})$$

$$\mathbf{f} = (-10x^7, -10y^7)^\top, \quad \Gamma = \Gamma_2, \quad (\text{P3})$$

$$\mathbf{f} = (-10x^{11}, -10y^{11})^\top, \quad \Gamma = \Gamma_2. \quad (\text{P4})$$

For (P1), we take $\Sigma^0 = E(1.0, 0.7)$ while for (P2), (P3), and (P4) we set $\Sigma^0 = E(1.0, 0.5)$. In all cases, the interior boundary is discretized with 30 discretization points. Meanwhile, except for (P1) where we take 70 nodal points, the exterior boundary is discretized with 100 nodal points.

Fig. 4 shows cross comparisons of optimal shapes computed via TD and CCBM. Results for Problems (P1), (P2), and (P3) have nearly identical shapes, but there is a noticeable difference for problem (P4). Despite this, the final free boundary obtained via TD closely resembles a superellipse or a squircle, which is the shape obtained via CCBM. Interestingly, even when the fixed boundary is axisymmetric, the computed optimal shapes are not. This is likely due to the value of the external force \mathbf{f} . Nonetheless, the fixed and free boundaries are concentric, and the cost values for all cases are close to zero, with J magnitude on the order of 10^{-8} or less and J_D magnitude on the order of 10^{-5} or less.

Fig. 5 and Fig. 6 display the shape evolution of the free boundaries for (P1) and (P4), respectively, obtained via TD and CCBM. The figures clearly depict the differences in the shape evolution. Additionally, the corresponding histories of cost and norm values for these problems are plotted alongside the figures.

Finally, Fig. 7–Fig. 10 visualize the imaginary parts of the Stokes' and adjoint flow fields, as well as the pressures at the initial and optimal shapes for (P1) and (P4). These figures demonstrate that the magnitudes of the flow fields and pressures at the optimal shapes are almost zero (around 10^{-3} or less), which is desirable.

4.2.2 Examples in three dimensions

Now we consider a test case in 3D. The assumptions are similar to the previous example. That is, we consider a gravity-like force $\mathbf{f} = (-10x, -10y, -10z)^\top \in \mathbb{R}^3$. This force is assumed to keep the fluid to surround an object that is spherical in shape having radius equal to 0.4. Again, the fluid flowing in the domain is triggered by an initial velocity. The value of α is again set to 0.01 and this time we take a complex shape for the initial guess as shown in Fig. 11.

We again look at the situations where we have coarse and fine mesh for the computational domain. For the latter (initial) setup, the tetrahedrons have maximum and minimum mesh width of $h_{\max} \approx 0.665$

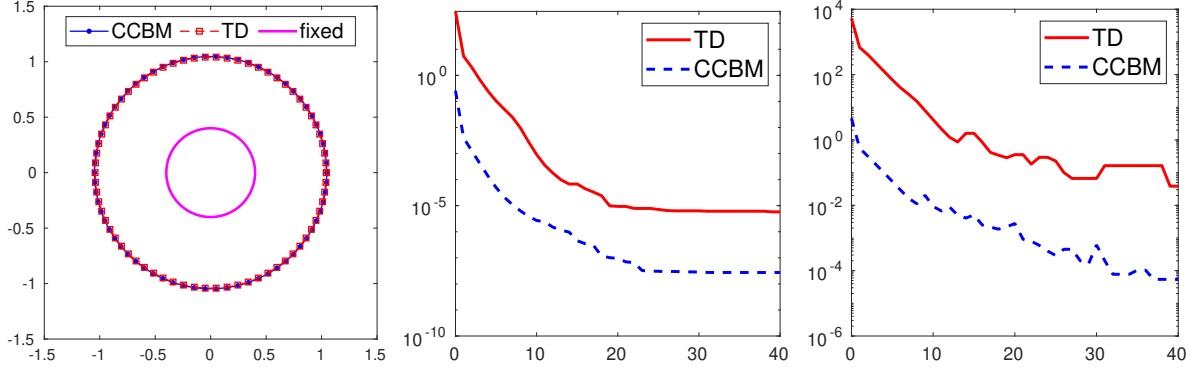


Fig. 1 Cross comparison of computed shapes (left plot), histories of cost values (middle plot), and H^1 gradient norms (right plot)

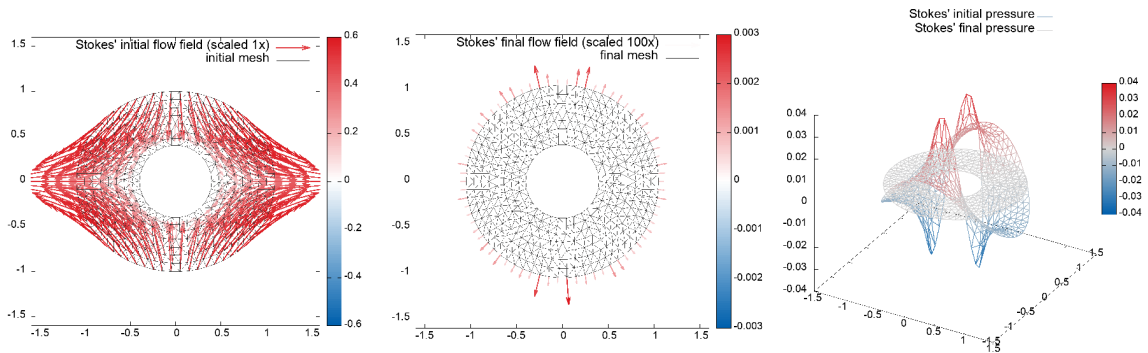


Fig. 2 Imaginary parts of the initial and final flow field and pressure of the Stokes system

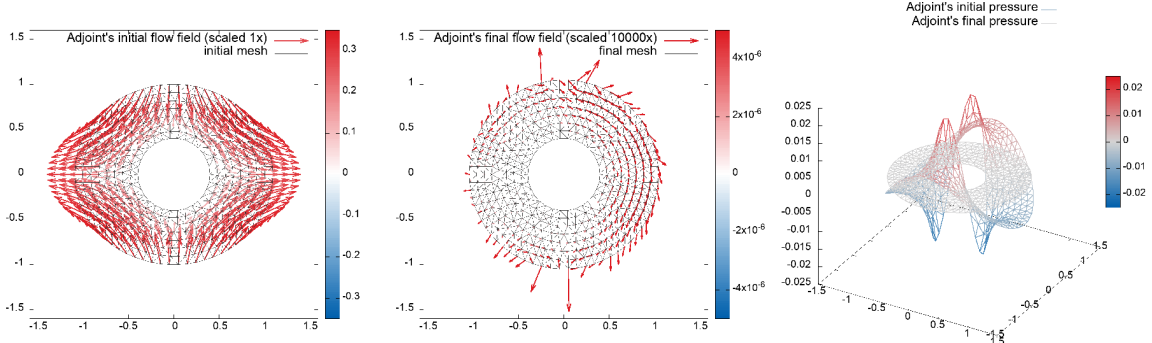


Fig. 3 Imaginary parts of the initial and final flow field and pressure of the adjoint system

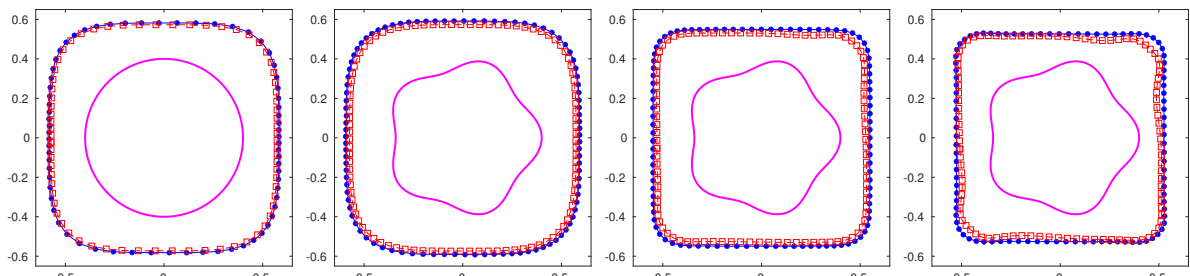


Fig. 4 (From left to right) Cross comparisons of computed shapes via TD and CCBM for problems (P1), (P2), (P3), and (P4). (See Fig. 1 for the legends.)

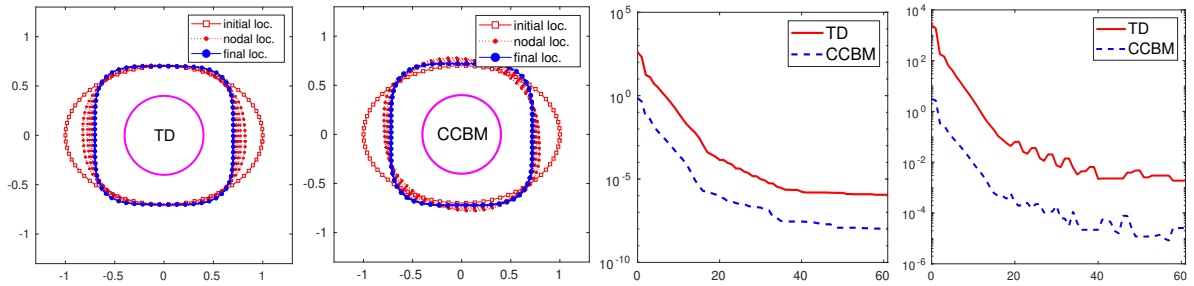


Fig. 5 (From left to right) Shape evolutions via TD and CCBM for problems (P1) and the corresponding plots for the histories of the costs and gradient norms.

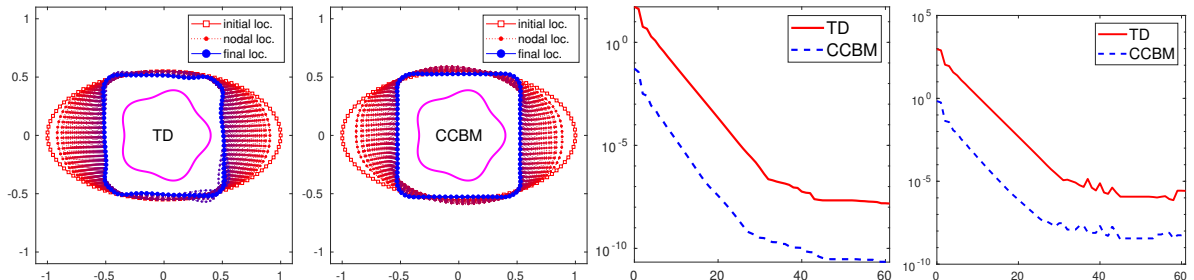


Fig. 6 (From left to right) Shape evolutions via TD and CCBM for problems (P4) and the corresponding plots for the histories of the costs and gradient norms.

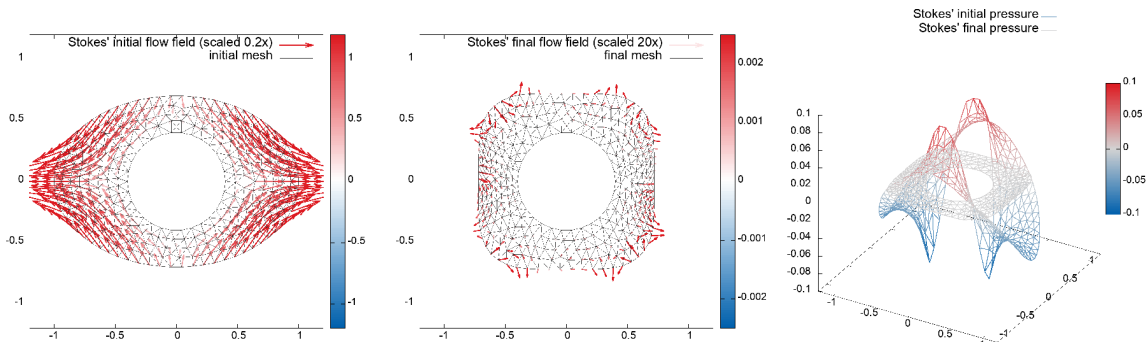


Fig. 7 Imaginary parts of the initial and final flow field and pressure of the Stokes system corresponding to problem (P1)

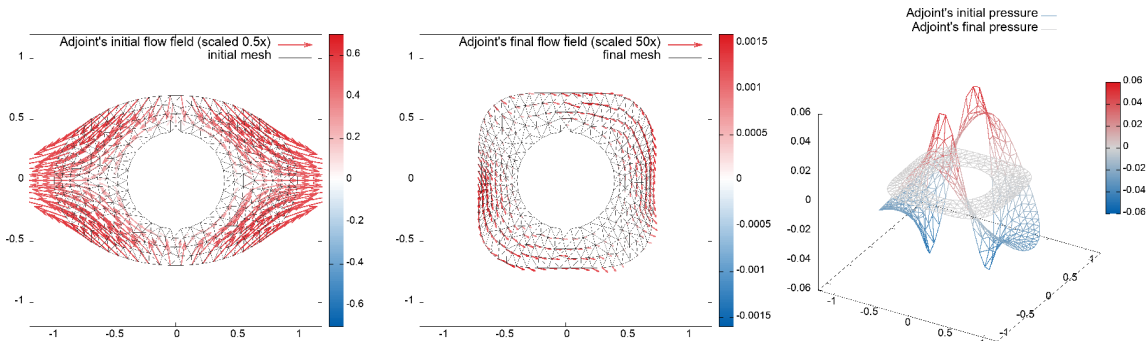


Fig. 8 Imaginary parts of the initial and final flow field and pressure of the adjoint system corresponding to problem (P1)

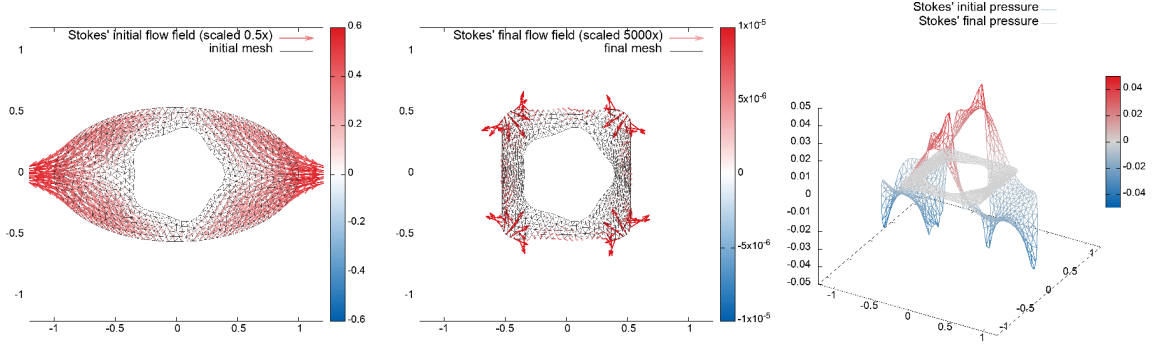


Fig. 9 Imaginary parts of the initial and final flow field and pressure of the Stokes system corresponding to problem (P4)

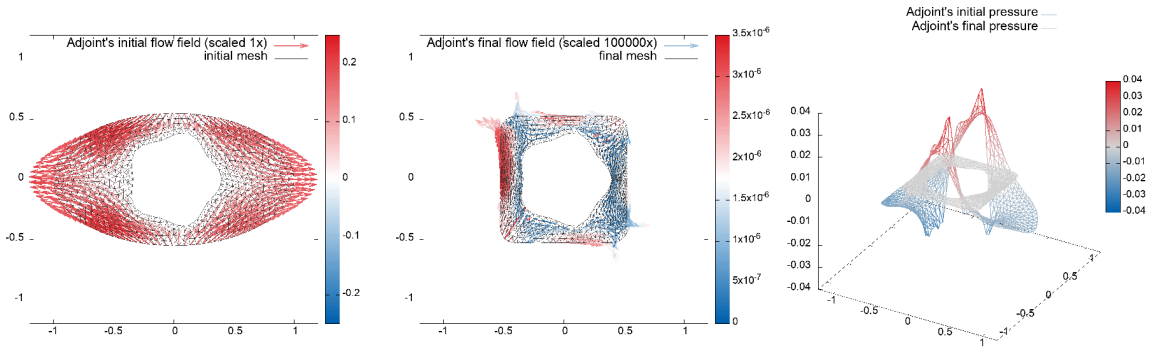


Fig. 10 Imaginary parts of the initial and final flow field and pressure of the adjoint system corresponding to problem (P4)

and $h_{\min} \approx 0.047$, respectively. Meanwhile, for the test experiment with fine mesh we take $h_{\max} \approx 0.487$ and $h_{\min} \approx 0.047$. The rest of the computational setup is similar to the case of two dimensions.

The computational results for coarse mesh are shown in Fig. 12–Fig. 15.¹¹ Fig. 12 shows that the sequence of shape approximations using CCBM differs from TD, as expected. Nevertheless, Fig. 13 shows that the computed optimal shapes obtained by the two methods are nearly identical. Meanwhile, Fig. 14–Fig. 15 display the initial and final imaginary parts of the Stokes' and adjoint's flow fields, and the pressure profiles¹² for the coarse-mesh experiment. These numerical results support Remark 2.1 and confirm the statement in Corollary 3.15, similar to the findings in 2D cases.

Fig. 16–Fig. 18 display the results for a finer computational mesh. In Fig. 16, the evolution from the initial domain to the optimal domain is displayed and is smooth with CCBM, unlike TD, which shows dents in the computed optimal shape. A comparison between the optimal shapes obtained from the two methods is shown in Fig. 17, further highlighting the superiority of CCBM. Fig. 18 reveals that the optimal shape achieved with CCBM is smoother than the one obtained with TD. These results clearly demonstrate the advantage of using CCBM over TD.

In Fig. 19, we plot the cost and gradient norm histories for both methods. It seems that CCBM converges faster to a stationary point on the coarse mesh compared to TD. Meanwhile, on the finer mesh, TD converges prematurely due to observed instabilities. These results indicate that CCBM is more robust than TD, as previously observed.

¹¹For the final pressure profile of the Stokes and the adjoint solutions, the maximum magnitude is found to be of order 10^{-3} and 10^{-4} , respectively.

¹²The pressure profiles are plotted in vectors (directed to the normal from the mesh node) whose length is scaled and colored by its magnitude.

Another set of examples but with different fixed surface and source function. We further illustrate the robustness of CCBM in solving 3D cases by giving another set of examples. Let us consider the following algebraic equation representing the surface of a sphube:

$$S(r, s) = x_1^2 + x_2^2 + x_3^2 - \frac{s^2}{r^2}x_1^2x_2^2 - \frac{s^2}{r^2}x_2^2x_3^2 - \frac{s^2}{r^2}x_1^2x_3^2 - \frac{s^4}{r^4}x_1^2x_2^2x_3^2 - r^2, \quad (r > 0, s \geq 0),$$

where $(x_1, x_2, x_3)^\top \in \mathbb{R}^3$, r represents the radius of the super-ellipsoid, and s dictates its squareness. For the additional experiments, we consider the following setups:

$$\mathbf{f} = (-10x, -10y, -10z)^\top, \quad (\text{P5})$$

$$\mathbf{f} = (-10x^3, -10y^3, -10z^3)^\top. \quad (\text{P6})$$

In both cases, $\Gamma = S(0.40, 0.85)$ and the initial guess for the exterior surface Σ is the same as in the one shown in Fig. 11; see Fig. 20 with a coarse mesh.

Figure 21 shows two sets of experiments: one with an initial mesh with $h_{\max} \approx 0.6$ and another one with a finer mesh with $h_{\max} \approx 0.55$. In both situations, we notice instabilities with the approximation due to TD. These phenomena, on the other hand, were not observed in the case of CCBM. Meanwhile, Fig. 22 displays the histories of cost and norms for both methods under coarse mesh from which we see that CCBM converges after around 35 iterations.

The results for problem (P6) are displayed in the rest of the figures. Fig. 23 and Fig. 24 respectively shows the optimal shapes under a coarse-mesh experiment with $h_{\max} \approx 0.64$ and a less coarse one with $h_{\max} \approx 0.60$. Both results reveal that TD is unstable while CCBM is not. As in previous cases, the instability of TD caused the algorithm to stop without reaching convergence. In these experiments, the step size was set to 0.33 and 0.10, respectively. A stable approximation of the optimal shape can, of course, be achieved for TD, but with much smaller step sizes and a larger number of iterations. Meanwhile, Fig. 25 illustrates the mesh profiles of the computed optimal shapes when initially $h_{\max} \approx 0.60$. Observably, CCBM produces an optimal shape resembling a sphube shape. Furthermore, Fig. 26 and Fig. 27 respectively display the imaginary parts of the velocity flow fields and pressure profiles (scaled for better display) for the Stokes' and the adjoint's equation, respectively. Clearly, these quantities significantly decrease in magnitude at the optimal shapes. Finally, Fig. 28 presents the histories of the costs and gradient norms for the experiment. We observe here that CCBM is (almost) in a state of convergence after 40 iterations. These numerical results, in conclusion, clearly demonstrate the superiority of CCBM over TD.

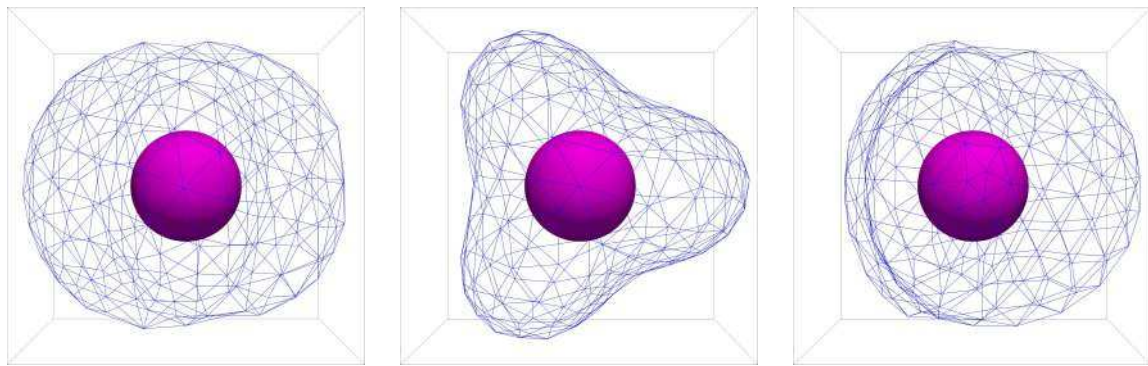


Fig. 11 Mesh profile (coarse mesh) of the initial guess viewed on different positions

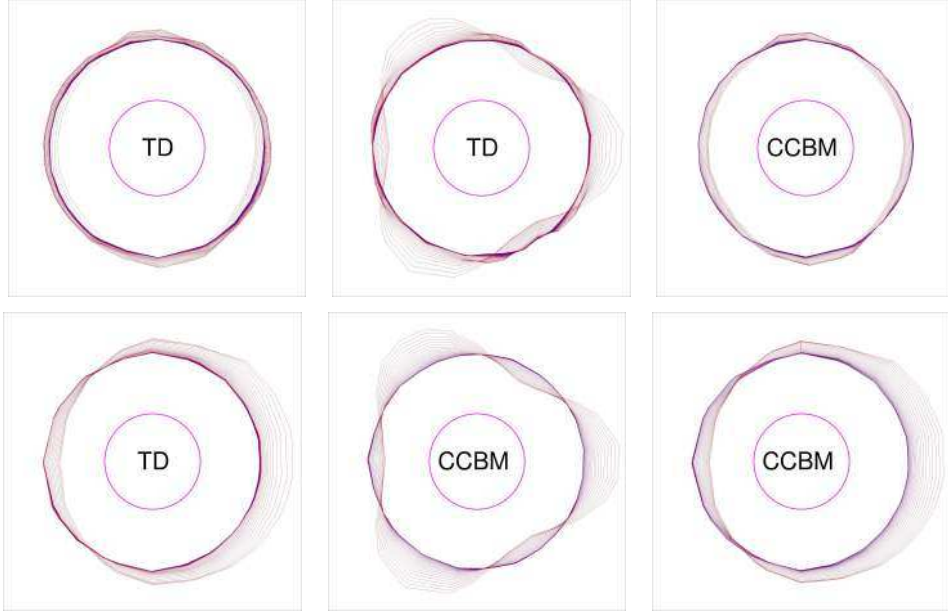


Fig. 12 Shape histories of the free boundary computed using TD and CCBM with coarser mesh viewed on the planes xz , yx , and yz (respectively, top and bottom plots)

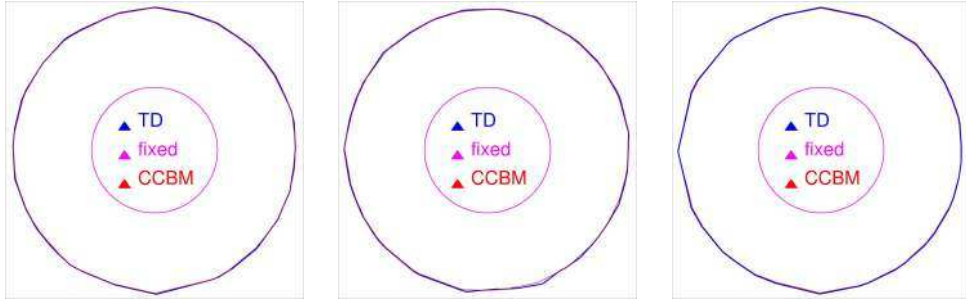


Fig. 13 Cross comparison of computed shapes (case of coarser meshes) viewed on the planes xz , yx , and yz (respectively, left, middle, and right plot)

5 Conclusions and Future Work

In this work, we have developed a coupled complex boundary method in shape optimization setting to solve a free boundary problem involving the Stokes equation. The shape gradient of the cost was rigorously computed, without relying on the shape derivative of the states and assuming only a mild regularity condition on the domain.

Using the shape gradient information, a Sobolev gradient-based descent scheme is formulated for numerically solving the minimization problem with the finite element method. Then, the method is tested in two- and three-dimensional problems, yielding promising numerical results. In fact, the new approach outperforms the classical least-squares approach of tracking Dirichlet data in terms of stability and demonstrates greater accuracy in obtaining the expected optimal shape solution.

For future work, we propose calculating and examining the shape Hessian of the cost functional to investigate the ill-posedness of the proposed shape optimization problem. This expression can then be used in a shape Newton method to numerically solve the minimization problem. Additionally, we plan to explore the application of the coupled complex boundary method in solving inverse obstacle problems within a shape optimization framework in our upcoming investigation.

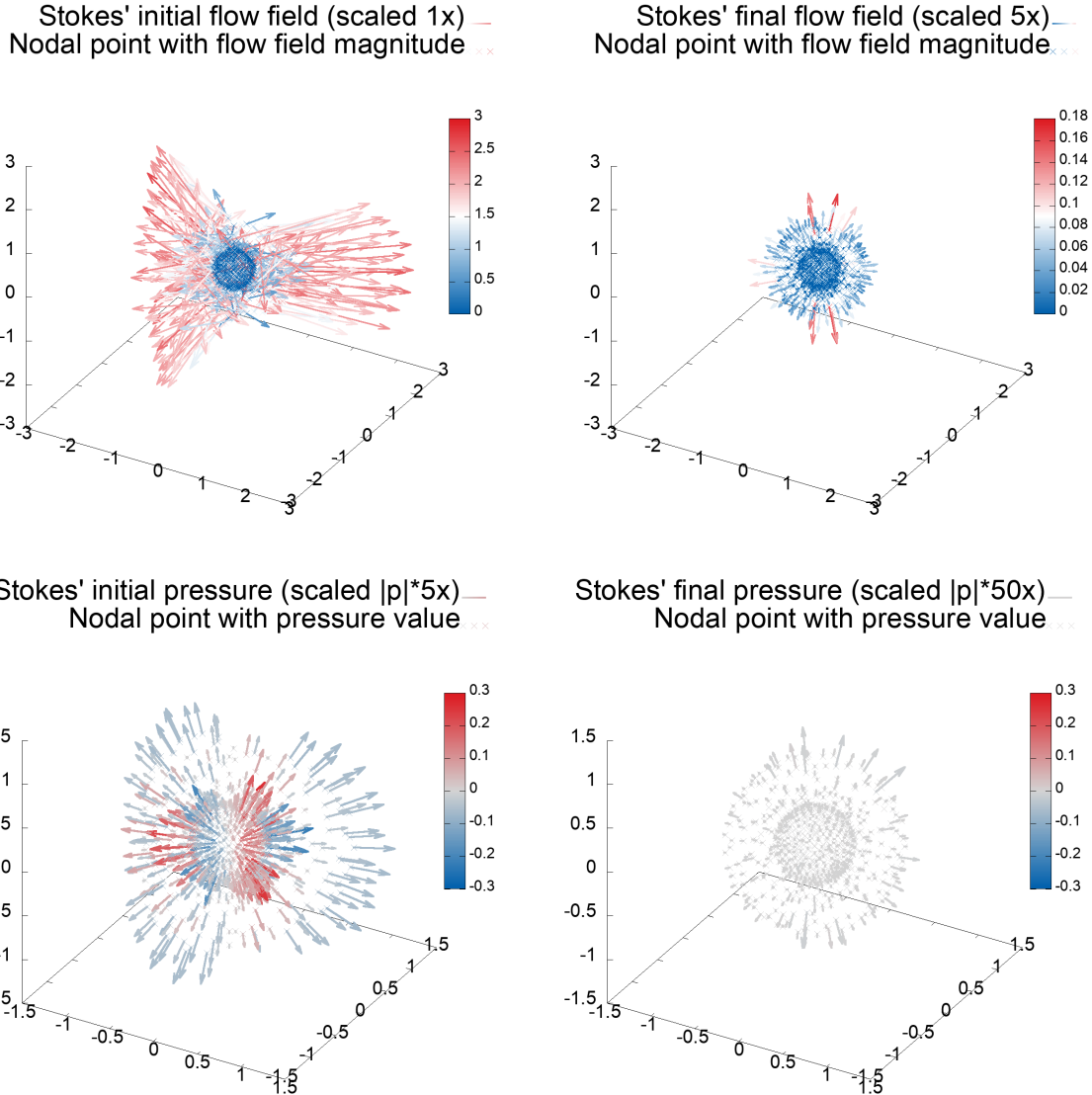


Fig. 14 Stokes' flow fields and pressure profiles at the initial and final shapes.

Acknowledgments. JFTR is partially supported by the JSPS Grant-in-Aid for Early-Career Scientists under Japan Grant Number 23K13012. HN is partially supported by JSPS Grants-in-Aid for Scientific Research under Grant Numbers JP20KK0058, JP21H04431, and JP20H01823. Both authors are also partially supported by the JST CREST Grant Number JPMJCR2014. The authors thank the three anonymous reviewers for their helpful and constructive comments that greatly contributed to improving the final version of the article.

Declarations

Conflict of interest The authors declare that they have no conflict of interest.

A On the well-posedness of the state problem

We provide here some details of the proof of Proposition 2.3. Firstly, we quote the following lemma (see, e.g., [9, Chap. 1.2]).

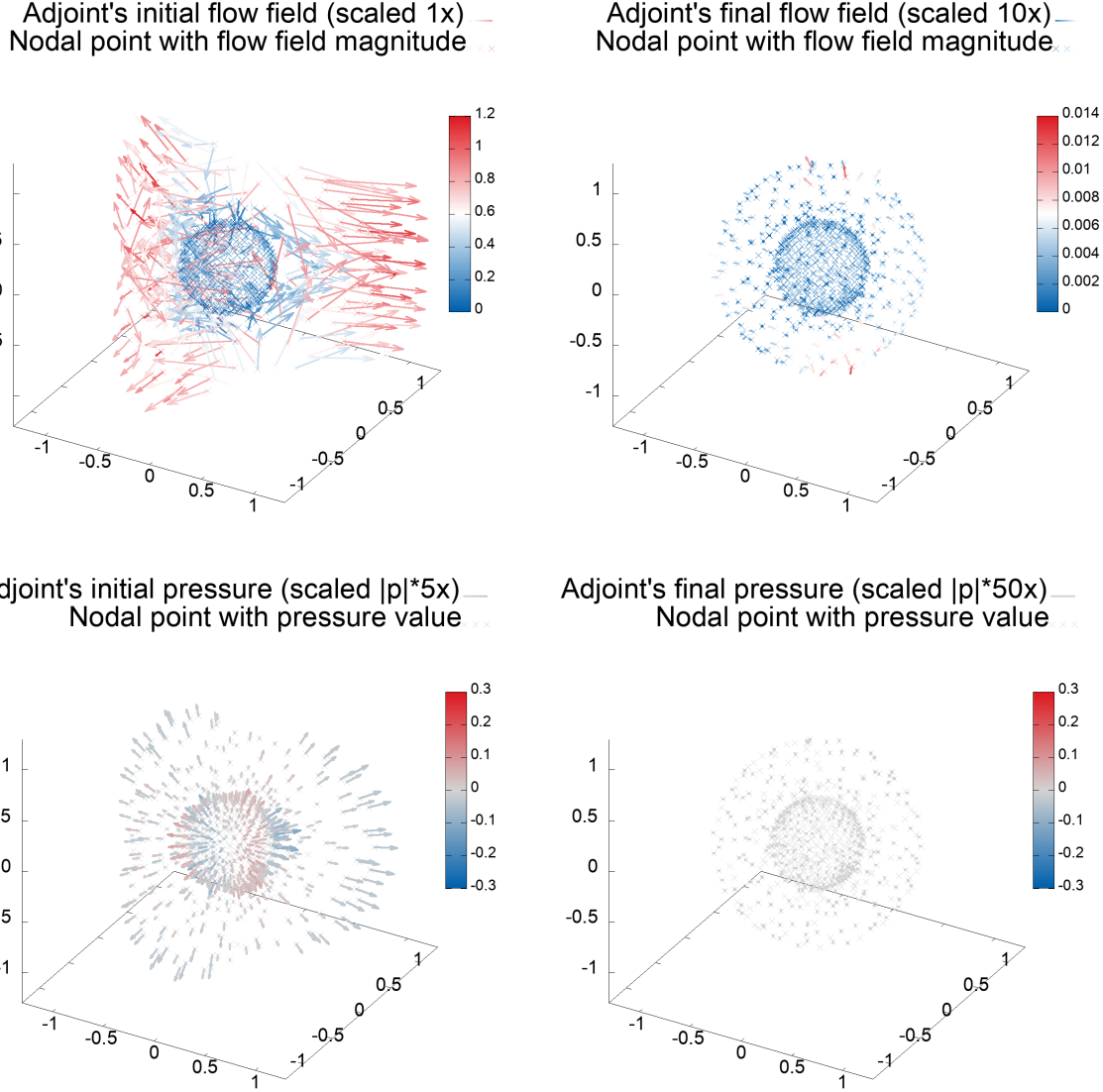


Fig. 15 Adjoint's flow fields and pressure profiles at the initial and final shapes.

Lemma A.1. Consider the maps $\mathcal{T} : \overset{\circ}{V} \mapsto \overset{\circ}{Q}$, $\mathcal{T}\varphi := -\nabla \cdot \varphi$, and $\mathcal{T}_\perp : \overset{\circ}{V}_\perp \mapsto \overset{\circ}{Q}$, $\mathcal{T}_\perp \varphi := -\nabla \cdot \varphi$. Then, \mathcal{T} is surjective, $\mathcal{T}_\perp \in \mathcal{L}(\overset{\circ}{V}, \overset{\circ}{Q})$, \mathcal{T}_\perp is bijective, and $\mathcal{T}_\perp \in \text{Isom}(\overset{\circ}{V}_\perp, \overset{\circ}{Q})$, i.e., there exists $\mathcal{T}_\perp^{-1} : \overset{\circ}{Q} \rightarrow \overset{\circ}{V}_\perp$, $\mathcal{T}_\perp^{-1} \in \mathcal{B} := \mathcal{L}(\overset{\circ}{Q}, \overset{\circ}{V}_\perp)$.

Let $\mathbf{f} \in L^2(\Omega)^d$ and $\varphi, \psi \in V_\Gamma$, $\lambda \in Q$. The continuity of the sesquilinear forms a and b as well as of the linear form F in (10) are easily verified. The same is true for the coercivity of the sesquilinear form a . Hence, we only argue about the inf-sup condition (13). For this purpose, we need to show that we can find $\beta_0 > 0$ such that

$$\sup_{\substack{\varphi \in V_\Gamma \\ \varphi \neq 0}} \frac{b(\varphi, \lambda)}{\|\varphi\|_X} \geq \beta_0 \|\lambda\|_Q, \quad \forall \lambda \in Q. \quad (\text{A.65})$$

Let $\lambda \in Q$ be fixed arbitrarily. We define $\lambda = \overset{\circ}{\lambda} + \lambda_*$ with $\overset{\circ}{\lambda} \in \overset{\circ}{Q}$ and $\lambda_* := \frac{1}{|\Omega|} \int_\Omega \lambda \, dx \in \mathbb{C}$. By Lemma A.1, there exists $\overset{\circ}{\varphi} \in \overset{\circ}{V}_\perp$ such that $-\nabla \cdot \overset{\circ}{\varphi} = \overset{\circ}{\lambda}$ ($= \mathcal{T}_\perp \overset{\circ}{\varphi}$). We let $\tilde{\varphi}_*$ be a fixed function in V_Γ such that



Fig. 16 Shape histories of the free boundary computed using TD and CCBM with finer mesh viewed on the planes xz , yx , and yz (respectively, top and bottom plots)

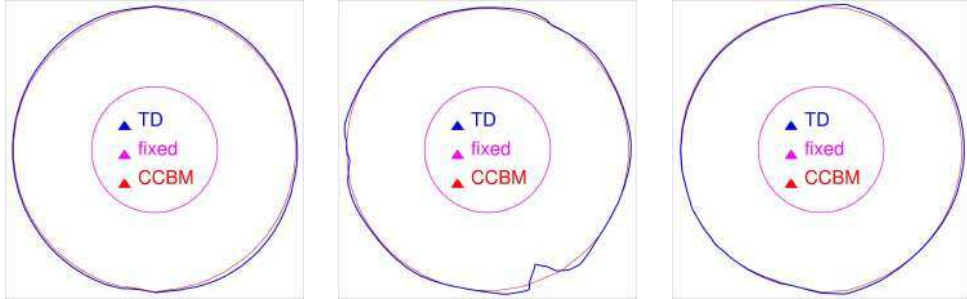


Fig. 17 Cross comparison of computed shapes under a finer mesh viewed on the planes xz , yx , and yz (respectively, left, middle, and right plot)

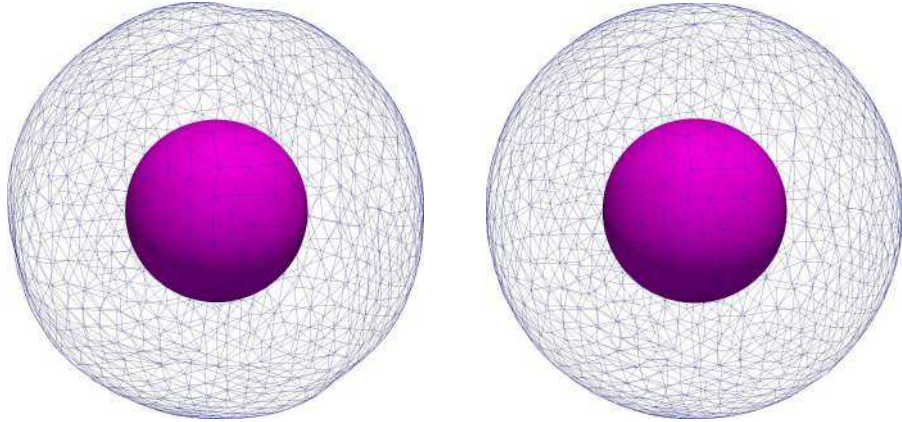


Fig. 18 Mesh profile of computed shapes (left plot: TD, right plot: CCBM) with finer mesh

$\int_{\Sigma} \tilde{\varphi}_* \cdot \mathbf{n} d\sigma \neq 0$ and define

$$\varphi_* := \tilde{\varphi}_* \left(\int_{\Sigma} \tilde{\varphi}_* \cdot \mathbf{n} d\sigma \right)^{-1} \in V_{\Gamma} \quad \text{satisfying} \quad \int_{\Sigma} \varphi_* \cdot \mathbf{n} d\sigma = -1. \quad (\text{A.66})$$

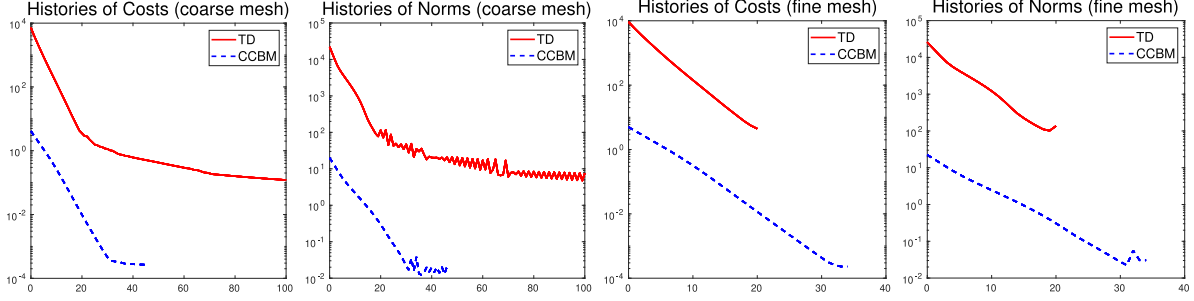


Fig. 19 Histories of cost and gradient norms

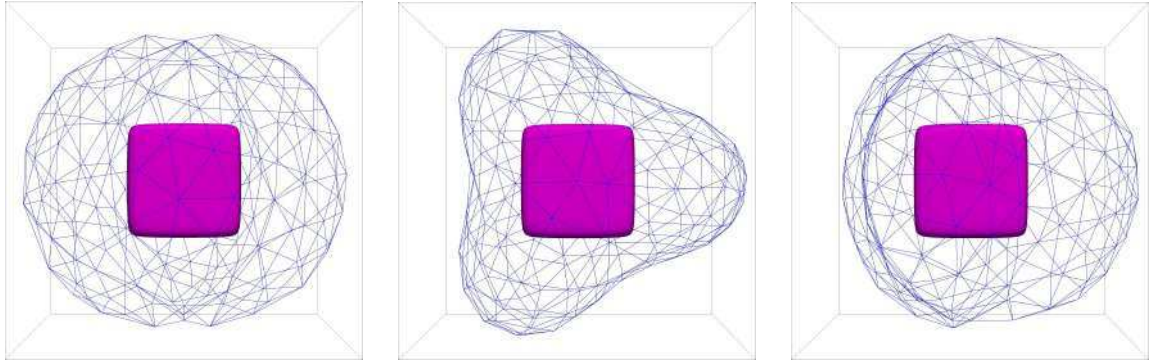


Fig. 20 Mesh profile of the initial guess viewed on different positions for problem (P5)

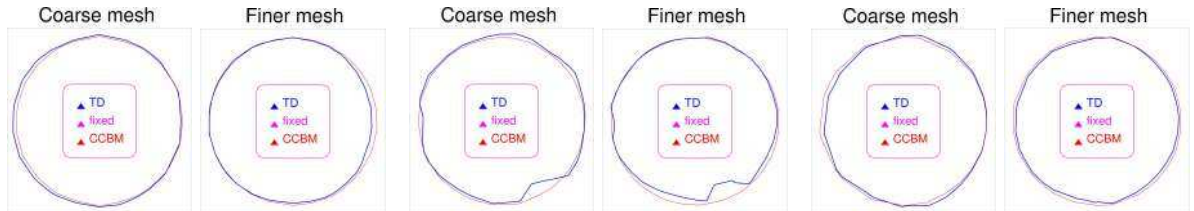


Fig. 21 Cross comparisons of computed shapes using a coarse mesh and a finer mesh viewed on planes xz , yx , and yz (respectively, left, middle, and right two columns) for problem (P5)

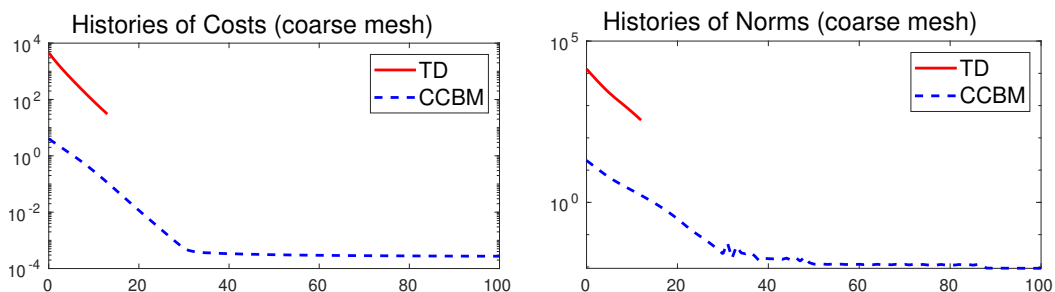


Fig. 22 Histories of cost and gradient norms under coarse mesh corresponding to problem (P5)

Now, let $\varphi = \overset{\circ}{\varphi} + t_0 \lambda_* \tilde{\varphi}_* \in V_\Gamma$ where $t_0 > 0$. Then, we obtain the inequality condition

$$\sup_{\substack{\varphi \in V_\Gamma \\ \varphi \neq 0}} \frac{b(\varphi, \lambda)}{\|\varphi\|_X} \geq \frac{b(\overset{\circ}{\varphi} + t_0 \lambda_* \tilde{\varphi}_*, \overset{\circ}{\lambda} + \lambda_*)}{\left\| \overset{\circ}{\varphi} + t_0 \lambda_* \tilde{\varphi}_* \right\|_X} =: \frac{N_1}{N_2}. \quad (\text{A.67})$$

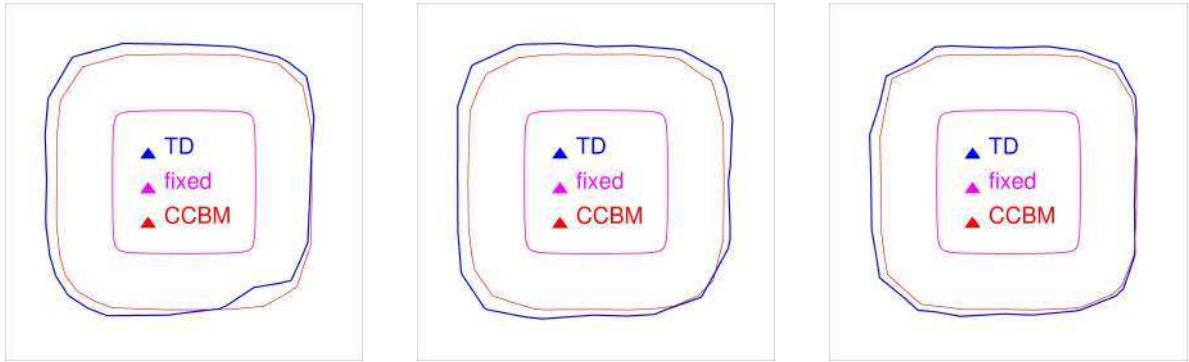


Fig. 23 Cross comparison of computed shapes under a coarse mesh viewed on the planes xz , yx , and yz (respectively, left, middle, and right plot) for problem (P6)

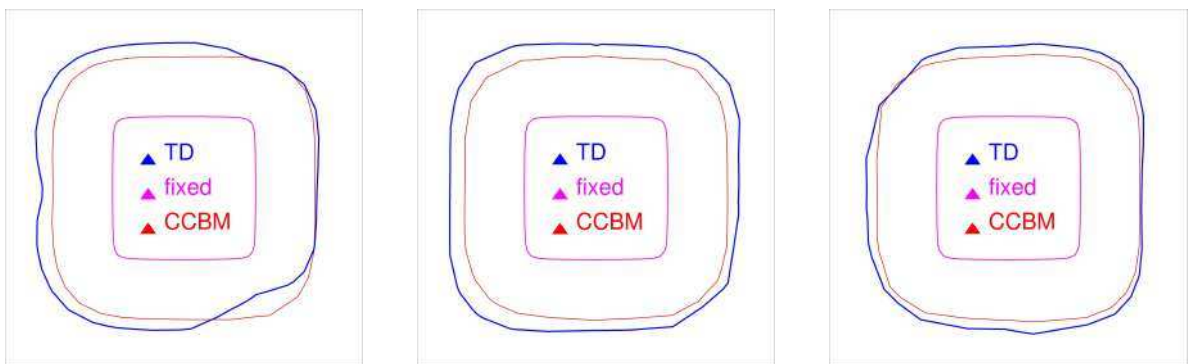


Fig. 24 Cross comparison of computed shapes under a finer mesh viewed on the planes xz , yx , and yz (respectively, left, middle, and right plot) for problem (P6)

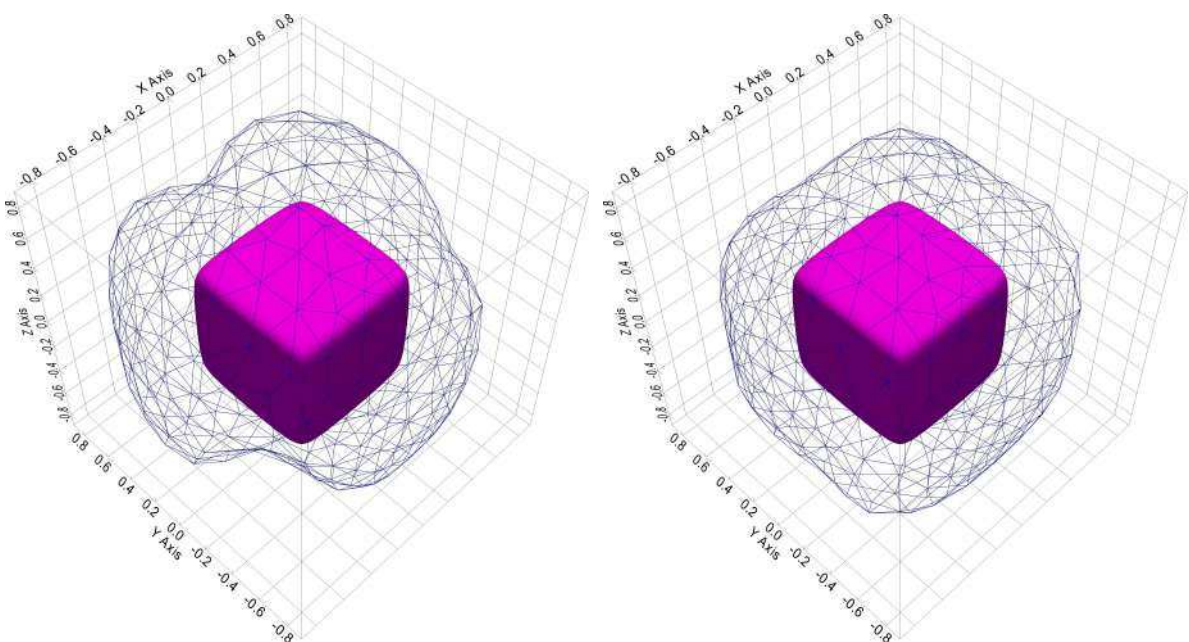


Fig. 25 Mesh profiles of the computed optimal shapes obtained via TD (left plot) and CCBM (right plot) for problem (P6)

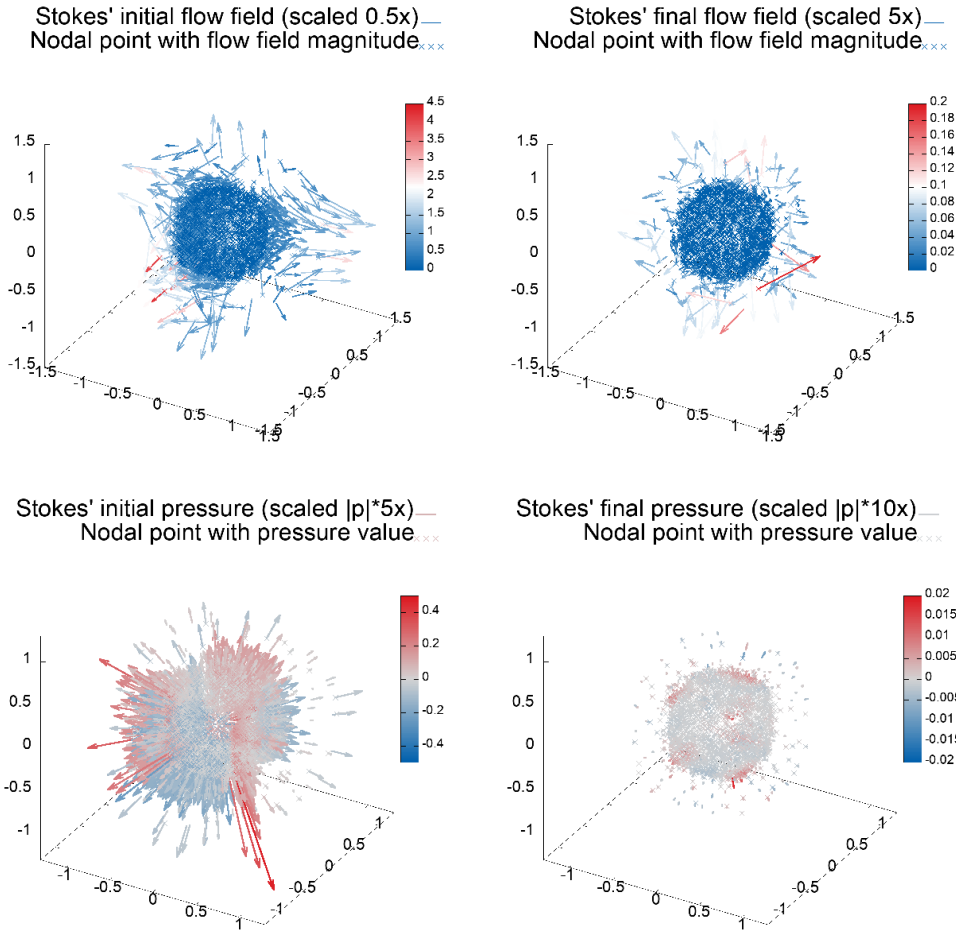


Fig. 26 Stokes' flow fields and pressure profiles at the initial and final shapes for problem (P6).

For the numerator N_1 , we have the following computations

$$\begin{aligned}
N_1 &= -(\nabla \cdot \overset{\circ}{\varphi}, \overset{\circ}{\lambda}) - (\nabla \cdot \overset{\circ}{\varphi}, \lambda_*) - t_0 \lambda_* (\nabla \cdot \widetilde{\varphi}_*, \overset{\circ}{\lambda}) - t_0 \lambda_* (\nabla \cdot \widetilde{\varphi}_*, \lambda_*) \\
&\stackrel{(1)}{=} \left\| \overset{\circ}{\lambda} \right\|_Q^2 - t_0 \lambda_* (\nabla \cdot \widetilde{\varphi}_*, \overset{\circ}{\lambda}) - t_0 \lambda_* (\nabla \cdot \widetilde{\varphi}_*, \lambda_*) \\
&\stackrel{(2)}{\geq} \left\| \overset{\circ}{\lambda} \right\|_Q^2 - t_0 |\lambda_*| \|\widetilde{\varphi}_*\|_{1,\Omega} \left\| \overset{\circ}{\lambda} \right\|_Q + t_0 |\lambda_*|^2 \\
&\stackrel{(3)}{=} \left\| \overset{\circ}{\lambda} \right\|_Q^2 - c_0 t_0 |\lambda_*| \left\| \overset{\circ}{\lambda} \right\|_Q + t_0 |\lambda_*|^2, \quad (\mathbb{R}^+ \ni c_0 = \|\widetilde{\varphi}_*\|_{1,\Omega}) \\
&\stackrel{(4)}{\geq} \left(1 - \frac{c_0 t_0}{2\varepsilon_0} \right) \left\| \overset{\circ}{\lambda} \right\|_Q^2 + t_0 \left(1 - \frac{\varepsilon_0 c_0}{2} \right) |\lambda_*|^2, \quad (\varepsilon_0 > 0), \\
&\geq \min \left\{ \left(1 - \frac{c_0 t_0}{2\varepsilon_0} \right), t_0 \left(1 - \frac{\varepsilon_0 c_0}{2} \right) \right\} \left(\left\| \overset{\circ}{\lambda} \right\|_Q^2 + |\lambda_*|^2 \right) \\
&=: c_1(c_0, t_0, \varepsilon) h(\lambda) =: c_1 h(\lambda).
\end{aligned}$$

Here, (1) is obtained from the fact that $\overset{\circ}{\varphi} \in \overset{\circ}{V}_0$ and the assumption that $-\nabla \cdot \overset{\circ}{\varphi} = \overset{\circ}{\lambda}$, (2) follows from Green's theorem, together with (A.66), (3) is due to the assumption that $\widetilde{\varphi}_*$ is fixed, so $\|\widetilde{\varphi}_*\|_{1,\Omega}$

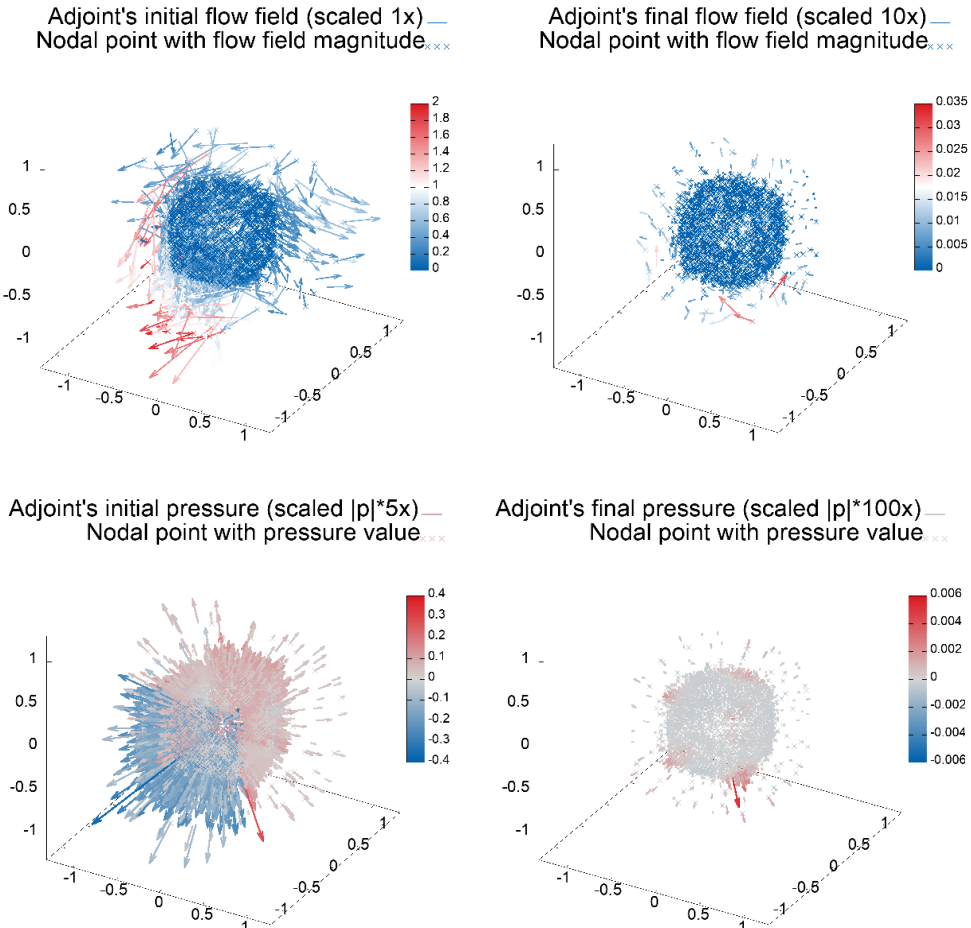


Fig. 27 Adjoints' flow fields and pressure profiles at the initial and final shapes for problem (P6).

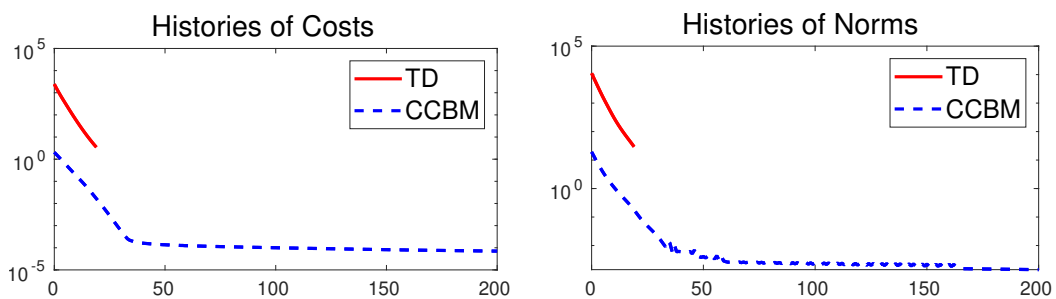


Fig. 28 Histories of cost and gradient norms under coarse mesh corresponding to problem (P6)

equates to some constant $c_0 > 0$, while inequality $\langle 4 \rangle$ is obtained because of Peter-Paul inequality¹³ applied to the product $|\lambda_*| \left\| \overset{\circ}{\lambda} \right\|_Q$.

¹³Here, of course, $\varepsilon_0 > 0$ is chosen such that $c_1 > 0$. For example, this condition holds if we choose $\varepsilon_0 = c_0^{-1} > 0$ and $t_0 = \varepsilon c_0^{-1} = c_0^{-2} > 0$.

Let us further estimate below the sum $h(\lambda)$. Note that

$$\|\lambda\|_Q^2 = \left\| \overset{\circ}{\lambda} + \lambda_* \right\|_Q^2 = \left\| \overset{\circ}{\lambda} \right\|_Q^2 + |\lambda_*|^2 |\Omega| \begin{cases} \leqslant \max\{1, |\Omega|\} h(\lambda) =: c_2^{-1} h(\lambda) \\ \geqslant \min\{1, |\Omega|\} h(\lambda) =: c_3^{-1} h(\lambda). \end{cases}$$

Thus, there actually exist constants $c_2, c_3 > 0$ such that $c_2 \|\lambda\|_Q^2 \leqslant h(\lambda) \leqslant c_3 \|\lambda\|_Q^2$. By these inequalities, we get an estimate for the numerator in (A.67):

$$b(\overset{\circ}{\varphi} + t_0 \lambda_* \tilde{\varphi}_*, \overset{\circ}{\lambda} + \lambda_*) \geqslant c_1 c_2 \|\lambda\|_Q^2. \quad (\text{A.68})$$

For the denominator N_2 in (A.67), we have the following estimations

$$\begin{aligned} N_2 &= \left\| \mathcal{T}_{\perp}^{-1} \overset{\circ}{\lambda} \right\|_{1,\Omega} + t_0 c_0 |\lambda_*| \leqslant \left\| \mathcal{T}_{\perp}^{-1} \right\|_{\mathcal{B}} \left\| \overset{\circ}{\lambda} \right\|_Q + t_0 c_0 |\lambda_*| \\ &\leqslant \sqrt{2} \max \left\{ \left\| \mathcal{T}_{\perp}^{-1} \right\|_{\mathcal{B}}, t_0 c_0 \right\} \left(\left\| \overset{\circ}{\lambda} \right\|_Q^2 + |\lambda_*|^2 \right)^{1/2} \\ &\leqslant \sqrt{2c_3} \max \left\{ \left\| \mathcal{T}_{\perp}^{-1} \right\|_{\mathcal{B}}, t_0 c_0 \right\} \|\lambda\|_Q. \end{aligned}$$

In above, we have used the fact that \mathcal{T}_{\perp}^{-1} is a bounded linear operator. Accordingly, $\|\cdot\|_{\mathcal{B}}$ denotes the operator norm for linear operators in $\mathcal{B} = \mathcal{L}(\overset{\circ}{Q}, \overset{\circ}{V}_{\perp})$. Combining the above estimate with (A.68), we finally get

$$\sup_{\substack{\varphi \in V_{\Gamma} \\ \varphi \neq 0}} \frac{b(\varphi, \lambda)}{\|\varphi\|_X} \geqslant \frac{N_1}{N_2} \geqslant \frac{c_1 c_2 \|\lambda\|_Q^2}{\sqrt{2c_3} \max \left\{ \left\| \mathcal{T}_{\perp}^{-1} \right\|_{\mathcal{B}}, t_0 c_0 \right\} \|\lambda\|_Q} =: \beta_0 \|\lambda\|_Q.$$

This proves (A.65), and thus (13).

B Computations of some identities

B.1 Expansion of I_t

We expand the determinant $I_t := \det(DT_t)$. Denoting the Kronecker delta function by δ_{ij} , the Jacobian of $T_t := id + t\theta$, $\theta \in \Theta^1$, is given by

$$DT_t = (M_{ij})_{1 \leqslant i,j \leqslant d}, \quad \text{where } M_{ij} = \delta_{ij} + t \frac{\partial V_i}{\partial x_j} =: \delta_{ij} + t m_{ij}, \quad \text{for } 1 \leqslant i, j \leqslant d.$$

Let \mathcal{S}_d be the set of all permutations of $N_d := \{1, \dots, d\}$ and sgn be the signum of the permutation σ of N_d (i.e., it is equal to $+1$ or -1 according to whether the minimum number of transpositions (pairwise interchanges) necessary to achieve it starting from N_d is even or odd). Moreover, let $\mathcal{I}_d := \{\sigma \in \mathcal{I}_d : \sigma(j) = j, j \in N'_d \subseteq N_d\}$ and ι be the identity permutation. By definition of the determinant [51, p. 29], we have

$$\begin{aligned} I_t &= \sum_{\sigma \in \mathcal{S}_d} \left(\text{sgn } \sigma \prod_{i=1}^d M_{i\sigma(i)} \right) \\ &= \sum_{\sigma=\iota} \prod_{i=1}^d \left(1 + t \frac{\partial V_i}{\partial x_i} \right) + \sum_{\sigma \in \mathcal{I}_d \setminus \{\iota\}} \left(\text{sgn } \sigma \prod_{i=1}^d M_{i\sigma(i)} \right) + \sum_{\sigma \in \mathcal{S}_d \setminus \mathcal{I}_d} \left(\text{sgn } \sigma \prod_{i=1}^d M_{i\sigma(i)} \right) \\ &=: S_1 + S_2 + S_3. \end{aligned}$$

Observe that we may write, for some function $\rho_1 \in \mathcal{C}^0 := \mathcal{C}(\mathbb{R}, \mathcal{C}^{0,1}(U))$, the first summand as $S_1 = 1 + t \operatorname{div} \theta + t^2 \rho_1(t, \theta)$. In addition, we can write the second sum as $t^2 \rho_2(t, \theta)$, for some function $\rho_2 \in \mathcal{C}^0$,

since each term S_2 consists of at least two factors of tm_{ij} , $i \neq j$, $i, j \in N_d$, $d \in \mathbb{N} \setminus \{1\}$. Meanwhile, all terms of S_3 have factors of the form tm_{ij} , $i \neq j$. So, the sum S_3 can be expressed as $t^d \rho_*(\boldsymbol{\theta})$ which can be written as $t^2 \rho_3(t, \boldsymbol{\theta})$, for some function $\rho_3 \in \mathcal{C}^0$. All together, we observe that $I_t = 1 + t \operatorname{div} \boldsymbol{\theta} + t^2 \tilde{\rho}(t, \boldsymbol{\theta})$, for some function $\tilde{\rho} \in \mathcal{C}^0$.

B.2 Derivative of $B_t |M_t \mathbf{n}|^{-2}$

Here we compute the derivative of $B_t |M_t \mathbf{n}|^{-2}$. Let us first recall that $B_t = I_t |M_t \mathbf{n}|$ and $M_t = (DT_t)^{-\top}$, and $B_0 = 1$ and $|M_0 \mathbf{n}| = |id\mathbf{n}| = |\mathbf{n}| = 1$. Then, considering two (column) vectors $\mathbf{a} := (a_1, \dots, a_d)^\top, \mathbf{b} := (b_1, \dots, b_d)^\top \in \mathbb{R}^d$ we have the following computations¹⁴

$$\frac{d}{dt} (|\mathbf{a} - t\mathbf{b} + O(t^2)|^2) = \sum_{i=1}^d 2(a_i - tb_i + O(t^2)) \cdot (-b_i + O(t)) = 2(-\mathbf{a} \cdot \mathbf{b} + O(t)).$$

Now, note that $M_t \mathbf{n} = (DT_t)^{-\top} \mathbf{n} = (id + tD\boldsymbol{\theta})^{-\top} \mathbf{n} = [id - t(D\boldsymbol{\theta})^\top + \tilde{R}(t)]\mathbf{n}$ (see (35)), where $\tilde{R}(t)$ is a $d \times d$ -matrix and is of order $O(t^2)$. Hence, considering (22) and the differentiability of $M_t \mathbf{n}$ is differentiable with respect to t , we derive the subsequent calculations from the earlier computation:

$$\frac{d}{dt} |M_t \mathbf{n}|^2 \Big|_{t=0} = \frac{d}{dt} \left(|\mathbf{n} - t(D\boldsymbol{\theta})^\top + \tilde{R}(t)|^2 \right) \Big|_{t=0} = -2\mathbf{n} \cdot [(D\boldsymbol{\theta})^\top \mathbf{n}] = -2(D\boldsymbol{\theta} \mathbf{n}) \cdot \mathbf{n}.$$

Finally, using the derivative $\frac{d}{dt} B_t \Big|_{t=0} = \operatorname{div} \boldsymbol{\theta} \Big|_\Sigma - (D\boldsymbol{\theta} \mathbf{n}) \cdot \mathbf{n}$, we get

$$\frac{d}{dt} \left(\frac{B_t}{|M_t \mathbf{n}|^2} \right) \Big|_{t=0} = \frac{\left(\frac{d}{dt} B_t \right) |M_t \mathbf{n}|^2 - B_t \left(\frac{d}{dt} |M_t \mathbf{n}|^2 \right)}{|M_t \mathbf{n}|^4} \Big|_{t=0} = \operatorname{div} \boldsymbol{\theta} \Big|_\Sigma + (D\boldsymbol{\theta} \mathbf{n}) \cdot \mathbf{n}.$$

C Computation of the shape gradient via chain rule

To validate the expression for the shape gradient, we give below the computation of the expression g_Σ under a $\mathcal{C}^{2,1}$ regularity assumption on the domain, supposing in addition that $\mathbf{f} \in H_{loc}^1(\mathbb{R}^d)^d$, specifically, we assume $\mathbf{f} \in H^1(U)^d$, where U is a fixed convex bounded open set in \mathbb{R}^d such that $U \supset \bar{\Omega}$. We note that the given regularity guarantees the existence of the material and the shape derivative of the state and because of this, the shape gradient of the cost can easily be established using Hadamard's domain differentiation formula: (see, e.g., [37, Thm. 4.2, p. 483]), [38, eq. (5.12), Thm. 5.2.2, p. 194] or [41, eq. (2.168), p. 113]):

$$\left\{ \frac{d}{dt} \int_{\Omega_t} f(t, x) dx_t \right\} \Big|_{t=0} = \int_{\Omega} \frac{\partial}{\partial t} f(0, x) dx + \int_{\partial\Omega} f(0, \sigma) \theta_n d\sigma \quad (\text{C.69})$$

(of course, with the assumption that the perturbation of Ω preserves its regularity).

Next, we restate Theorem 3.4, but with higher regularity assumption.

Theorem C.1. *Let $\Omega \in \mathcal{C}^{2,1}$ and $\boldsymbol{\theta} \in \Theta^2$. Then, the shape derivative of J at Ω along $\boldsymbol{\theta}$ is given by $dJ(\Omega)[\boldsymbol{\theta}] = \int_{\Sigma} g_\Sigma \theta_n d\sigma$, where g_Σ is the expression in (26).*

Before we prove the above theorem, we briefly prepare the following lemmata which will be useful in the derivation of the shape derivative.

Lemma C.2. *Let $\Omega \in \Theta^2$ and \mathbf{n} be the outward unit normal to Σ . Then, it holds that $D\tilde{\mathbf{n}}\mathbf{n} = (D\tilde{\mathbf{n}})^\top \mathbf{n} = (\nabla \tilde{\mathbf{n}})\mathbf{n} = 0$ on Σ , where $\tilde{\mathbf{n}}$ is a unitary \mathcal{C}^1 extension of the outward unit normal vector \mathbf{n} to Σ .*

¹⁴Here, the expression $O(t)$ represents a generic remainder term.

Throughout the rest of this appendix, we will write the operator $\frac{\partial}{\partial x_j}$ simply as ∂_j .

Proof. Because Ω is $C^{2,1}$ regular, then by Proposition 5.4.8 of [38, p. 218] (see also [52, Lem. 16.1, p. 390]), there exists a C^1 unitary extension $\tilde{\mathbf{n}} := (\tilde{n}_1, \dots, \tilde{n}_d)^\top$ ¹⁵ of \mathbf{n} . So, in an open neighborhood of Σ , we have $|\tilde{\mathbf{n}}|^2 = \langle \tilde{\mathbf{n}}, \tilde{\mathbf{n}} \rangle = 1$. Thus, for each $j = 1, \dots, d$, we have $\partial_j(|\tilde{\mathbf{n}}|^2) = \partial_j(\tilde{n}_i^2) = 2\tilde{n}_i \partial_j \tilde{n}_i = 0$, or equivalently,

$$\nabla(|\tilde{\mathbf{n}}|^2) = \nabla(\tilde{n}_i^2) = 2\tilde{n}_i \nabla \tilde{n}_i = 2\tilde{n}_i (\partial_j \tilde{n}_i \mathbf{e}_j) = \mathbf{0}, \quad (\text{C.70})$$

where $\mathbf{e}_j := (\underbrace{0, \dots, 0}_{j}, 1, 0, \dots, 0)^\top \in \mathbb{R}^d$ is the j th vector of the canonical basis in \mathbb{R}^d . So, we have $(D\tilde{\mathbf{n}})^\top \tilde{\mathbf{n}} = (\partial_k \tilde{n}_i \tilde{n}_j) \mathbf{e}_k$. Comparing this with equation (C.70), we deduce that $\langle (D\tilde{\mathbf{n}})\mathbf{n}, \mathbf{n} \rangle = \langle \mathbf{n}, (D\tilde{\mathbf{n}})^\top \mathbf{n} \rangle = 0$ on Γ from which we infer the conclusion. \square

Remark C.3. In light of the previous lemma, and recalling the definition of the tangential Jacobian matrix from Definition 3.1, we see that for the C^1 unitary extension $\tilde{\mathbf{n}}$ of \mathbf{n} , we clearly have the identity $D\tilde{\mathbf{n}}|_{\Sigma} = D\mathbf{n} = D_{\Sigma}\mathbf{n} = (D_{\Sigma}\mathbf{n})^\top$ (refer to [37, eq. (5.17) – (5.19), p. 497] for the last equation).

Lemma C.4. Let $\Omega \in \Theta^2$ and \mathbf{n} be the outward unit normal to Σ . Then, for the solution \mathbf{u} of (7), we have $\partial_{\mathbf{n}}(\mathbf{u} \cdot \mathbf{n}) = \partial_{\mathbf{n}}\mathbf{u} \cdot \mathbf{n}$ on Σ .

Proof. Firstly, we note that $\partial_{\mathbf{n}} n_j = \mathbf{n}^\top \nabla n_j n_k \partial_k n_j$. Moreover, from the proof of the previous lemma, we know that $(D\tilde{\mathbf{n}})\tilde{\mathbf{n}} = (\partial_j \tilde{n}_k \tilde{n}_j) \mathbf{e}_k = \mathbf{0}$ from which it can be deduced that $n_j \partial_j n_k = 0$ on Σ , for all $k = 1, \dots, d$. In addition, we have the following identity

$$\partial_{\mathbf{n}} \mathbf{u} \cdot \mathbf{n} = (D\mathbf{u})\mathbf{n} \cdot \mathbf{n} = (\partial_j u_k n_j) \mathbf{e}_k \cdot n_i \mathbf{e}_i = (\partial_j u_k n_j) n_k. \quad (\text{C.71})$$

Here, we have used the identity $\mathbf{e}_i \cdot \mathbf{e}_j = \delta_{ij}$ and δ_{ij} is the Kronecker delta function. Thus, we get the equation $\partial_{\mathbf{n}}(\mathbf{u} \cdot \mathbf{n}) = \partial_{\mathbf{n}}(u_k n_k) = (\partial_{\mathbf{n}} u_k n_k + u_k \partial_{\mathbf{n}} n_k) = (n_j \partial_j u_k) n_k$. The desired identity then follows by comparing the previous equation with (C.71). \square

Lemma C.5. Let $\Omega \in \Theta^2$ and \mathbf{n} be the outward unit normal to Σ . Then, for the solution \mathbf{u} of (7), we have $\partial_{\mathbf{n}}[(\mathbf{u} \cdot \mathbf{n})\mathbf{n}] = [\partial_{\mathbf{n}}(\mathbf{u} \cdot \mathbf{n})]\mathbf{n}$ on Σ .

Proof. Let $\tilde{\mathbf{n}}$ be the C^1 extension of \mathbf{n} as before and denote $\mathbf{b} = a\tilde{\mathbf{n}} := (u_i \tilde{n}_i) \tilde{\mathbf{n}}$ with $\mathbf{b} := (b_1, \dots, b_d) = (a\tilde{n}_1, \dots, a\tilde{n}_d)$. Note that

$$(D\mathbf{b})\tilde{\mathbf{n}} = (\partial_j b_k \tilde{n}_j) \mathbf{e}_k. \quad (\text{C.72})$$

Moreover, we have the identity $\partial_j b_k = \partial_j(a\tilde{n}_k) = (\partial_j u_i \tilde{n}_i + u_i \partial_j \tilde{n}_i)\tilde{n}_k + (u_i \tilde{n}_i) \partial_j \tilde{n}_k$. Inserting this expression to (C.72), and then applying Lemma C.4, we get

$$\begin{aligned} (D\mathbf{b})\tilde{\mathbf{n}} &= ([(\partial_j u_i \tilde{n}_i) \tilde{n}_k] \tilde{n}_j) \mathbf{e}_k + ([u_i \tilde{n}_i] \partial_j \tilde{n}_k) \tilde{n}_j \mathbf{e}_k \\ &= (D\mathbf{u}\tilde{\mathbf{n}} \cdot \mathbf{n}) \tilde{n}_k \mathbf{e}_k + u_n (\partial_j \tilde{n}_k \tilde{n}_j) \mathbf{e}_k = (D\mathbf{u}\tilde{\mathbf{n}} \cdot \tilde{\mathbf{n}}) \tilde{\mathbf{n}}. \end{aligned}$$

Thus, we have $\partial_{\mathbf{n}}[(\mathbf{u} \cdot \mathbf{n})\mathbf{n}] = [\partial_{\mathbf{n}}(\mathbf{u} \cdot \mathbf{n})]\mathbf{n}$ on Σ , as desired. \square

¹⁵The same is used in Lemma C.4 and Lemma C.5.

Proof of Proposition C.1. Let us assume that Ω is of class $C^{2,1}$ and $\boldsymbol{\theta} \in \Theta^2$. Using classical regularity theory, we have $\mathbf{u}_r, \mathbf{u}_i \in H^3(\Omega)^d$ and $p_r, p_i \in H^2(\Omega)$. Because we have sufficient regularity for \mathbf{u}, p, Ω , and $\boldsymbol{\theta}$, then we can apply formula (C.69) to obtain – noting that $\boldsymbol{\theta} = \mathbf{0}$ on Γ – the derivative

$$dJ(\Omega)[\boldsymbol{\theta}] = \int_{\Omega} (\mathbf{u}_i \cdot \mathbf{u}'_i + p_i p'_i) dx + \frac{1}{2} \int_{\Sigma} (|\mathbf{u}_i|^2 + |p_i|^2) \theta_n d\sigma =: \mathbb{I}_1 + \mathbb{I}_2. \quad (\text{C.73})$$

Hereafter, we proceed in four steps:

Step 1. We establish the strong form of the shape derivatives \mathbf{u}' and p' which is characterized by the complex PDE system (C.78).

Step 2. We prove the differentiability of $J(\Omega)$ in the direction of $(\delta \tilde{\mathbf{u}}, \delta \tilde{p}) \in X \times Q$.

Step 3. We justify the structure of the adjoint system (27).

Step 4. We obtain the expression for the shape gradient via the adjoint method.

Step 1. We recall the variational equation (11). Because Ω, \mathbf{u}, p , and $\boldsymbol{\theta}$ are regular enough, then the solution $(\mathbf{u}, p) \in X \times Q$ is shape differentiable and we can differentiate (11) (formally) to get

$$\begin{aligned} & \int_{\Omega} \alpha \nabla \mathbf{u}' : \nabla \bar{\psi} dx + i \int_{\Sigma} (\mathbf{u}' \cdot \mathbf{n}) \bar{\psi}_n d\sigma - \int_{\Omega} p' (\nabla \cdot \bar{\psi}) dx - \int_{\Omega} \bar{\lambda} (\nabla \cdot \mathbf{u}') dx \\ &= - \int_{\Sigma} \alpha (\nabla \mathbf{u} : \nabla \bar{\psi} - p (\nabla \cdot \bar{\psi})) \theta_n d\sigma - i \int_{\Sigma} \mathbf{u} \cdot \mathbf{n}' \bar{\psi}_n d\sigma - i \int_{\Sigma} u_n \bar{\psi} \cdot \mathbf{n}' d\sigma \\ & \quad - i \int_{\Sigma} \left[\frac{\partial}{\partial \mathbf{n}} ((u_n) \mathbf{n}) + \kappa u_n \mathbf{n} \right] \cdot \bar{\psi} \theta_n d\sigma + \int_{\Sigma} \mathbf{f} \cdot \bar{\psi} \theta_n d\sigma, \end{aligned} \quad (\text{C.74})$$

where the shape derivative \mathbf{n}' of the normal vector \mathbf{n} is given by $\mathbf{n}' = -\nabla_{\Sigma} \theta_n$ (see part of the proof of Proposition 5.4.14 in [38, p. 222] for this identity).

From the previous equation we can derive a BVP for (\mathbf{u}', p') . Namely, choosing $\psi \in \mathcal{C}_0^\infty(\Omega)^d$ and $\lambda \in \mathcal{C}_0^\infty(\Omega)$ ¹⁶ reveals that (via IBP)

$$-\alpha \Delta \mathbf{u}' + \nabla p' = \mathbf{0} \quad \text{in } \Omega \quad \text{and} \quad \nabla \cdot \mathbf{u}' = \mathbf{0} \quad \text{in } \Omega, \quad (\text{C.75})$$

which hold in the distributional sense. That is, we have obtained the first equation above from

$$\langle -\alpha \Delta \mathbf{u}' + \nabla p', \bar{\psi} \rangle_{[\mathcal{C}_0^\infty(\Omega)^d]', \mathcal{C}_0^\infty(\Omega)^d} = \int_{\Omega} (\alpha \nabla \mathbf{u}' : \nabla \bar{\psi} - p' (\nabla \cdot \bar{\psi})) dx = 0,$$

and the second one from a similar argument, i.e., we check that $\nabla \cdot \mathbf{u}' = \mathbf{0}$ in $[\mathcal{C}_0^\infty(\Omega)^d]'$.

Meanwhile, because $\boldsymbol{\theta} \in \Theta^2$, i.e., $\boldsymbol{\theta}$ vanishes on Γ , the boundary condition on Γ satisfied by \mathbf{u}' easily follows. That is, we have $\mathbf{u}' = \mathbf{0}$ on Γ .

To proceed further, we underline here that $\Omega \in C^{2,1}$, and since we have that $(\mathbf{u}, p) \in \mathbf{H}^3(\Omega)^d \times \mathbf{H}^2(\Omega)$, we know that $\nabla \mathbf{u}' \in \mathbf{L}^2(\Omega)^{d \times d}$ and $\nabla p' \in \mathbf{L}^2(\Omega)^d$.

We next exhibit the boundary condition on Σ . We choose¹⁷ $\varphi \in \mathcal{C}^\infty(\Sigma)^d$ and $\mu \in \mathcal{C}^\infty(\Sigma)$. Accordingly, we can find an extension $\psi \in \mathcal{C}^\infty(\Omega)^d$ and $\lambda \in \mathcal{C}^\infty(\Omega)$ such that $\psi|_{\Sigma} = \varphi$ and $\lambda|_{\Sigma} = \mu$, and $\partial_{\mathbf{n}} \psi|_{\Sigma} = \mathbf{0}$

¹⁶For clarity, we mention here that there is slight abuse of notations. Specifically, $\psi \in \mathcal{C}_0^\infty(\Omega)^d$ and $\lambda \in \mathcal{C}_0^\infty(\Omega)$ means that $\psi_r, \psi_i \in \mathcal{C}_0^\infty(\Omega)^d$ and $\lambda_r, \lambda_i \in \mathcal{C}_0^\infty(\Omega)$ where $\mathcal{C}_0^\infty(\Omega)^d$ and $\mathcal{C}_0^\infty(\Omega)$ denotes the usual space of infinitely differentiable (vector-valued and scalar-valued) functions, respectively.

¹⁷Here we choose a test function $\psi \in \mathbf{H}^2(\Omega)^d$, and because $\Omega \in C^{2,1}$, it follows that – by Stein's extension theorem [53, Thm. 5.24, p. 154] – we can construct an extension of ψ in $\mathbf{H}^2(\mathbb{R}^{d \times d})$ (still denoted by ψ).

and $\partial_{\mathbf{n}} \lambda|_{\Sigma} = 0$. Applying IBP on the left hand side of (C.74) and using (C.75), we get

$$\begin{aligned} & \int_{\Sigma} [\alpha \partial_{\mathbf{n}} \mathbf{u}' + i(\mathbf{u}' \cdot \mathbf{n}) \mathbf{n} - p' \mathbf{n}] \cdot \bar{\psi} d\sigma \\ &= - \int_{\Sigma} [\alpha \nabla \mathbf{u} : \nabla \bar{\psi} - p(\nabla \cdot \bar{\psi})] \theta_n d\sigma + \int_{\Sigma} \mathbf{B}_1[\theta_n] \cdot \bar{\psi} d\sigma, \end{aligned}$$

where $\mathbf{B}_1[\theta_n] := -i[(\mathbf{u} \cdot \mathbf{n}') \mathbf{n} + u_n \mathbf{n}'] - i[\partial_{\mathbf{n}}(u_n \mathbf{n}) + \kappa u_n \mathbf{n}] \theta_n + \mathbf{f} \theta_n$. At this juncture, let us recall the definition of tangential gradient and divergence from subsection 3.2, to deduce the identity

$$\int_{\Sigma} p \nabla \cdot \bar{\psi} \theta_n d\sigma = \int_{\Sigma} [p \operatorname{div}_{\Sigma} \bar{\psi} + \partial_{\mathbf{n}} \bar{\psi} \cdot (p \mathbf{n})] \theta_n d\sigma,$$

and make use of the identities $(\partial_{\mathbf{n}} \mathbf{u} \otimes \mathbf{n}) : (\partial_{\mathbf{n}} \bar{\psi} \otimes \mathbf{n}) = \partial_{\mathbf{n}} \mathbf{u} \cdot \partial_{\mathbf{n}} \bar{\psi}$ and $\nabla \mathbf{u} : (\partial_{\mathbf{n}} \bar{\psi} \otimes \mathbf{n}) = \partial_{\mathbf{n}} \mathbf{u} \cdot \partial_{\mathbf{n}} \bar{\psi} = \nabla \bar{\psi} : (\partial_{\mathbf{n}} \mathbf{u} \otimes \mathbf{n})$ (cf. equation in remark found in [41, p. 87]) to obtain

$$\nabla \mathbf{u} : \nabla \bar{\psi} = \nabla_{\Sigma} \mathbf{u} : \nabla_{\Sigma} \bar{\psi} + \partial_{\mathbf{n}} \mathbf{u} \cdot \partial_{\mathbf{n}} \bar{\psi}.$$

Using the tangential Green's formula and applying IBP on Σ , we can write

$$\begin{aligned} & \int_{\Sigma} p \theta_n \operatorname{div}_{\Sigma} \bar{\psi} d\sigma = \int_{\Sigma} [\kappa p \theta_n \mathbf{n} - \nabla_{\Sigma}(p \theta_n)] \cdot \bar{\psi} d\sigma =: \int_{\Sigma} \mathbf{B}_2[\theta_n] \cdot \bar{\psi} d\sigma, \\ & - \int_{\Sigma} \alpha(\nabla_{\Sigma} \mathbf{u} : \nabla_{\Sigma} \bar{\psi}) \theta_n d\sigma = \int_{\Sigma} \bar{\psi} \cdot \{\operatorname{div}_{\Sigma} [\alpha(\nabla_{\Sigma} \mathbf{u}) \theta_n] - [\alpha \kappa(\nabla_{\Sigma} \mathbf{u}) \theta_n \mathbf{n}]\} d\sigma \\ &= \int_{\Sigma} \bar{\psi} \cdot \{\operatorname{div}_{\Sigma} [\alpha(\nabla_{\Sigma} \mathbf{u}) \theta_n]\} d\sigma =: \int_{\Sigma} \bar{\psi} \cdot \mathbf{B}_3[\theta_n] d\sigma, \end{aligned} \quad (\text{C.76})$$

where the last equality is due to the fact that $\nabla_{\Sigma} \mathbf{u} \mathbf{n} = \mathbf{0}$. Using these identities, together with the fact that $-\alpha \partial_{\mathbf{n}} \mathbf{u} + p \mathbf{n} = i u_n \mathbf{n}$ and $\partial_{\mathbf{n}} \bar{\psi} = \mathbf{0}$ on Σ , we get

$$\begin{aligned} & \int_{\Sigma} (\alpha \partial_{\mathbf{n}} \mathbf{u}' + i(\mathbf{u}' \cdot \mathbf{n}) \mathbf{n} - p' \mathbf{n}) \cdot \bar{\psi} d\sigma \\ &= - \int_{\Sigma} \alpha(\nabla_{\Sigma} \mathbf{u} : \nabla_{\Sigma} \bar{\psi} - p(\nabla_{\Sigma} \cdot \bar{\psi})) \theta_n d\sigma + i \int_{\Sigma} u_n \mathbf{n} \theta_n \cdot \partial_{\mathbf{n}} \bar{\psi} d\sigma + \int_{\Sigma} \mathbf{B}_1 \cdot \bar{\psi} d\sigma \\ &= \int_{\Sigma} \mathbf{B}[\theta_n] \cdot \bar{\psi} d\sigma, \end{aligned}$$

where

$$\begin{aligned} \mathbf{B}[\theta_n] &:= \mathbf{B}_1[\theta_n] + \mathbf{B}_2[\theta_n] + \mathbf{B}_3[\theta_n] \\ &= \{-i[(\mathbf{u} \cdot \mathbf{n}') \mathbf{n} + u_n \mathbf{n}'] - i[\partial_{\mathbf{n}}(u_n \mathbf{n}) + \kappa u_n \mathbf{n}] \theta_n + \mathbf{f} \theta_n\} \\ &\quad + \{\kappa p \theta_n \mathbf{n} - \nabla_{\Sigma}(p \theta_n)\} + \{\operatorname{div}_{\Sigma} [\alpha(\nabla_{\Sigma} \mathbf{u}) \theta_n]\} \\ &= \mathbf{f} \theta_n - \nabla_{\Sigma}(p \theta_n) + \operatorname{div}_{\Sigma} [\alpha(\nabla_{\Sigma} \mathbf{u}) \theta_n] + i[(\mathbf{u} \cdot \nabla_{\Sigma} \theta_n) \mathbf{n} + u_n \nabla_{\Sigma} \theta_n] \\ &\quad - [i(\partial_{\mathbf{n}} u_n) \mathbf{n} + i \kappa u_n \mathbf{n} - \kappa p \mathbf{n}] \theta_n, \end{aligned}$$

where the latter equation follows from Lemma C.5 and the formula $\mathbf{n}' = -\nabla_{\Sigma} \theta_n$.

We underline here that $\mathbf{B}[\theta_n] \in \mathbf{H}^{1/2}(\Sigma)^d$. Indeed, since Ω is of class $C^{2,1}$, the normal vector \mathbf{n} is $C^{1,1}(N^{\varepsilon})$ regular and $\kappa \in C^{0,1}(N^{\varepsilon}) \subset W^{1,\infty}(N^{\varepsilon}) \subset H^1(N^{\varepsilon})$, where N^{ε} is a small neighborhood of $\partial\Omega$ [37, Sec. 7.8]. Therefore, (using the density in $L^2(\Omega)^d$ of the traces on Σ of functions in $\mathbf{H}^2(\Omega)^d$) we get

$$\alpha \partial_{\mathbf{n}} \mathbf{u}' + i(\mathbf{u}' \cdot \mathbf{n}) \mathbf{n} - p' \mathbf{n} = \mathbf{B}[\theta_n], \quad \text{on } \Sigma.$$

In the following lines, we simplify the expression $\mathbf{B}[\theta_n]$ by utilizing identities from Lemma 3.2 and the definitions of tangential operators, including the Laplace-Beltrami operator and its decomposition $\Delta\varphi = \Delta_\Sigma\varphi + \kappa D\varphi\mathbf{n} + D^2\varphi\mathbf{n}\cdot\mathbf{n}$ (see, e.g., [37, p. 28] or [38, Prop. 5.4.12, eq. (5.59), p. 220]). Also, we note that, in Ω , we have $-\alpha\Delta\mathbf{u} + \nabla p = \mathbf{f}$. So, we get the following equations on Σ :

$$\begin{aligned}\nabla_\Sigma(p\theta_n) &= \theta_n\nabla_\Sigma p + p\nabla_\Sigma(\theta_n), \\ \operatorname{div}_\Sigma(\alpha\nabla_\Sigma\mathbf{u}\theta_n) &= -\theta_n(\mathbf{f} + \kappa\partial_\mathbf{n}\mathbf{u} + \partial_{\mathbf{n}\mathbf{n}}^2\mathbf{u} - \nabla p) + \alpha\nabla\mathbf{u}\nabla_\Sigma\theta_n.\end{aligned}$$

Because $p\mathbf{n} - \alpha\partial_\mathbf{n}\mathbf{u} = iu_n\mathbf{n}$ on Σ , the latter equation further implies that

$$\begin{aligned}\kappa p\mathbf{n}\theta_n + [\mathbf{f}\theta_n + \operatorname{div}_\Sigma(\alpha\nabla_\Sigma\mathbf{u}\theta_n)] &= \kappa p\mathbf{n}\theta_n + [-\theta_n(\kappa\partial_\mathbf{n}\mathbf{u} + \partial_{\mathbf{n}\mathbf{n}}^2\mathbf{u} - \nabla p) + \alpha\nabla\mathbf{u}\nabla_\Sigma\theta_n] \\ &= i\kappa u_n\mathbf{n}\theta_n - \theta_n(\partial_{\mathbf{n}\mathbf{n}}^2\mathbf{u} - \nabla p) + \alpha\nabla\mathbf{u}\nabla_\Sigma\theta_n.\end{aligned}$$

These computations, together with Lemma C.5 and the identities¹⁸

$$\begin{aligned}\nabla p - \nabla_\Sigma p &= \partial_\mathbf{n} p\mathbf{n}, \\ \nabla_\Sigma\theta_n \cdot \mathbf{u} - \theta_n(D\mathbf{u}\mathbf{n} \cdot \mathbf{n}) &= \nabla_\Sigma\theta_n \cdot \mathbf{u} + \theta_n \operatorname{div}_\Sigma \mathbf{u} \\ &= \operatorname{div}_\Sigma(\theta_n\mathbf{u}),\end{aligned}$$

on Σ , lead us to conclude that $\mathbf{B}[\theta_n]$ can be written equivalently as follows:

$$\begin{aligned}\mathbf{B}[\theta_n] &= \mathbf{f}\theta_n - \nabla_\Sigma(p\theta_n) + \operatorname{div}_\Sigma[\alpha(\nabla_\Sigma\mathbf{u})\theta_n] + i\operatorname{div}_\Sigma(\theta_n\mathbf{u})\mathbf{n} + iu_n\nabla_\Sigma\theta_n \\ &\quad + \kappa(p\mathbf{n} - iu_n\mathbf{n})\theta_n \\ &= [\alpha\nabla\mathbf{u} + (u_n - p)id]\nabla_\Sigma\theta_n - [-\partial_\mathbf{n} p\mathbf{n} + \partial_{\mathbf{n}\mathbf{n}}^2\mathbf{u} + i\partial_\mathbf{n}(u_n)\mathbf{n}]\theta_n \\ &\quad - i(\mathbf{u}\cdot\nabla_\Sigma\theta_n)\mathbf{n}.\end{aligned}\tag{C.77}$$

In summary, the shape derivative (\mathbf{u}', p') of (\mathbf{u}, p) which solves equation (7) is given by

$$\left\{\begin{array}{ll}-\alpha\Delta\mathbf{u}' + \nabla p' = \mathbf{0} & \text{in } \Omega, \\ \nabla\cdot\mathbf{u}' = \mathbf{0} & \text{in } \Omega, \\ \mathbf{u}' = \mathbf{0} & \text{on } \Gamma, \\ -p'\mathbf{n} + \alpha\partial_\mathbf{n}\mathbf{u}' + i(\mathbf{u}'\cdot\mathbf{n})\mathbf{n} = \mathbf{B}[\theta_n] & \text{on } \Sigma.\end{array}\right.\tag{C.78}$$

Step 2. Because we have sufficient regularity on the unknowns, the derivatives (see [37, Chap. 2, Sec. 2]) $J'(\Omega)\delta\tilde{\mathbf{u}}$ and $J'(\Omega)\delta\tilde{p}$ exist and are easily computed as

$$J'(\Omega)\delta\tilde{\mathbf{u}} = \int_\Omega \mathbf{u}_i \cdot \delta\tilde{\mathbf{u}} dx \quad \text{and} \quad J'(\Omega)\delta\tilde{p} = \int_\Omega p_i \delta\tilde{p} dx.$$

Step 3. Now, to derive and justify the structure of the adjoint system (27), we let $\bar{\mathbf{x}} := (\mathbf{u}, p) \in \mathcal{X} := X \times Q$, $\xi := (\psi, \mu) \in \mathcal{X}$, $\bar{\mathbf{y}} := (\mathbf{v}, q) \in \mathcal{X}$, and define the operator $\mathcal{E}_{\bar{\mathbf{x}}}(\bar{\mathbf{x}}, \Omega)\xi \in \mathcal{L}(X, X^*)$ such that (cf. (28))

$$\langle \mathcal{E}_{\bar{\mathbf{x}}}(\bar{\mathbf{x}}, \Omega)\xi, \bar{\mathbf{y}} \rangle_{\mathcal{X}^*, \mathcal{X}} := \tilde{a}(\psi, \mathbf{v}) + b(\mathbf{v}, \mu) + b(\psi, q).$$

This operator is bijective if and only if for every $\varphi \in X^*$ and $\lambda \in Q^*$, there exists a unique solution $\bar{\mathbf{y}} := (\mathbf{v}, q) \in \mathcal{X}$ to the variational equation (cf. (29))

$$\langle \mathcal{E}_{\bar{\mathbf{x}}}(\bar{\mathbf{x}}, \Omega)\xi, \bar{\mathbf{y}} \rangle_{\mathcal{X}^*, \mathcal{X}} = (\varphi, \psi) + (\mu, \lambda),$$

¹⁸Since $\operatorname{div}_\Sigma \mathbf{u} = 0$, then by the definition of the tangential divergence of a vector function, see Definition 3.1, we actually have $\operatorname{div}_\Sigma \mathbf{u} = -(D\mathbf{u}\mathbf{n} \cdot \mathbf{n})$ on Σ .

for all $\xi \in \mathcal{X}$. The existence of a unique solution to this equation – with $\varphi = \mathbf{u}_i \in V_\Gamma$ and $\lambda = p_i \in Q$ – can be established using similar arguments issued for the well-posedness of the state problem (7) (see subsection 2.2). So, we omit the details.

Now, since $(\mathbf{u}, p) \in (V_\Gamma \times Q) \cap (\mathbf{H}^3(\Omega)^d \times \mathbf{H}^2(\Omega))$, then by the previous step together with Remark 3.5, there is a unique adjoint state $(\mathbf{v}, q) \in (V_\Gamma \times Q) \cap (\mathbf{H}^3(\Omega)^d \times \mathbf{H}^2(\Omega))$ which satisfies (29). By standard arguments as in *Step 1* – applying IBP and/or Green's formula – we recover (27).

Step 4. For the final step, we will write the shape derivative of J given by (C.73) via the adjoint method – eliminating the shape derivative of the states \mathbf{u}' and p' appearing in \mathbb{I}_1 . To do this, let us first consider the weak formulation of (C.78): find $(\mathbf{u}', p') \in V_\Gamma \times Q$ such that

$$\begin{cases} a(\mathbf{u}', \varphi) + b(\varphi, p') = \int_{\Sigma} \mathbf{B}[\theta_n] \cdot \bar{\varphi} d\sigma, & \forall \varphi \in V_\Gamma, \\ b(\mathbf{u}', \lambda) = 0, & \forall \lambda \in Q. \end{cases} \quad (\text{C.79})$$

Following similar arguments carried out in subsection 2.2, the existence of weak solution to the above problem is a consequence of the complex version of the Lax-Milgram lemma [36, Thm. 1, p. 376] (see also [54, Lem. 2.1.51, p. 40]).

Now, by taking $(\varphi, \lambda) = (\mathbf{v}, q) \in V_\Gamma \times Q$, we get

$$a(\mathbf{u}', \mathbf{v}) + b(\mathbf{v}, p') = \int_{\Sigma} \mathbf{B}[\theta_n] \cdot \bar{\mathbf{v}} d\sigma \quad \text{and} \quad b(\mathbf{u}', q) = 0.$$

On the other hand, let us take $(\psi, \mu) = (\mathbf{u}', p') \in V_\Gamma \times Q$ in the variational equation (29) of the adjoint system (27). This lead us to

$$\tilde{a}(\mathbf{v}, \mathbf{u}') + b(\mathbf{u}', q) = \tilde{F}(\mathbf{u}') \quad \text{and} \quad b(\mathbf{v}, p') = (p', p_i).$$

Taking the complex conjugate of both sides of the equations above, and then combining it with the previous two, yields the following identity

$$\int_{\Omega} (\mathbf{u}_i \cdot \mathbf{u}' + p_i p') dx = \int_{\Sigma} \mathbf{B}[\theta_n] \cdot \bar{\mathbf{v}} d\sigma.$$

Comparing the imaginary parts of both sides of the above equation gives us

$$\mathbb{I}_1 = \int_{\Omega} (\mathbf{u}_i \cdot \mathbf{u}'_i + p_i p'_i) dx = \Im \left\{ \int_{\Omega} (\mathbf{u}_i \cdot \mathbf{u}' + p_i p') dx \right\} = \Im \left\{ \int_{\Sigma} \mathbf{B}[\theta_n] \cdot \bar{\mathbf{v}} d\sigma \right\}.$$

Adding this to \mathbb{I}_2 then concludes the proof. \square

References

- [1] Bouchon, F., Peichl, G.H., Sayeh, M., Touzani, R.: A free boundary problem for the Stokes equation. *ESAIM Control Optim. Calc. Var.* **23**, 195–215 (2017)
- [2] Flucher, M., Rumpf, M.: Bernoulli's free-boundary problem, qualitative theory and numerical approximation. *J. Reine. Angew. Math.* **486**, 165–204 (1997)
- [3] Alt, A., Caffarelli, L.A.: Existence and regularity for a minimum problem with free boundary. *J. Reine. Angew. Math.* **325**, 105–144 (1981)
- [4] Kasumba, H.: Shape optimization approaches to free-surface problems. *Int. J. Numer. Meth. Fluids* **74**, 818–845 (2014)

- [5] Babuška, I.: The Theory of Small Changes in the Domain of Existence in the Theory of Partial Differential Equations and Its Applications. *Differential Equations and their Applications*. Academic Press, New York (1963)
- [6] Saito, H., Scriven, L.E.: Study of coating flow by the finite element method. *J. Comput. Phys.* **42**, 53–76 (1981)
- [7] Beavers, G.J., Joseph, D.D.: Boundary conditions of a naturally permeable wall. *J. Fluid Mech.* **30**, 197–207 (1967)
- [8] Liakos, A.: Discretization of the Navier-Stokes equations with slip boundary condition. *Num. Meth. for Partial Diff. Eq.* **1**(1–18) (2001)
- [9] Girault, V., Raviart, P.A.: *Finite Element Methods for Navier–Stokes Equations*. Springer, Berlin (1986)
- [10] Galdi, G.P.: *An Introduction to the Mathematical Theory of the Navier-Stokes Equations. Springer Tracts in Natural Philosophy*. Springer, New York (1994)
- [11] Alessandrini, B., Delhommeau, G.: Simulation of three-dimensional unsteady viscous free surface flow around a ship model. *Int. J. Numer. Methods Fluids* **19**(4), 321–342 (1994)
- [12] Volkov, O., Protas, B., Liao, W., Glander, D.W.: Adjoint-based optimization of thermo-fluid phenomena in welding processes. *J. Eng. Math.* **65**(3), 201–220 (2009)
- [13] Wei, S., Smith, R.W., Udaykumar, H.S., Rao, M.M.: *Computational Fluid Dynamics with Moving Boundaries*. Taylor & Francis, Inc., Bristol, PA, USA (1996)
- [14] Kärkkäinen, K.T., Tiihonen, T.: Free surfaces: shape sensitivity analysis and numerical methods. *Int. J. Numer. Methods Eng.* **44**(8), 1079–1098 (1999)
- [15] VanBrummelen, E.H., Raven, H.C., Koren, B.: Efficient numerical solution of steady free-surface Navier-Stokes flow. *J. Comput. Phys.* **174**(1), 120–137 (2001)
- [16] Brummelen, E.H.V., Segal, A.: Numerical solution of steady free-surface flows by the adjoint optimal shape design method. *Int. J. Numer. Methods Fluids* **41**(1), 3–27 (2003)
- [17] Eppler, K., Harbrecht, H.: Tracking Neumann data for stationary free boundary problems. *SIAM J. Control Optim.* **48**, 2901–2916 (2009)
- [18] Eppler, K., Harbrecht, H.: Tracking the Dirichlet data in L^2 is an ill-posed problem. *J. Optim. Theory Appl.* **145**, 17–35 (2010)
- [19] Haslinger, J., Ito, K., Kozubek, T., Kunisch, K., Peichl, G.H.: On the shape derivative for problems of Bernoulli type. *Interfaces Free Bound.* **11**, 317–330 (2009)
- [20] Haslinger, J., Kozubek, T., Kunisch, K., Peichl, G.H.: Shape optimization and fictitious domain approach for solving free-boundary value problems of Bernoulli type. *Comput. Optim. Appl.* **26**(3), 231–251 (2003)
- [21] Ito, K., Kunisch, K., Peichl, G.H.: Variational approach to shape derivative for a class of Bernoulli problem. *J. Math. Anal. Appl.* **314**(2), 126–149 (2006)
- [22] Abda, A.B., Bouchon, F., Peichl, G.H., Sayeh, M., Touzani, R.: A Dirichlet-Neumann cost functional approach for the Bernoulli problem. *J. Eng. Math.* **81**, 157–176 (2013)

- [23] Bacani, J.B.: Methods of shape optimization in free boundary problems. PhD thesis, Karl-Franzens-Universität-Graz, Graz, Austria (2013)
- [24] Eppler, K., Harbrecht, H.: On a Kohn-Vogelius like formulation of free boundary problems. *Comput. Optim. App.* **52**, 69–85 (2012)
- [25] Laurain, A., Privat, Y.: On a Bernoulli problem with geometric constraints. *ESAIM Control Optim. Calc. Var.* **18**, 157–180 (2012)
- [26] Tiihonen, T.: Shape optimization and trial methods for free boundary problems. *RAIRO Modél. Math. Anal. Numér.* **31**, 805–825 (1997)
- [27] Cheng, X.L., Gong, R.F., Han, W., Zheng, X.: A novel coupled complex boundary method for solving inverse source problems. *Inverse Problems*, 055002 (2014)
- [28] Cheng, X.L., Gong, R.F., Han, W.: A coupled complex boundary method for the cauchy problem. *Inverse Probl. Sci. Eng.* **24**(9), 1510–1527 (2016)
- [29] Gong, R., Cheng, X., Han, W.: A coupled complex boundary method for an inverse conductivity problem with one measurement. *Appl. Anal.* **96**(5), 869–885 (2017)
- [30] Zheng, X., Cheng, X., Gong, R.: A coupled complex boundary method for parameter identification in elliptic problems. *Int. J. Comput. Math.* **97**(5), 998–1015 (2020)
- [31] Afraites, L.: A new coupled complex boundary method (CCBM) for an inverse obstacle problem. *Discrete Contin. Dyn. Syst. Ser. S* **15**(1), 23–40 (2022)
- [32] Rabago, J.F.T.: On the new coupled complex boundary method in shape optimization framework for solving stationary free boundary problems. *Math. Control Relat. Fields* (2022)
- [33] Ouaissa, H., Chakib, A., Nachaoui, A., Nachaoui, M.: On numerical approaches for solving an inverse Cauchy Stokes problem. *Appl. Math. Optim.* **85**(Art. 3), 37 (2022)
- [34] Bacani, J.B., Peichl, G.H.: On the first-order shape derivative of the Kohn-Vogelius cost functional of the Bernoulli problem. *Abstr. Appl. Anal.* **2013**, 19–384320 (2013)
- [35] Ito, K., Kunisch, K., Peichl, G.H.: Variational approach to shape derivatives. *ESAIM Control Optim. Calc. Var.* **14**, 517–539 (2008)
- [36] Dautray, R., Lions, J.-L.: Mathematical Analysis and Numerical Methods for Science and Technology vol. 2. Springer, Heidelberg (1998)
- [37] Delfour, M.C., Zolésio, J.-P.: Shapes and Geometries: Metrics, Analysis, Differential Calculus, And Optimization, 2nd edn. *Adv. Des. Control*, vol. 22. SIAM, Philadelphia (2011)
- [38] Henrot, A., Pierre, M.: Shape Variation and Optimization: A Geometrical Analysis. *Tracts in Mathematics*, vol. 28. European Mathematical Society, Zürich (2018)
- [39] Murat, F., Simon, J.: Sur le contrôle par un domaine géométrique. Research report 76015, Univ. Pierre et Marie Curie, Paris (1976)
- [40] Simon, J.: Differentiation with respect to the domain in boundary value. *Numer. Funct. Anal. Optim.* **2**, 649–687 (1980)
- [41] Sokołowski, J., Zolésio, J.-P.: Introduction to Shape Optimization: Shape Sensitivity Analysis. Springer Series in Computational Mathematics. Springer, Berlin, Heidelberg (1992)

- [42] Simon, J.: Domain variations for drag in stokes flow. In: Li, X., Yong, J. (eds.) Control Theory of Distributed Parameter Systems and Applications. Lecture Notes in Control and Information Sciences, vol. 159, pp. 28–42. Springer, Berlin, Heidelberg
- [43] Caubet, F., Dambrine, M., Kateb, D., Timimoun, C.Z.: A Kohn-Vogelius formulation to detect an obstacle immersed in a fluid. *Inverse Probl. Imaging* **7**(1), 123–157 (2013)
- [44] Dziri, R., Zolésio, J.-P.: An energy principle for a free boundary problem for navier-stokes equations. In: Partial Differential Equation Methods in Control and Shape Analysis. Lecture Notes in Pure and Applied Mathematics, vol. 188, pp. 133–151. Dekker, New York (1997)
- [45] Rabago, J.F.T., Azegami, H.: A second-order shape optimization algorithm for solving the exterior Bernoulli free boundary problem using a new boundary cost functional. *Comput. Optim. Appl.* **77**(1), 251–305 (2020)
- [46] Neuberger, J.W.: Sobolev Gradients and Differential Equations. Springer, Berlin (1997)
- [47] Doğan, G., Morin, P., Nocchetto, R.H., Verani, M.: Discrete gradient flows for shape optimization and applications. *Comput. Methods Appl. Mech. Engrg.* **196**, 3898–3914 (2007)
- [48] Novruzi, A., Roche, J.-R.: Newton’s method in shape optimisation: a three-dimensional case. *BIT Numer. Math.* **40**, 102–120 (2000)
- [49] Simon, J.: Second variation for domain optimization problems. In: Kappel, F., Kunisch, K., Schapacher, W. (eds.) Control and Estimation of Distributed Parameter Systems. International Series of Numerical Mathematics, vol. 91, pp. 361–378. Birkhäuser, Basel (1989)
- [50] Hecht, F.: New development in FreeFem++. *J. Numer. Math.* **20**, 251–265 (2012)
- [51] Johnson, C.R., Horn, R.A.: Matrix Analysis. Cambridge University Press, Cambridge (2013)
- [52] Gilbarg, D., Trudinger, N.S.: Elliptic Partial Differential Equations of Second Order. Springer, Berlin, Heidelberg (1988)
- [53] Adams, R.A., Fournier, J.J.F.: Sobolev Spaces. Pure and Applied Mathematics, vol. 140. Academic Press, Amsterdam (2003)
- [54] Sauter, S.A., Schwab, C.: Boundary Element Methods. Springer, Berlin, Heidelberg (2011)